RESONANCE STUDIES OF ARTIFICIAL EARTH SATELLITES

MARK STEVEN GILTHORPE

Doctor of Philosophy

THE UNIVERSITY OF ASTON IN BIRMINGHAM

March 1991

THE UNIVERSITY OF ASTON IN BIRMINGHAM

Resonance Studies of Artificial Earth Satellites

Mark Steven Gilthorpe

Doctor of Philosophy

1991

THESIS SUMMARY

Orbit determination from artificial satellite observations is a key process in obtaining information about the Earth and its environment. A study of the perturbations experienced by these satellites enables knowledge to be gained of the upper atmosphere, the gravity field, ocean tides, solid–Earth tides and solar radiation.

The gravity field is expressed as a double infinite series of associated Legendre functions (tesseral harmonics). In contemporary global gravity field models the overall geoid is well determined. An independent check on these gravity field harmonics of a particular order may be made by analysis of satellites that pass through resonance of that order. For such satellites the perturbations of the orbital elements close to resonance are analysed to derive lumped harmonic coefficients. The orbital parameters of 1984–106A have been determined at 43 epochs, during which time the satellite was close to 14^{th} order resonance. Analysis of the inclination and eccentricity yielded 6 lumped harmonic coefficients or order 14 whilst analysis of the mean motion yielded additional pairs of lumped harmonics of orders 14, 28 and 42, with the 14^{th} order harmonics superseding those obtained from analysis of the inclination.

This thesis concentrates in detail on the theoretical changes of a near–circular satellite orbit perturbed by the Earth's gravity field under the influence of minimal air–drag whilst in resonance with the Earth. The satellite 1984–106A experienced the interesting property of being temporarily trapped with respect to a secondary resonance parameter due to the low air–drag in 1987. This prompted the theoretical investigation of such a phenomenon. Expressions obtained for the resonance parameter lead to the determination of 8 lumped harmonic coefficients, coincidental to those already obtained. All the derived lumped harmonic values are used to test the accuracy of contemporary gravity field models and the underlying theory in this thesis.

KEYWORDS AND PHRASES

- Resonance
- Lumped Harmonics
- Near–Circular Orbits
- Gravity Field
- Tesseral Harmonics

DEDICATION

I dedicate this thesis to my parents for their endless support and encouragement throughout the years.

ACKNOWLEDGEMENTS

I would like to express my gratitude to the Science and Engineering Research Council, to the Ministry of Defence and to the University of Aston for financial support.

I would also like to thank Dr. Philip Moore for his patience and support given as a supervisor and a friend and Lynn Burton for making an excellent job of typing this thesis.

LIST OF CONTENTS

List of Tables

List of Figures

CHAPTER I

INTRODUCTION

Throughout the years science has given rise to many ingenious methods of exploration and investigation. Since the launching of the first satellite in 1957, orbit determination from satellite observations has been an essential process in obtaining information about the upper atmosphere, the gravity field, ocean tides, solid-Earth tides and solar radiation. The perturbations experienced by these satellites saw the advent of a whole new scientific approach to the investigation of the Earth and its environment.

Over the past decade substantial improvements have been made in modelling the Earth's external gravity field. The global models GEM–T1 (Marsh et al, 1988), GEM–T2 (Marsh et al, 1989) and the more recent PGS-3337 (Marsh et al, 1990) were derived by analysing thousands of optical, laser and doppler measurements of several satellites. The gravity field is expressed as a double infinite series of associated Legendre functions (tesseral harmonics). In the global models the overall geoid is well determined, but individual tesseral harmonics of high degree and order may be poorly determined. An independent check on these gravity field harmonics of a particular order may be made by analysis of satellites that pass through resonance of that order. For such satellites the perturbations of the orbital elements close to resonance are analysed to derive lumped harmonic coefficients. Such lumped values are applicable to a particular inclination. However, by studying satellites over the full range of orbital inclinations, individual coefficients can be derived by the weighted least-squares analysis of the lumped harmonic values and their analytical formulation (King–Hele et al, 1979 and 1986).

The availability of observations for the USSR satellite Cosmos 1603 (1984-106A) enables lumped harmonic values to be derived from both the inclination and eccentricity in a procedure which is now familiar (King–Hele, 1985). The results obtained from the eccentricity yield an improvement on values obtained previously. The values obtained from the inclination are comparable to previously derived values, but are superseded by

more accurate results from analysis of the change in the mean motion. This is the first time that reliable values are obtained in this manner, and their nominal accuracy proves to be much better than in any previous evaluation.

During the period of observation Cosmos 1603 experienced low drag, a direct consequence of its perigee height of 840km and the low solar activity in 1987. The combination of low drag and the near commensurability of the satellite with respect to the secondary resonance parameter $\Phi - \omega$, where Φ is the primary resonance variable and ω the argument of perigee, yields the physically interesting property of the satellite being temporarily 'trapped' in resonance. For this USSR satellite the resonance effects are sufficiently large such that they dominate the low drag effects, with the result that $\Phi - \omega$ exhibits libration about its mean value. In consequence, the eccentricity increases quasi–secularly whilst the perigee height decreases.

The secondary resonance phenomenon observed for Cosmos 1603 sparked off a detailed discussion of near-circular orbits perturbed by resonance in the presence of low air-drag. In particular, the consequence of minimal drag effects prompted an extended examination of the resonance angle, with the aim of obtaining expressions for Φ given explicitly in terms of time. Studies have previously been carried out in this area by Gedeon (1969) and Sochilina (1982). Initially the theory is developed for the resonance parameter incorporating the dominant resonance term only. Drag is introduced through a small correction term which models air-density variation. Finally the smaller resonance terms are introduced. The resulting expressions facilitate the evaluation of lumped harmonic coefficients using both the primary resonance parameter Φ and the secondary resonance parameter Φ - ω. The derived values are in good agreement with those obtained here from the eccentricity and the mean motion. The determination of lumped harmonic values is achieved using the secondary resonance parameter in conjunction with the variables $\xi = e \cos \omega$ and $\eta = e \sin \omega$, as used for near-circular orbits. The resonance problem for two degrees of freedom has been examined previously by Moore (1983 and 1984). Although this approach is more demanding than the method employed

for the eccentricity alone, accurate values are obtained. This technique utilizes the modelling of the resonance angle in the presence of low air-drag.

The equations of motion described by ξ and η are investigated in detail. Analytical solutions are obtained for shallow Φ resonance and for both deep and shallow $\Phi - \omega$ resonance. The occurrence of deep secondary resonance as experienced by Cosmos 1603 gives an excellent opportunity to investigate the validity of the theory developed. In particular the equations of motion, represented analytically as an infinite series of Bessel functions, prove to be sufficiently accurate to yield lumped harmonic values comparable to those obtained from numerical techniques alone. The occurrence of frozen orbits is briefly examined, with the view to reducing the rates of change of e and ω for a near-circular orbit experiencing dominant resonance perturbations.

Finally, air-drag is introduced analytically to the equations of motion for ξ and η, which are then developed to yield a unified solution combining gravity and drag. The main observation of the effect of even minimal drag in contrast to the drag-free result is that the eccentricity tends to zero.

This thesis examines in detail the theoretical changes of a satellite orbit perturbed by the Earth's non-uniform gravity field under the influence of minimal air-drag and other small forces, e.g. luni-solar perturbations. In particular, the phenomenon of 'resonance' is explored. The theory and numerical results presented in this thesis add to our knowledge of the Earth's gravity field and especially to our understanding of the resultant satellite motion.

CHAPTER II

ORBITAL PERTURBATIONS

§2.1 GRAVITY

A satellite in orbit about the Earth can be treated, to a first approximation, as a particle under an inverse square law of attraction, since the departure of the Earth from a perfect sphere is small. The resulting motion is described by an ellipse which lies in a plane that intersects the centre of mass of the Earth (which will henceforth be referred to as the Earth's centre). The acceleration of the satellite towards the Earth's centre can thus be written

$$a = \frac{\mu}{r^2} \tag{2.1}$$

where $\mu = GM$, G is the universal gravitational constant, M is the mass of the Earth and r is the radial distance of the satellite from the Earth's centre. This acceleration is the magnitude of a vector **a** directed along the line between the satellite and the centre of the Earth. The vector **a** of magnitude a, i.e. (2.1), will be obtained by expressing the acceleration as a gradient of a scalar, called a potential. Thus,

$$\mathbf{a} = \nabla V \tag{2.2}$$

where

$$V = \frac{\mu}{r} \, . \tag{2.3}$$

In (2.3) V is shown as a positive quantity, which is consistent with the sign convention of astronomy and geodesy. In physics V is conventionally taken to be negative.

To describe orbital motion it is desirable to develop a coordinate system that reflects the structure of the dynamical system. We will see initially that motion follows the path of an ellipse and later that this ellipse is slowly changing in shape and orientation. Due to

symmetry of the geometry, it is therefore preferable to develop elliptical motion in polar coordinates and to convert the solution of the equations of motion from cartesian coordinates to spherical polar coordinates. The aim ultimately is to make a final transformation to the *orbital elements* coordinate system.

Elliptical Motion

The equation of motion for a particle in a vacuum, moving under Newton's inverse square law of gravitational attraction, is described in polar coordinates (r, θ) by (King–Hele, 1987)

$$\ddot{r} - r\dot{\theta}^2 = -\frac{\mu}{r^2} , \tag{2.4}$$

where dots denote differentiation with respect to time. If there are no perturbations and the only force acting is the radial attraction then the transverse acceleration is zero, i.e.

$$\frac{1}{r}\frac{d}{dt}\left(r^2\,\dot{\theta}\right) = 0$$

or

$$r^2\,\dot{\theta} = \text{constant} = h, \qquad \text{say.} \tag{2.5}$$

Using equation (2.5), the general solution to (2.4) is

$$\frac{1}{r} = \frac{\mu}{h^2}\left[1 + e\cos(\theta - B)\right] , \tag{2.6}$$

where e and B are constants. It is convenient to choose the θ–axis so that $B = 0$ and then (2.6) becomes

$$\frac{1}{r} = \frac{1}{p}\left(1 + e\cos\theta\right) \tag{2.7}$$

where

$$h^2/\mu = p.$$

This is the polar equation of a conic with eccentricity e, semi–latus rectum p and one focus at the centre of the Earth. If $e < 1$, the orbit is an ellipse and if $e > 1$, the orbit is a hyperbola. The angle θ is called the true anomaly. From here onwards only the ellipse is considered.

The semi–major axis of this ellipse can be written as (King–Hele, 1987)

$$a = \frac{1}{2}(r_a + r_p) = \frac{p}{(1 - e^2)}$$

where $r_a = a(1 + e)$ and $r_p = a(1 - e)$ are the apogee and perigee distances respectively, as shown in Fig. 2.1.

Thus, (2.7) becomes

$$r = \frac{a(1 - e^2)}{(1 + e \cos \theta)}$$

which is the standard equation for an elliptic orbit.

In place of the true anomaly it is useful to use E, the eccentric anomaly, which is related to the true anomaly by

$$\begin{aligned} r \cos \theta &= a(\cos E - e) &&= q_1 \\ r \sin \theta &= a(1 - e^2)^{1/2} \sin E &&= q_2 \end{aligned} \qquad (2.8)$$

where q_1 and q_2 are the components of $\mathbf{q}$, the position vector in the plane of the ellipse. Figure 2.1 illustrates some of the parameters described.

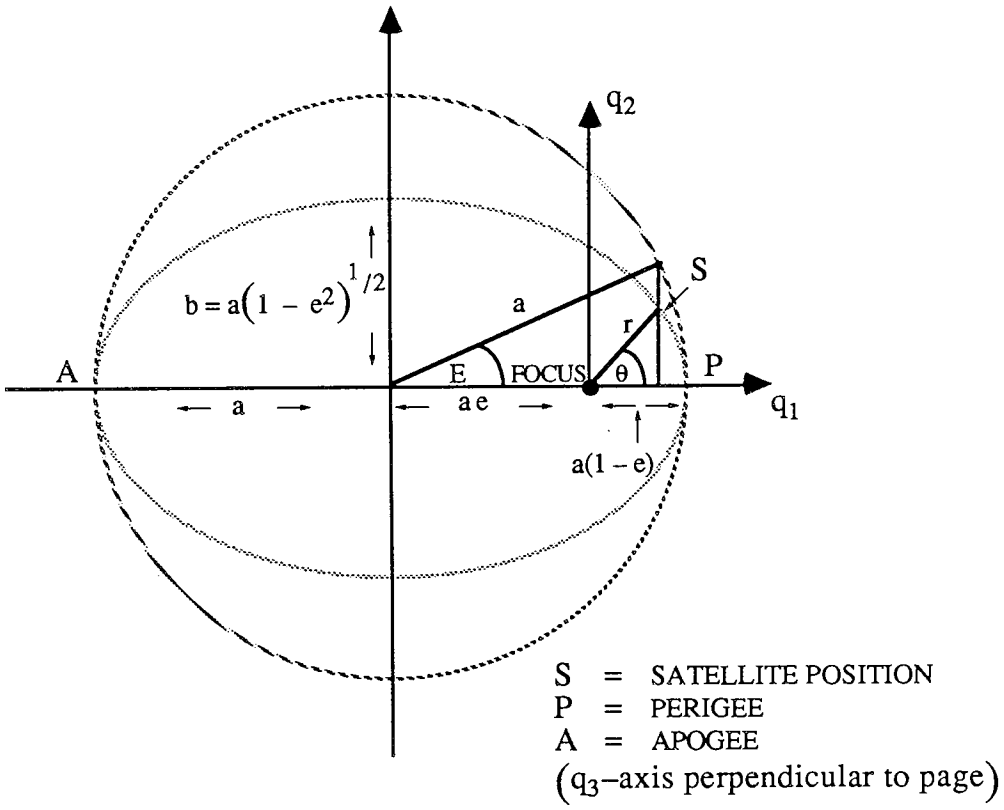

Fig. 2.1. The orbital ellipse.

From (2.8) it follows that

$$r = \sqrt{q_1^2 + q_2^2} = a(1 - e \cos E). \tag{2.9}$$

On differentiating (2.9) and then utilising (2.8), we have

$$dr = ae \sin E \, dE = \frac{q_2 \, e}{(1 - e^2)^{1/2}} \, dE \tag{2.10}$$

and similarly with equation (2.7)

$$dr = \frac{r^2 \, e \sin \theta}{a(1 - e^2)} \, d\theta = \frac{q_2 r \, e}{a(1 - e^2)} \, d\theta \, . \tag{2.11}$$

Equating (2.10) and (2.11) and using equation (2.5), we obtain

$$a^2 (1 - e \cos E) \, dE = (\mu a)^{1/2} \, dt \, . \tag{2.12}$$

Hence the velocity components $\dot{q}_1$ and $\dot{q}_2$ may be written, utilizing equations (2.8) and (2.12), as

$$\begin{aligned} \dot{q}_1 &= \frac{dq_1}{dE}\frac{dE}{dt} = -\left(\frac{\mu}{a}\right)^{1/2}\frac{\sin E}{(1-e\cos E)} \\ \dot{q}_2 &= \frac{dq_2}{dE}\frac{dE}{dt} = \left(\frac{\mu}{a}\right)^{1/2}\frac{(1-e^2)^{1/2}\cos E}{(1-e\cos E)} \end{aligned} \qquad (2.13)$$

Six orbital elements are required to specify the motion of a satellite in its ellipse, replacing the six cartesian elements $\{x, y, z, \dot{x}, \dot{y}, \dot{z}\}$. These orbital elements may be denoted by the set of parameters $\{a, e, i, \Omega, \omega, \theta\}$ where i, Ω and ω are defined in Fig. 2.2 – i is the inclination of the orbital plane to the equator, Ω the right ascension of the ascending node and ω the argument of perigee. The ascending node is the point, N, where the satellite crosses the equator going north. The Equinox, γ, is the fixed point in the sky which serves as a reference for measuring star positions and Ω is measured positively eastwards from that point.

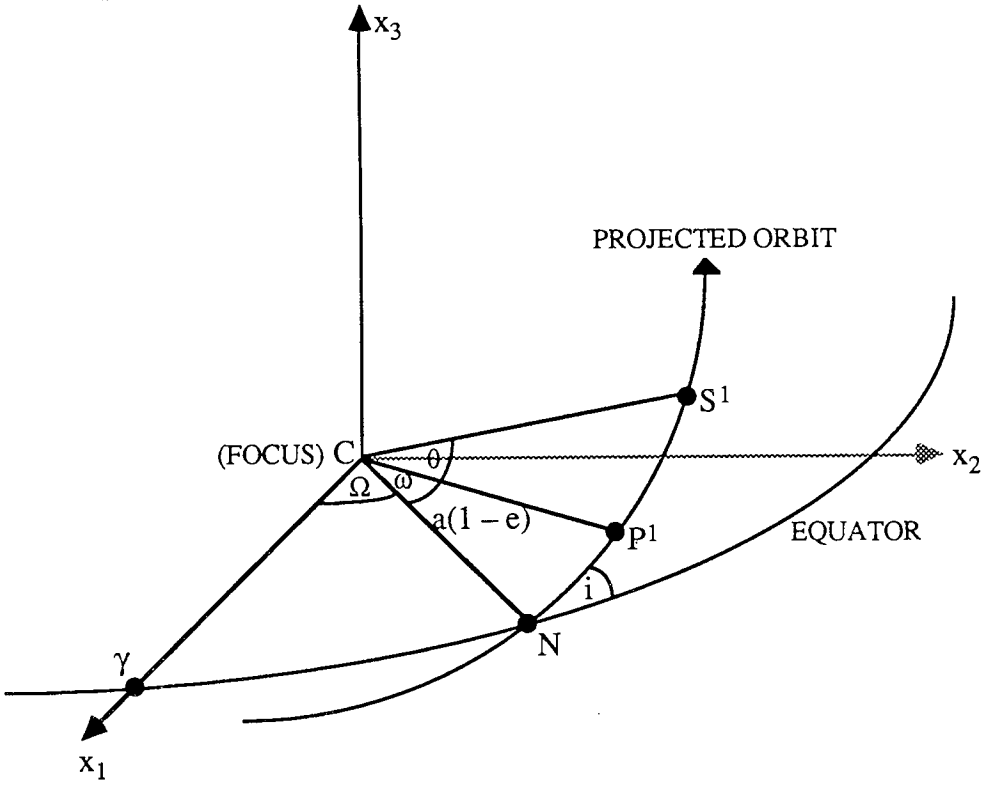

C = CENTRE OF EARTH

γ = EQUINOX

N = ASCENDING NODE

S^1 = PROJECTED SATELLITE POSITON

P^1 = PROJECTED PERIGEE POSITION

Fig. 2.2. Orbital orientation.

Sometimes the mean motion, n, is specified instead of a, since, applying Kepler's law, $n^2a^3 = \mu$ and the true anomaly may be replaced by either the eccentric anomaly, E, or the mean anomaly, M, written

$$M = M_0 + nt$$

where M_0 is the value of M at the epoch $t = 0$.

It is easier to understand the physical interpretation of some of the parameters described, by examination of Figures 2.1 and 2.2 – a and e define the shape of the orbit; i and Ω give the orientation of the orbital plane in space and ω defines the position of perigee in the ellipse, whilst θ, E or M give the angular positon of the satellite relative to perigee. We choose to use M in preference to θ or E. The set of six elements $\{a, e, i, \Omega, \omega, M\}$ are known as Keplerian elements and at any instant describe the position of a satellite in an Earth–centred, inertially fixed coordinate system.

The relationship between the orbital coordinate system, $\mathbf{q} = \mathbf{q}(q_1, q_2, q_3)$ and the rectangular coordinate system, $\mathbf{x} = \mathbf{x}(x_1, x_2, x_3)$, is given by three independent rotations (see Fig. 2.2). Transforming from the **x**–system to the **q**–system comprises of :-

i) a counter–clockwise rotation about the x_3–axis from the Equinox to the ascending node, N, denoted $\mathbf{R}_3(\Omega)$,

ii) a counter–clockwise rotation about the x_1–axis from the equatorial plane to the orbital plane, denoted $\mathbf{R}_1(i)$, and

iii) a counter–clockwise rotation about the x_3–axis from the node, N, to the argument of perigee, P, denoted $\mathbf{R}_3(\omega)$.

Hence,

$$\mathbf{R}_{qx} = \mathbf{R}_3(\omega)\ \ \mathbf{R}_1(i)\ \ \mathbf{R}_3(\Omega)$$
$$\mathbf{R}_{xq} = \mathbf{R}_3(-\Omega)\ \ \mathbf{R}_1(-i)\ \ \mathbf{R}_3(-\omega)$$

where $\mathbf{R}_{qx}$ is the transformation matrix converting from $\mathbf{x}$–coordinates to $\mathbf{q}$–coordinates and $\mathbf{R}_{xq}$ is the the transformation matrix converting from $\mathbf{q}$–coordinates to $\mathbf{x}$–coordinates. Clearly $\mathbf{R}_{xq}$ is the inverse of $\mathbf{R}_{qx}$, i.e. $\mathbf{R}_{xq} = \mathbf{R}_{qx}^{-1}$.

Using the standard form of rotation matrix $\mathbf{R}_i(\theta)$ to rotate the coordinate system through θ degrees, counter–clockwise, about the x_i–axis, $\mathbf{R}_{xq}$ is written as

$$\mathbf{R}_{xq} = \begin{bmatrix} \cos\Omega\cos\omega - \sin\Omega\cos i\sin\omega & -\cos\Omega\sin\omega - \sin\Omega\cos i\cos\omega & \sin\Omega\sin i \\ \sin\Omega\cos\omega + \cos\Omega\cos i\sin\omega & -\sin\Omega\sin\omega + \cos\Omega\cos i\cos\omega & -\cos\Omega\sin i \\ \sin i\sin\omega & \sin i\cos\omega & \cos i \end{bmatrix}.$$

Thus the relationship between the Keplerian elements $\{a, e, i, \Omega, \omega, M\}$ and the six cartesian elements $\{x, y, z, \dot{x}, \dot{y}, \dot{z}\}$ is given by

$$\begin{aligned} \mathbf{x} &= \mathbf{R}_{xq}\{\Omega, i, \omega\}\ \mathbf{q}\ \{a, e, M\} \\ \dot{\mathbf{x}} &= \mathbf{R}_{xq}\{\Omega, i, \omega\}\ \dot{\mathbf{q}}\ \{a, e, M\} \end{aligned} \tag{2.14}$$

where $\mathbf{q}$ and $\dot{\mathbf{q}}$ can be written, from equations (2.8) and (2.13) after utililizing $n^2a^3 = \mu$, as

$$\mathbf{q} = \begin{bmatrix} a(\cos E - e) \\ a(1 - e^2)^{1/2}\sin E \\ 0 \end{bmatrix}; \qquad \dot{\mathbf{q}} = \frac{na}{(1 - e\cos E)} \begin{bmatrix} -\sin E \\ (1 - e^2)^{1/2}\cos E \\ 0 \end{bmatrix} \tag{2.15}$$

where E is a function of the mean anomaly M, obtained by integrating (2.12) (Kaula, 1966), namely

$$E - e\sin E = M.$$

The developments this far apply solely to motion in a purely central field, but interest in orbital perturbations is mainly due to the fact that the Earth's gravitational field is non–central, that is (2.2) holds but V has a non central form. This is a direct consequence of the Earth having a non–uniform shape and density distribution. Consider the effect

of several particles of masses M_i at distance r_i. The combined acceleration in (2.2) can be expressed as the gradient of a potential which is the sum of potentials V_i, given by equation (2.3). If these particles are conglomerated to form a continuous body of variable density ρ, this summation can be replaced by an integration over the volume of the body. Thus, in the cartesian coordinate system, this may be summarized by,

$$V = G \iiint \frac{\rho(x, y, z)}{r(x, y, z)} \, dx \, dy \, dz. \tag{2.16}$$

However, we wish to express V in terms of the Keplerian elements and then develop the equations of motion in this coordinate system.

At a particular instant in time the Keplerian ellipse is known as the instantaneous or osculating orbit. The six elements $\{a, e, i, \Omega, \omega, M\}$ are called osculating elements. If V differs from a central field very slightly (as in the case for the Earth) then the parameters of the ellipse will change slowly, allowing the use of osculating elements as a convenient coordinate system.

The three 2nd order equations of motion in cartesian coordinates can be expressed as six 1st order equations by treating the velocity components as variables, independent of the position components. Thus,

$$\begin{aligned} \frac{d}{dt} x_i &= \dot{x}_i \\ \frac{d}{dt} \dot{x}_i &= \frac{\partial V}{\partial x_i} \end{aligned} \qquad (i = 1, 2, 3)$$

where x_i and $\dot{x}_i$ denote inertially fixed rectangular components of position and velocity, respectively. Representing the rates of change of the six Keplerian elements by ds_k/dt, where s_k denotes any of $\{a, e, i, \Omega, \omega, M\}$ and using the chain rule, then

$$\frac{\partial x_i}{\partial s_k} \cdot \frac{ds_k}{dt} = \dot{x}_i \tag{2.17}$$

and $(i = 1, 2, 3)$

$$\frac{\partial \dot{x}_i}{\partial s_k} \cdot \frac{ds_k}{dt} = \frac{\partial V}{\partial x_i} \tag{2.18}$$

where the summation convention is assumed whenever there is a repeated subscript; the subscripts k running from 1 to 6.

Multiplying (2.17) by $-\partial \dot{x}_i/\partial s_\ell$, multiplying (2.18) by $\partial x_i/\partial s_\ell$ and adding yields,

$$\left[s_\ell, s_k\right] \frac{ds_k}{dt} = \frac{\partial F}{\partial s_\ell} \tag{2.19}$$

where

$$\left[s_\ell, s_k\right] = \frac{\partial x_i}{\partial s_\ell} \cdot \frac{\partial \dot{x}_i}{\partial s_k} - \frac{\partial \dot{x}_i}{\partial s_\ell} \cdot \frac{\partial x_i}{\partial s_k} \tag{2.20}$$

which is known as Lagrange's bracket and

$$F = V - T$$

which is known as the force function. This is the negative of the total energy as used in physics. V is the negative of the potential energy and T is the kinetic energy, written

$$T = \frac{1}{2} \dot{x}_i \dot{x}_i = \frac{1}{2}\left(\dot{q}_1^2 + \dot{q}_2^2\right) = \frac{\mu}{r} - \frac{\mu}{2a} \tag{2.21}$$

from (2.15). It is usual to express the force function, using (2.21), as

$$F = \frac{\mu}{r} + R - T = \frac{\mu}{2a} + R. \tag{2.22}$$

The function R, comprising of all terms in V except the central term, is known as the disturbing function.

Inspection of (2.20) reveals that $[s_k, s_\ell] = -[s_\ell, s_k]$ and hence $[s_k, s_k]$ vanishes. Thus there are fifteen different Lagrange brackets to be evaluated. These are determined by differentiating equation (2.14). A useful property of Lagrange brackets that facilitates their evaluation is their time invariance, that is

$$\frac{\partial}{\partial t}\,[s_\ell, s_k] = 0,$$

hence $\mathbf{q}$ and $\dot{\mathbf{q}}$ that appear in (2.14) can be evaluated at any convenient point, such as perigee, where $E = 0$.

The complete set of non–zero results is, (Kaula, 1966)

$$\begin{aligned}
[\Omega, i] &= -[i, \Omega] = -na^2(1-e^2)^{1/2}\sin i,\\
[\Omega, a] &= -[a, \Omega] = (1-e^2)^{1/2}\cos i\, na/2,\\
[\Omega, e] &= -[e, \Omega] = -na^2 e\cos i/(1-e^2)^{1/2},\\
[\omega, a] &= -[a, \omega] = (1-e^2)^{1/2}\, na/2,\\
[\omega, e] &= -[e, \omega] = -na^2 e/(1-e^2)^{1/2},\\
[a, M] &= -[M, a] = -na/2.
\end{aligned} \tag{2.23}$$

The substitution of expressions (2.22) and (2.23) into (2.19) and the solution of the six simultaneous equations for the ds_k/dt yield Lagrange's planetary equations (Kaula, 1966),

$$\begin{aligned}
\frac{da}{dt} &= \frac{2}{na}\,\frac{\partial R}{\partial M},\\
\frac{de}{dt} &= \frac{1-e^2}{na^2 e}\,\frac{\partial R}{\partial M} - \frac{(1-e^2)^{1/2}}{na^2 e}\,\frac{\partial R}{\partial \omega},\\
\frac{di}{dt} &= \frac{\cos i}{na^2(1-e^2)^{1/2}\sin i}\,\frac{\partial R}{\partial \omega} - \frac{1}{na^2(1-e^2)^{1/2}\sin i}\,\frac{\partial R}{\partial \Omega},
\end{aligned}$$

$$\frac{d\Omega}{dt} = \frac{1}{na^2(1-e^2)^{1/2}\sin i}\frac{\partial R}{\partial i},$$

$$\frac{d\omega}{dt} = -\frac{\cos i}{na^2(1-e^2)^{1/2}\sin i}\frac{\partial R}{\partial \omega} + \frac{(1-e)^{1/2}}{na^2 e}\frac{\partial R}{\partial e},$$

$$\frac{dM}{dt} = n - \frac{1-e^2}{na^2 e}\frac{\partial R}{\partial e} - \frac{2}{na}\frac{\partial R}{\partial a}.$$

(2.24)

The Earth's spherical harmonic potential

A particular component a_x, of the acceleration vector **a**, derived from a point mass potential of equation (2.3), may be written as

$$a_x = \frac{\partial V}{\partial x} = -\mu\frac{x}{r^3}$$

and for the second derivative,

$$\frac{\partial^2 V}{\partial x^2} = \mu\left(-\frac{1}{r^3} + \frac{3x^2}{r^5}\right).$$

Adding together all three components of the second derivative yields Laplace's equation,

$$\nabla^2 V = \frac{\partial^2 V}{\partial x^2} + \frac{\partial^2 V}{\partial y^2} + \frac{\partial^2 V}{\partial z^2} = \mu\left(-\frac{3}{r^3} + \frac{3\left(x^2+y^2+z^2\right)}{r^5}\right) = 0.$$

The same result would be achieved for any element of mass $\rho dx\, dy\, dz$ in the potential V of equation (2.16). It follows, therefore, that the gravitational potential (central and non–central parts) satisfies Laplace's equation. To obtain an expression for V in terms of the osculating elements it is necessary to solve Laplace's equation in spherical polar coordinates and then transform the solution to Keplerian coordinates. Laplace's equation in spherical coordinates becomes

$$r^2\nabla^2 V = \frac{\partial}{\partial r}\left(r^2\frac{\partial V}{\partial r}\right) + \frac{1}{\cos\phi}\frac{\partial}{\partial\phi}\left(\cos\phi\frac{\partial V}{\partial\phi}\right) + \frac{1}{\cos^2\phi}\frac{\partial^2 V}{\partial\lambda^2} = 0 \qquad (2.25)$$

where r is the radial distance, ϕ the latitude and λ the longitude (measured eastward). These coordinates are related to the cartesian coordinates by

$$\begin{aligned} x &= r \cos\phi \cos\lambda \\ y &= r \cos\phi \sin\lambda \\ z &= r \sin\phi \end{aligned} .$$

To express the variations of the potential V in spherical polars, it would be convenient if V had the form

$$V = R(r)\,\Phi(\phi)\,\Lambda(\lambda)$$

where R, Φ and Λ are each explicit functions of only r, ϕ and λ respectively. The solution to (2.25) can be obtained in this form and may be written (Kaula, 1966) as

$$V = \frac{\mu}{r}\left[1 - \sum_{\ell=2}^{\infty} J_\ell \left(\frac{a_e}{r}\right)^\ell P_\ell(\sin\phi) + \sum_{\ell=2}^{\infty}\sum_{m=1}^{\ell} \left(\frac{a_e}{r}\right)^\ell P_\ell^m(\sin\phi)\left[C_{\ell m}\cos m\lambda + S_{\ell m}\sin m\lambda\right]\right] \tag{2.26}$$

where, a_e is the Earth's equatorial radius, $P_\ell(\sin\phi)$ is the Legendre polynomial of degree ℓ and argument $\sin\phi$, $P_\ell^m(\sin\phi)$ is the associated Legendre function of order m and degree ℓ, J_ℓ are the zonal harmonic coefficients and $C_{\ell m}$ and $S_{\ell m}$ are the tesseral harmonic coefficients. To make terms and coefficients more readily comparable in numerical work, it is generally more convenient to use normalized functions and coefficients, namely

$$\bar{C}_{\ell m} = C_{\ell m}/N_{\ell m} \; ; \qquad \bar{S}_{\ell m} = S_{\ell m}/N_{\ell m}$$

and

$$\bar{F}_{\ell mp}(i) = N_{\ell m}\, F_{\ell mp}(i)$$

where the normalizing factor is given by

$$N_{\ell m}^2 = \frac{(\ell - m)!\,(2\ell + 1)(2 - \delta_{0m})}{(\ell + m)!}$$

and the Kronecker delta δ_{0m} is equal to 1 for $m = 0$ and 0 for $m \neq 0$.

Conversion of the spherical harmonic potential is achieved after extensive manipulation of algebra and trigonometric terms (Kaula, 1966). The potential is expressed in terms of the six Keplerian elements, by

$$V = \sum_{\ell=0}^{\infty} \sum_{m=0}^{\ell} \sum_{p=0}^{\ell} \sum_{q=-\infty}^{\infty} \left(\frac{\mu}{a}\right)\left(\frac{a_e}{a}\right)^{\ell} \bar{F}_{\ell mp}(i)\, G_{\ell pq}(e) \left\{ \begin{bmatrix} \bar{C}_{\ell m} \\ -\bar{S}_{\ell m} \end{bmatrix}_{\ell-m\ \text{odd}}^{\ell-m\ \text{even}} \cos \psi_{\ell mpq} + \right.$$

$$\left. + \begin{bmatrix} \bar{S}_{\ell m} \\ \bar{C}_{\ell m} \end{bmatrix}_{\ell-m\ \text{odd}}^{\ell-m\ \text{even}} \sin \psi_{\ell mpq} \right\} \qquad (2.27)$$

where $$\psi_{\ell mpq} = (\ell - 2p)\omega + (\ell - 2p + q)M + m(\Omega - \theta)\,. \qquad (2.28)$$

Here, θ denotes the Greenwich Sidereal Time and $F_{\ell mp}(i)$ is Kaula's inclination function given by

$$F_{\ell mp}(i) = \sum_{t} \frac{(2\ell - 2t)!}{t!(\ell - t)!(\ell - m - 2t)!\, 2^{2\ell-2t}} \sin^{\ell-m-2t} i$$

$$\times \sum_{s=0}^{m} \binom{m}{s} \cos^{s} i \sum_{c} \binom{\ell - m - 2t + s}{c} \binom{m - s}{p - t - c} (-1)^{c-k}$$

where k is the integer part of $(\ell - m)/2$, t is summed from 0 to the lesser of p or k and c is summed over all values making the binomial coefficients non–zero.

$G_{\ell pq}(e)$ is a function of eccentricity given by (Tisserand, 1889, p256), where

$$G_{\ell pq}(e) = (-1)^{|q|}\left(1+\beta^2\right)^{\ell}\beta^{|q|}\sum_{k=0}^{\infty} P_{\ell pqk}\, Q_{\ell pqk}\, \beta^{2k} \tag{2.29}$$

given

$$\beta = \frac{e}{1+\sqrt{1-e^2}};$$

$$P_{\ell pqk} = \sum_{r=0}^{h}\binom{2p'-2\ell}{h-r}\frac{(-1)^r}{r!}\left(\frac{(\ell-2p'+q')e}{2\beta}\right)^r$$

$$h = k + q',\ q' > 0; \qquad h = k,\ q' < 0;$$

and

$$Q_{\ell pqk} = \sum_{r=0}^{h}\binom{-2p'}{h-r}\frac{1}{r!}\left(\frac{(\ell-2p'+q')e}{2\beta}\right)^r$$

$$h = k,\ q' > 0; \qquad h = k - q',\ q' < 0;$$

$$p' = p,\ q' = q \quad \text{for} \quad p \le \ell/2; \qquad p' = \ell - p,\ q' = -q \quad \text{for} \quad p > \ell/2\ .$$

The disturbing potential

Writing

$$\varphi^{A}_{\ell mpq} = \begin{bmatrix}\bar{C}_{\ell m}\\ -\bar{S}_{\ell m}\end{bmatrix}^{\ell-m\ \text{even}}_{\ell-m\ \text{odd}} \sin\psi_{\ell mpq} - \begin{bmatrix}\bar{S}_{\ell m}\\ \bar{C}_{\ell m}\end{bmatrix}^{\ell-m\ \text{even}}_{\ell-m\ \text{odd}} \cos\psi_{\ell mpq}$$

$$\varphi^{B}_{\ell mpq} = \begin{bmatrix}\bar{C}_{\ell m}\\ -\bar{S}_{\ell m}\end{bmatrix}^{\ell-m\ \text{even}}_{\ell-m\ \text{odd}} \cos\psi_{\ell mpq} + \begin{bmatrix}\bar{S}_{\ell m}\\ \bar{C}_{\ell m}\end{bmatrix}^{\ell-m\ \text{even}}_{\ell-m\ \text{odd}} \sin\psi_{\ell mpq} \tag{2.30}$$

the non–central part of the geopotential (2.27) is given by

$$R = \sum_{\ell=2}^{\infty}\sum_{m=0}^{\ell}\sum_{p=0}^{\ell}\sum_{q=-\infty}^{\infty}\left(\frac{\mu}{a}\right)\left(\frac{a_e}{a}\right)^{\ell}\bar{F}_{\ell mp}(i)\, G_{\ell pq}(e)\, \varphi^{B}_{\ell mpq}\,. \tag{2.31}$$

Denoting

$$\bar{F}'_{\ell mp}(i) = \frac{\partial \bar{F}_{\ell mp}(i)}{\partial i} \quad \text{and} \quad G'_{\ell pq}(e) = \frac{\partial G_{\ell pq}(e)}{\partial e}$$

and considering a general term, $R_{\ell mpq}$, of the disturbing potential and upon utilizing equations (2.28) and (2.30) the derivatives in Lagrange's planetary equations (2.24), may be written

$$\begin{aligned}
\frac{1}{na^2}\frac{\partial R_{\ell mpq}}{\partial a} &= -\frac{(\ell+1)}{a} n \left(\frac{a_e}{a}\right)^{\ell} \bar{F}_{\ell mp}(i)\, G_{\ell pq}(e)\, \varphi^{B}_{\ell mpq} \\
\frac{1}{na^2}\frac{\partial R_{\ell mpq}}{\partial e} &= n \left(\frac{a_e}{a}\right)^{\ell} \bar{F}_{\ell mp}(i)\, G'_{\ell pq}(e)\, \varphi^{B}_{\ell mpq} \\
\frac{1}{na^2}\frac{\partial R_{\ell mpq}}{\partial i} &= n \left(\frac{a_e}{a}\right)^{\ell} \bar{F}'_{\ell mp}(i)\, G_{\ell pq}(e)\, \varphi^{B}_{\ell mpq} \\
\frac{1}{na^2}\frac{\partial R_{\ell mpq}}{\partial \omega} &= -n \left(\frac{a_e}{a}\right)^{\ell} \bar{F}_{\ell mp}(i)\, G_{\ell pq}(e)\, [\ell-2p]\, \varphi^{A}_{\ell mpq} \\
\frac{1}{na^2}\frac{\partial R_{\ell mpq}}{\partial \Omega} &= -n \left(\frac{a_e}{a}\right)^{\ell} \bar{F}_{\ell mp}(i)\, G_{\ell pq}(e)\, [m]\, \varphi^{A}_{\ell mpq} \\
\frac{1}{na^2}\frac{\partial R_{\ell mpq}}{\partial M} &= -n \left(\frac{a_e}{a}\right)^{\ell} \bar{F}_{\ell mp}(i)\, G_{\ell pq}(e)\, [\ell-2p+q]\, \varphi^{A}_{\ell mpq} .
\end{aligned} \tag{2.32}$$

Linear Perturbations

The term of the gravitational field which dominates the disturbing function R, is that with $(\ell, m) = (2, 0)$, since $C_{20}\ (\text{or } -J_2)$ is at least 100 times greater than any other $C_{\ell m}$. Thus, we write

$$R_{20} = \frac{\mu C_{20}}{a}\left(\frac{a_e}{a}\right)^2 \sum_{p,q} F_{20}(i)\, G_{2pq}(e) \cos[(2-2p)\omega + (2-2p+q)M]$$

summing over p and q only. Assuming that the coefficients in R_{20} are of about the same magnitude, the terms that do not contain M will be dominant, since M completes a full cycle in the relatively brief period of one orbital revolution.

The summation limits in (2.27) and (2.29) indicates that the only term of R_{20} from which M is absent is when (p, q) = (1, 0), this being

$$R_{2010} = \frac{\mu C_{20}}{a}\left(\frac{a_e}{a}\right)^2 F_{201}(i)\, G_{210}(e). \tag{2.33}$$

Evaluating F_{201} and G_{210} and replacing C_{20} by $-J_2$, Lagrange's planetary equations yield

$$\begin{aligned}
\dot{a} &= \dot{e} = \dot{i} = 0 \\
\dot{\omega} &= 3n\, J_2 \left(\frac{a_e}{a}\right)^2 \frac{1}{(1-e^2)^2}\left[1 - 5/4\, \sin^2 i\right] \\
\dot{\Omega} &= 3n\, J_2 \left(\frac{a_e}{a}\right)^2 \frac{1}{(1-e^2)^2}\frac{\cos i}{2} \\
\dot{M} &= n + \frac{3n}{2} J_2 \left(\frac{a_e}{a}\right)^2 \frac{1}{(1-e^2)^{3/2}}\left[1 - 3/4\, \sin^2 i\right] .
\end{aligned}$$

These are the first order linear perturbations experienced by the osculating elements, due to the dominant J_2 zonal harmonic.

Tesseral contribution and resonance

Resonance occurs if the disturbing potential is constant or slowly changing. R, as given by equation (2.31), involves time through the two quantities $(\omega+M)$ and $(\Omega-\theta)$. Hence, there will be resonance whenever

$$\alpha(\dot{\omega} + \dot{M}) + \beta(\dot{\Omega} - \dot{\theta}) \simeq 0 \tag{2.34}$$

where α and β are two mutually prime integers. The physical interpretation of equation (2.34) is that $\beta : \alpha$ resonance occurs if a satellite performs β nodal

revolutions for α rotations of the Earth, relative to the precessing orbital plane. The resonance variable, Φ, can thus be taken as

$$\Phi_{\alpha\beta} = \alpha(\omega + M) + \beta(\Omega - \theta) \tag{2.35}$$

and equation (2.28) becomes

$$\psi_{\ell mpq} = \gamma\Phi_{\alpha\beta} - q\omega$$

where ℓ, m, p and q are subject to the inequalities $2 \le \ell \le \infty$, $1 \le m \le \ell$ and $0 \le p \le \ell$; and the equations linking ℓ, m, p and q with α, β and γ are

$$\ell - 2p + q = \alpha\gamma, \quad m = \beta\gamma \quad \text{and} \quad \gamma = 1, 2 \ldots . \tag{2.36}$$

We introduce another parameter, k, given by $k = \alpha\gamma - q$, which is used throughout resonance theory. Purely for notational convenience in subsequent chapters pertaining to resonance, we define

$$\phi^{A}_{\ell m} = \varphi^{A}_{\ell m,\frac{1}{2}(\ell-\alpha\gamma),0} = \begin{bmatrix} \bar{C}_{\ell m} \\ -\bar{S}_{\ell m} \end{bmatrix}_{\ell-m\ \text{odd}}^{\ell-m\ \text{even}} \sin\gamma\Phi_{\alpha\beta} - \begin{bmatrix} \bar{S}_{\ell m} \\ \bar{C}_{\ell m} \end{bmatrix}_{\ell-m\ \text{odd}}^{\ell-m\ \text{even}} \cos\gamma\Phi_{\alpha\beta}$$

$$\phi^{B}_{\ell m} = \varphi^{B}_{\ell m,\frac{1}{2}(\ell-\alpha\gamma),0} = \begin{bmatrix} \bar{C}_{\ell m} \\ -\bar{S}_{\ell m} \end{bmatrix}_{\ell-m\ \text{odd}}^{\ell-m\ \text{even}} \cos\gamma\Phi_{\alpha\beta} + \begin{bmatrix} \bar{S}_{\ell m} \\ \bar{C}_{\ell m} \end{bmatrix}_{\ell-m\ \text{odd}}^{\ell-m\ \text{even}} \sin\gamma\Phi_{\alpha\beta} \ . \tag{2.37}$$

For a satellite experiencing $\beta : \alpha$ resonance, the rate of change of inclination i, produced by a relevant pair of coefficients, $\bar{C}_{\ell m}$ and $\bar{S}_{\ell m}$, may be written (King–Hele et al, 1979),

$$\frac{di}{dt} = \frac{n(1-e^2)^{-1/2}}{\sin i}\left(\frac{a_e}{a}\right)^{\ell} \bar{F}_{\ell mp}(i)\, G_{\ell pq}(e)\,(k\cos i - m)\,\Re\left[j^{\ell-m+1}\left(\bar{C}_{\ell m} - j\bar{S}_{\ell m}\right)\exp\left[j(\gamma\,\Phi - q\,\omega)\right]\right] \tag{2.38}$$

where $\Re$ denotes the "real part of", $j = \sqrt{-1}$ and $\bar{F}_{\ell mp}(i)$ is Allan's normalized inclination function (Allan, 1973), written as

$$F_{\ell mp}(i) = j^{\ell-m}\,\frac{(\ell+m)!}{2^{\ell}\,p!\,(\ell-p)!}\sum_{k}(-)^k \binom{2\ell-2p}{k}\binom{2p}{\ell-m-k} * c^{3\ell-m-2p-2k}\; s^{m-\ell+2p+2k}$$

where $c = \cos i/2$, $s = \sin i/2$, and the summation is over all permissible values of k, i.e. from $k = \max(0,\ \ell-m-2p)$ to $k = \min(\ell-m,\ 2\ell-2p)$.

This expression along with the *real* and *imaginary* notation in $\frac{di}{dt}$ is preferred here because historically it is this notation that has been consistently used in all previous work pertaining to analysis of orbital resonances. To avoid confusion, this notation will be used in chapter 3 only and nowhere else. Allan's inclination function differs from Kaula's by a factor of $(-j)$ for odd $\ell-m$.

By similar analysis, the rate of change of eccentricity, e, caused by the (ℓ, m) harmonic near $\beta : \alpha$ resonance can be written (Gooding et al, 1989) as

$$\frac{de}{dt} = n(1-e^2)^{1/2}\left(\frac{a_e}{a}\right)^{\ell}\bar{F}_{\ell mp}(i)\,G_{\ell pq}(e)\left\{\frac{(k+q)(1-e^2)^{1/2}-k}{e}\right\} * \Re\left[j^{\ell-m+1}\left(\bar{C}_{\ell m} - j\bar{S}_{\ell m}\right)\exp\left[j(\gamma\,\Phi - q\,\omega)\right]\right] \tag{2.39}$$

whilst the rate of change of the mean motion n is given by

$$\frac{dn}{dt} = -3n^2 \alpha\gamma \left(\frac{a_e}{a}\right)^{\ell} \bar{F}_{\ell mp}(i)\, G_{\ell pq}(e)\, \Re\left[j^{\ell-m+1} \left(\bar{C}_{\ell m} - j\bar{S}_{\ell m}\right) \exp\left[j(\gamma\,\Phi - q\,\omega)\right]\right] . \tag{2.40}$$

§2.2 ATMOSPHERIC DRAG

The chief perturbations of the atmosphere on a satellite orbit are secular changes experienced by the semi–major axis and the eccentricity, with smaller effects on the inclination caused by atmospheric rotation. On examining the changes in the semi–major axis and eccentricity it can be shown (King–Hele, 1987) that

$$\frac{da}{dE} = -a^2\, \rho\delta \frac{(1 + e\cos E)^{3/2}}{(1 - e\cos E)^{1/2}} \tag{2.41}$$

and

$$\frac{de}{dE} = -a\,\rho\delta \left(\frac{1 + e\cos E}{1 - e\cos E}\right)^{1/2} \left(1 - e^2\right)\cos E \tag{2.42}$$

where ρ is atmospheric density, E is the eccentric anomaly and δ is a scaling coefficient incorporating the drag coefficient C_D, the surface to mass ratio S/M and the effect of atmospheric rotation, F, given by

$$\delta = \frac{F\,S\,C_D}{M} . \tag{2.43}$$

The air density at a particular height fluctuates in accordance with solar activity and geomagnetic activity and follows a day–to–night variation which is particularly significant for heights above 250km. In addition, the density varies with latitude and season. The upper atmosphere is heated predominantly by *extreme ultraviolet radiation* or EUV. This radiation has a short–periodic and a long–periodic variation. The short–periodic variation of 27 days is commensurate with the rotation period of the sun, whilst the long–period variation, of approximately 11 years, is a result of sunspot activity. A common measure of EUV is the 10.7cm solar flux, denoted $F_{10.7}$, (which has units of

10^{-22} Wm^{-2} Hz^{-1}). This index is taken daily and yields the night–time minimum temperature of the upper atmosphere through the empirical model of Jacchia (CIRA, 1972), namely

$$T_c = 379 + 3.24\,\bar{F}_{10.7} + 1.3\left(F_{10.7} - \bar{F}_{10.7}\right) \text{ K} \qquad (2.44)$$

where $\bar{F}_{10.7}$ is the mean value of $F_{10.7}$ over four solar rotations (108 days) centred on the day in question.

The average daily temperature, $T_{(av)}$, can be obtained approximately from T_c by multiplying the latter by the factor 1.15, (CIRA, 1972). Although this may only be an estimate, this direct relationship between T_c and $T_{(av)}$ is found to be good for the whole range of heights.

Atmospheric density varies with temperature and it is therefore important to be aware of the extent of both short–term and long–term fluctuations in the average daily temperature. Air–density can be evaluated, for fixed heights, from the average daily temperature by means of tables, such as CIRA (COSPAR International Reference Atmosphere). An example of this variation with temperature, for a height of 840km, is given in Fig. 2.3.

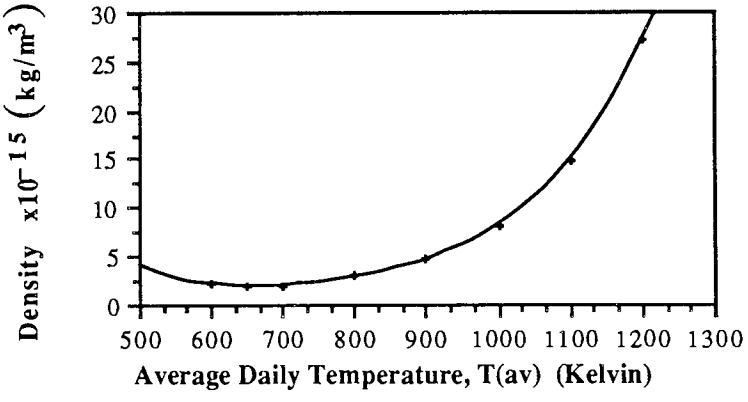

Figure 2.3 Variation of density with temperature at perigee height of 840km.

In developing a density model appropriate for orbital theory, we cannot account for all the irregularities in solar activity. The aim of any model, therefore, is to provide a smooth curve for the theoretical density changes, giving rise to mean elements and their rates of change, upon which will be superimposed small, irregular oscillations. These fluctuations will not affect the equations which are independent of time.

From knowledge of the atmosphere, the density can be assumed to exhibit an exponential decrease with height y (King–Hele, 1987),

$$\rho \alpha \exp\left[-y/H\right]$$

where H is a scalar (called the *density scale height*). The value of H can be obtained from tables such as those given by CIRA (1972). Thus the atmosphere may initially be taken to be spherically symmetric with an exponential variation of density with height. This may be improved by considering the atmosphere to be oblate, allowing density scale height to vary with altitude and incorporating day–to–night variation for heights over 250km. For our purposes, however, a simple model will suffice.

By this formalism air density may be written (Cook and King–Hele, 1965)

$$\rho = \rho_0 \exp\left[-\frac{r - r_0}{H}\right] \tag{2.45}$$

where ρ_0 is the density at distance r_0 from the Earth's centre. r_0 is usually taken to be the initial perigee distance, $a_0(1 - e_0)$.

Upon utilizing the relationship

$$r = a(1 - e\cos E)$$

equation (2.45) becomes

$$\rho = \rho_0 \exp\left(\frac{a_0 - a}{H} - \frac{a_0\, e}{H} + \frac{a\, e}{H}\cos E\right). \tag{2.46}$$

The changes in a and e during one revolution, Δa and Δe, say, are obtained by integrating (2.41) and (2.42) from $E = 0$ to $E = 2\pi$. Substitution of (2.46) into these equations yields

$$\Delta a = -a^2 \rho_0 \delta \exp\left[\beta(a_0 - a) - z\right] \int_0^{2\pi} \frac{(1 + e\cos E)^{3/2}}{(1 - e\cos E)^{1/2}} \exp[z\cos E]\, dE$$

and

$$\Delta e = -a \rho_0 \delta \exp\left[\beta(a_0 - a) - z\right](1 - e^2) \int_0^{2\pi} \left(\frac{1 + e\cos E}{1 - e\cos E}\right)^{1/2} \exp[z\cos E]\cos E\, dE$$

where $\beta = 1/H$ and $z = a_0 e/H$ is treated as a constant.

Expanding the integrands as a power series in e, we have to O(e)

$$\Delta a = -a^2 \rho_0 \delta \exp\left[\beta(a_0 - a) - z\right] \int_0^{2\pi} \exp[z\cos E]\,\{1 + 2e\cos E\}\, dE \tag{2.47}$$

and

$$\Delta e = -a \rho_0 \delta \exp\left[\beta(a_0 - a) - z\right] \int_0^{2\pi} \exp[z\cos E]\,\{1 + e\cos E\}\cos E\, dE. \tag{2.48}$$

Using the integral representation of the Bessel function of the first kind and imaginary argument of order n, $I_n(z)$, given by

$$I_n(z) = \frac{1}{2\pi} \int_0^{2\pi} \exp\left[z\cos\theta\right] \cos n\theta\, d\theta$$

the terms in (2.47) and (2.48) may be integrated individually, yielding

$$\Delta a = -2\pi a^2 \rho_0 \delta \exp\left[\beta(a_0-a)-z\right]\left\{I_0(z) + 2e\, I_1(z)\right\} \tag{2.49}$$

and

$$\Delta e = -2\pi a \rho_0 \delta \exp\left[\beta(a_0-a)-z\right]\left\{I_1(z) + \frac{e}{2}\left[I_0(z) + I_2(z)\right]\right\}. \tag{2.50}$$

Using the recurrence relationship (King–Hele, 1987)

$$I_{n-1}(z) + I_{n+1}(z) = 2I'_n(z)$$

where $I'_n(z)$ denotes $\frac{dI_n}{dz}$, and the infinite expansion of $I_n(z)$, namely

$$I_n(z) = \sum_{m=0}^{\infty} \frac{(z/2)^{n+2m}}{m!(n+m)!},$$

equations (2.49) and (2.50) reduce to

$$\Delta a = -2\, a^2 \rho_0 \delta\pi\ (1 + 2ze) \exp\left[\beta(a_0-a)-z\right],$$

and

$$\Delta e = -a \rho_0 \delta\pi\ (z + e) \exp\left[\beta(a_0-a)-z\right],$$

for small z and e. Simplifying further by taking 'a' to be constant and putting $a = a_0$, we have

$$\Delta a = -2\, a^2 \rho_0 \delta\pi\ (1 + 2ze) \exp[-z], \tag{2.51}$$

and

$$\Delta e = -a\,\rho_0 \delta\pi\,(z + e)\exp[-z]\,. \tag{2.52}$$

Atmospheric rotation

As previously mentioned, the effect of atmospheric rotation on a satellite orbit is small, but still important. The force of the rotating atmosphere acts normal to the plane of orbit, consequently perturbing the inclination. The rate of change of the inclination can be written (King–Hele, 1987) as

$$\frac{di}{dt} = \frac{-\rho\, v r^2\, w\delta}{2\sqrt{\mu\, Fa(1 - e^2)}} \sin i \cos^2(\omega + \theta) \tag{2.53}$$

where v is the velocity of the satellite relative to the Earth's centre and w is the angular velocity of the atmosphere with respect to the Earth.

Rewriting (2.53) in terms of E and integrating from 0 to 2π, the change in the inclination over one revolution for small z and e is given by

$$\Delta i = -\left(\frac{a}{\mu F}\right)^{1/2} \frac{\pi a^2\, w\delta}{2}\, \rho_0 \exp[-z] \sin i + 0(e)\,. \tag{2.54}$$

§2.3 SOLAR RADIATION PRESSURE (SRP)

The acceleration due to direct SRP, $\ddot{\underline{x}}_{SRP}$, is modelled by (Aksnes, 1976)

$$\ddot{\underline{x}}_{SRP} = -\nu\, C_R\, S/m\, P \frac{(AU)^2}{|\underline{x} - \underline{x}_{SUN}|}\, \hat{\mathbf{x}}_S \tag{2.55}$$

where ν is the eclipse factor (which equals zero if the satellite is in the Earth's shadow, one if it is in total sunlight with a smoothing function to account for the transition between the two); C_R is the solar reflectivity coefficient to account for the reflectivity characteristics of the spacecraft (usually between 1.0 and 2.0); S/m is the surface–to–mass ratio; P the force per unit area exerted at the Earth by the sun when its geocentric

distance is one astronomical unit (AU) in km; $\underline{x}$ is the position of the satellite while $\underline{x}_{SUN}$ is the position of the sun and $\hat{\mathbf{x}}_S$ is a unit vector from the satellite to the sun (all in the geocentric reference frame, J2000).

When converted to Keplerian elements, equation (2.55) yields the perturbation on the semi–major axis, (Asknes, 1976)

$$\delta a = 2a^3 F \left| S \cos E + T\left(1 - e^2\right)^{1/2} \sin E \right|_{E_1}^{E_2} \qquad (2.56)$$

for a satellite that moves from eccentricity anomaly E_1 to E_2 $\left(\text{add } 2\pi \text{ to } E_2 \text{ if } E_2 < E_1\right)$, where S and T are direction cosines (components of a unit vector) of the force along the satellite radius r and perpendicular to r in the orbital plane, respectively; F is constant where μF, $\left(\mu = n^2a^3\right)$, is the force per unit mass of the satellite.

Equation (2.56) does not contain terms in E alone, but only in sin E and cos E. If the satellite remains in sunlight there would be no perturbations in a.

The effects of SRP on the semi–major axis (hence the mean motion) are purely the consequence of the transition from sunlight to shadow and shadow to sunlight. These perturbations are comparatively small since there is no secular change due to SRP which compounds over time.

§2.4 LUNI–SOLAR AND OTHER THIRD BODY ATTRACTION

Third body attraction can be calculated for the Sun, Moon, Venus, Mars, Jupiter and Saturn. Referring to Figure 2.4 the accelerating force, $\ddot{\underline{x}}_{TB}$, at the point $\underline{x}$ is given by (Brouwer and Clemence, 1961)

$$\ddot{\underline{x}}_{TB} = \sum_j G M_j \left\{ \frac{\underline{x}_j - \underline{x}}{\Delta_j^3} - \frac{\underline{x}_j}{r_j^3} \right\}$$

where $r = |\underline{x}|$, $r_j = |\underline{x}_j|$ and $\Delta_j = |\underline{x} - \underline{x}_j|$. M_j represents the mass of the j^{th} body with the summation being taken over all those bodies just mentioned.

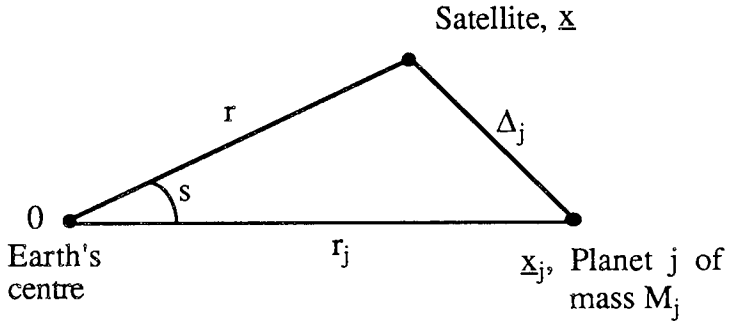

Figure 2.4. Third body attraction.

CHAPTER III

DETERMINATION OF ORBITS AND ANALYSIS OF ORBITAL RESONANCES FOR THE USSR SATELLITE 1984–106A

This chapter details the orbital analysis of the U.S.S.R. satellite, Cosmos 1603 (1984–106A), which prompted the theoretical discussion and developments that follow in subsequent chapters. COSMOS 1603 was launched on 28 September 1984 into an orbit of 51° inclination. The satellite was manoeuvred from a 51° to a 66° orbit and then to a 70° orbit, probably on the day of launch. In the 70° orbit, the perigee was near 851km and apogee near 857km, giving an orbital eccentricity near 0.002. The lifetime is estimated to be 300 years (RAE Table of Earth Satellites, King–Hele et al., 1981). The shape, size and weight are unknown.

§3.1 ORBITAL ANALYSIS

The orbit of Cosmos 1603 has been determined at 43 epochs between 4 January and 7 December 1987, utilizing 3033 observations. Approximately 85% of these were supplied by the U.S. Naval Research Laboratory, the remainder comprised of 257 visual observations (supplied by a volunteer network of observers, then coordinated by the Earth Satellite Research Unit at Aston University) and 183 Hewitt camera observations, of which 120 were from the Australian camera at Siding Springs (S) and 63 from the Royal Greenwich Observatory (R). The lack of observations from other sources necessitated the evaluation of orbital elements at five epochs solely from the U.S. Naval radar observations, despite the inherent risk of bias from the narrow latitudinal spread. A breakdown of the number and type of observations used on each of the 43 runs is given in Table 3.1.

The most accurate group of observations are those from the Hewitt cameras. These observations which were available on 23 transits (6(R), 14(S) and 3 from both), have an accuracy of 2 arc secs. in position and 1ms in time. The second most accurate group

consists of the U.S. Naval observations. Some 2593 were available with an accuracy of about 2 arc mins. in right ascension and declination and 1km range. The remaining 257 visual observations usually had accuracies between 1 and 4 arc mins. in angular measurements.

Run	Hewitt Camera (R)	Hewitt Camera (S)	U.S. Radar	Visual	Total
1		12	53		65
2		10	58		68
3	8	4	39	8	59
4	8	8	36	39	91
5			76	2	78
6		4	63	6	73
7		4	46		50
8			58		58
9			63	2	65
10		8	65	5	78
11	4	4	74	2	84
12			71	19	90
13		4	84	6	94
14		4	74		78
15			69	11	80
16	8		48	21	77
17	2		81	3	86
18			90	2	92
19		4	65		69
20		14	66		80
21			62		62
22			76		76
23	8		64		72
24			69		69
25			60		60
26		8	70		78
27		4	51	6	61
28		4	51	2	57
29	8		50	26	84
30	9		63	22	94
31	8		42	19	69
32			46	22	68
33		12	57	1	58
34		12	56	2	70
35			50		62
36			65	2	67
37			52	5	57
38			49	3	52
39			56	3	59
40			47	9	56
41			53	3	56
42			66	1	67
43			59	5	64
	63	120	2593	257	3033

Table 3.1 Sources of the observations used in each run.

The 43 sets of orbital elements determined by the RAE orbit refinement program, PROP 6 (Gooding and Taylor, 1968 and Gooding, 1974), are listed in Table 3.2 with their standard deviations. Also in Table 3.2 is the value of ε given by the final run, where ε^2 is the sum of the squares of the weighted residuals divided by the number of degrees of freedom.

The mean anomaly, M, is represented in the PROP 6 model by the polynomial

$$M = \sum_{i=0}^{5} M_i \, t^i$$

where the actual number of coefficients to be used is a parameter of the program. The time, t, is measured from the epoch, which corresponds to 0hrs on the day indicated. (M_1 is the mean motion.) In detail, 41 of the orbits required three coefficients in the expansion of M whilst 2 required four coefficients.

The average value of the S.D. (Standard Deviation) of the inclination, i, is 0.0007°. The S.D.'s of the eccentricity, e, vary between 2×10^{-6} and 16×10^{-6} giving accuracy of perigee height of 116m at worst. The right ascension of the ascending node, Ω, has an average S.D. of 0.00006°. For the argument of perigee, ω, and the mean anomaly at epoch, M_0, the S.D.'s are comparable, being of the order 0.1° mostly, but increasing occasionally to as much as 0.9°. The mean motion, M_1, is everywhere accurate to $2 \times 10^{-5}\%$.

No.	MJD	Date (1987)	a	e	i	Ω	ω	M_0	M_1	M_2	M_3	ε
1	46799 H	4 Jan	7231.7897 1	0.001520 4	71.01527 88	313.3597 5	138.143 93	319.052 93	5083.1282 1	–0.00012 6		0.54
2	46807 H	12 Jan	7231.7940 2	0.001702 4	71.01843 55	296.6573 6	130.121 70	299.961 70	5083.1237 2	–0.00038 5		0.46
3	46819 H	24 Jan	7231.8029 3	0.001909 6	71.01602 100	271.6083 7	118.471 206	90.361 206	5083.1113 3	–0.00077 1		0.41
4	46826 H	31 Jan	7231.8159 4	0.001953 4	71.01372 24	256.9870 3	111.563 126	28.917 127	5083.1025 4	–0.00597 32		1.00
5	46832	6 Feb	7231.8249 2	0.002071 5	71.00923 68	244.4568 5	105.392 311	284.581 310	5083.0907 2	–0.00098 13		0.35
6	46840 H	14 Feb	7231.8386 2	0.002123 5	71.00752 50	227.7494 6	98.554 261	263.986 260	5083.0761 3	–0.00073 7		0.41
7	46848 H	22 Feb	7231.8549 3	0.002166 4	71.00812 46	211.0413 4	92.071 84	242.891 4	5083.0590 3	–0.00115 10		0.25
8	46864	10 Mar	7231.8863 2	0.002162 5	71.01114 75	177.6281 6	77.399 268	202.019 267	5083.0261 3	–0.00104 10		0.33
9	46873	19 Mar	7231.9018 2	0.002103 6	71.00975 85	158.8341 7	68.793 273	224.162 273	5083.0096 3	–0.00062 8		0.38
10	46881 H	27 Mar	7231.9116 5	0.001988 8	71.00546 12	142.1255 91	61.474 393	203.409 392	5082.9971 5	–0.00013 16		0.60

No.	MJD	Date (1987)	a	e	i	Ω	ω	M_0	M_1	M_2	M_3	ε
11	46889 H	4 Apr	7231.9259 6	0.001874 4	71.00474 12	125.4118 1	52.746 179	183.979 173	5082.9839 6	–0.00162 18	0.000416 85	0.48
12	46895	10 Apr	7231.9300 5	0.001830 10	71.00106 85	112.8806 7	46.248 296	79.291 295	5082.9794 5	–0.00055 22		0.43
13	46903 H	18 Apr	7231.9360 1	0.001729 8	70.99992 77	96.1666 2	35.881 166	61.367 166	5082.9731 2	–0.00052 6		0.41
14	46912 H	27 Apr	7231.9401 2	0.001552 5	71.00458 41	77.3651 5	25.246 142	85.126 142	5082.9690 2	–0.00027 7		0.33
15	46919	4 May	7231.9417 3	0.001412 12	71.00363 95	62.7439 8	15.925 237	24.629 237	5082.9672 3	0.00041 20		0.41
16	46925 H	10 May	7231.9395 7	0.001279 16	71.00613 125	50.2129 12	6.380 376	282.908 376	5082.9717 8	0.00088 46		0.60
17	46931 H	16 May	7231.9362 3	0.001191 14	71.00928 86	37.6799 11	356.690 367	181.342 368	5082.9733 3	0.00117 13		0.65
18	46939	24 May	7231.9296 3	0.001059 15	71.00549 129	20.9657 10	343.476 399	166.272 399	5082.9801 3	0.00061 5		0.60
19	46946 H	31 May	7231.9205 9	0.000921 11	71.00701 103	6.3468 9	328.436 580	111.621 580	5082.9897 9	0.00124 21	0.000352 107	0.60
20	46954 H	8 Jun	7231.9042 2	0.000867 2	71.00765 25	349.6333 2	303.467 196	108.484 196	5083.0069 2	0.00117 12		0.75

No.	MJD	Date (1987)	a	e	i	Ω	ω	M_0	M_1	M_2	M_3	ε
21	46963	17 Jun	7231.8841	0.000751	71.00504	330.8330	280.255	145.228	5083.0280	0.00124		0.34
			2	5	90	7	757	758	2	9		
22	46972	26 Jun	7231.8619	0.000792	71.00894	312.0328	251.332	187.887	5083.0516	0.00129		0.30
			1	4	69	5	552	552	2	54		
23	46981	5 Jul	7231.8391	0.000921	71.01343	293.2377	229.121	224.054	5083.0759	0.00030		0.40
	H		2	2	37	5	451	451	2	11		
24	46988	12 Jul	7231.8224	0.001034	71.01204	278.6189	212.023	172.144	5083.0934	0.00135		0.26
			2	7	61	5	290	290	3	11		
25	46995	19 Jul	7231.8070	0.001192	71.01141	264.0010	198.628	116.663	5083.1097	0.00081		0.29
			2	8	71	5	232	232	2	10		
26	47003	27 Jul	7231.7909	0.001326	71.01218	247.2953	187.581	100.550	5083.1267	0.00036		0.51
	H		1	4	77	6	182	182	1	11		
27	47011	4 Aug	7231.7808	0.001524	71.00862	230.5895	173.716	87.361	5083.1387	0.00081		0.20
	H		2	5	58	4	126	126	2	8		
28	47022	15 Aug	7231.7671	0.001745	71.00932	207.6173	158.457	200.557	5083.1494	0.00030		0.18
	H		4	5	83	6	132	132	4	15		
29	47031	24 Aug	7231.7681	0.001928	71.01220	188.8239	147.063	226.682	5083.1514	–0.00025		0.39
	H		2	10	90	7	233	233	2	10		
30	47039	1 Sep	7231.7687	0.002063	71.01676	172.0182	137.606	209.230	5083.1503	–0.00024		0.63
	H		4	9	58	11	403	402	4	13		

No.	MJD	Date (1987)	a	e	i	Ω	ω	M_0	M_1	M_2	M_3	ε
31	47047 H	9 Sep	7231.7704 4	0.002193 7	71.01829 63	155.4187 10	129.460 397	190.458 396	5083.1487 4	–0.00041 19		0.73
32	47055	17 Sep	7231.7762 2	0.002364 5	71.01414 58	138.7152 5	119.768 153	173.204 152	5083.1423 2	–0.00055 8		0.25
33	47064 H	26 Sep	7231.7876 1	0.002484 4	71.00967 56	119.9224 4	109.804 143	197.787 142	5083.1343 1	–0.00051 5		0.22
34	47073 H	5 Oct	7231.7944 3	0.002508 2	71.00685 33	101.1256 5	101.786 182	220.336 183	5083.1221 3	–0.00085 7		0.62
35	47080	12 Oct	7231.8071 2	0.002569 5	71.01042 35	86.5031 2	94.888 135	158.446 135	5083.1095 2	–0.00057 13		0.56
36	47088	20 Oct	7231.8207 2	0.002651 4	71.00758 53	69.7953 5	86.273 200	139.761 199	5083.0950 2	–0.00094 11		0.27
37	47095	27 Oct	7231.8340 2	0.002647 4	71.01064 60	55.1764 5	79.682 192	77.376 191	5083.0811 2	–0.00103 10		0.31
38	47101	2 Nov	7231.8438 3	0.002627 5	71.01166 73	42.6475 6	73.685 248	332.749 247	5083.0708 3	–0.00102 20		0.32
39	47108	9 Nov	7231.8564 3	0.002568 6	71.01151 75	28.0287 6	66.519 209	270.769 208	5083.0576 3	–0.00092 16		0.35
40	47116	17 Nov	7231.8701 3	0.002459 9	71.01114 94	11.3222 9	59.368 286	250.224 286	5083.0435 3	–0.00108 11		0.40

No.	MJD	Date (1987)	a	e	i	Ω	ω	M_0	M_1	M_2	M_3	ε
41	47123	24 Nov	7231.8793	0.002379	71.00815	356.6988	50.404	189.863	5083.0332	–0.00082		0.30
			2	8	86	7	213	212	3	18		
42	47130	1 Dec	7231.8874	0.002274	71.00539	342.0749	42.054	128.821	5083.0246	–0.00060		0.34
			3	9	81	7	213	212	3	13		
43	47136	7 Dec	7231.8940	0.002188	71.00359	329.5390	34.637	25.286	5083.0175	–0.00069		0.36
			5	11	86	7	221	220	5	27		

MJD = modified Julian day number, a = semi–major axis (km), e = eccentricity, i = inclination(deg), Ω = right ascension of ascending node(deg), ω = argument of perigee (deg), M_0 = mean anomaly at epoch (deg), M_1 = mean motion (deg/day), M_2, M_3 = later coefficients in the polynomial for M, ε = measure of fit, H denotes Hewitt Camera observations within the orbit.

Table 3.2 The 43 sets of orbital elements with their standard deviations and the value of epsilon.

Bias may occur in orbits derived principally from U.S. Naval radar observations with just a few observations from other sources. An example of this is given by orbit 8. Here the fit is considered good, with epsilon as small as 0.33 whilst the S.D. of inclination is $0.75 \times 10^{-3}°$. This orbit was derived solely from U.S. Naval observations. In comparison, Orbit 4 which contained 16 Hewitt camera observations together with 39 visual observations, yielded a more realistic value of epsilon of 1.00, whilst the S.D. for inclination was only $0.24 \times 10^{-3}°$. This clearly indicates both the value of Hewitt camera observations in determining accurate elements and the extent that small epsilons may be deceptive for orbits determined mainly from U.S. Naval observations.

§3.2 14th ORDER RESONANCE FOR COSMOS 1603 (1984–106A)

The function $G_{\ell pq}(e)$ in equations (2.38), (2.39) and (2.40) are of order $\frac{1}{|q|!}\left(\frac{1}{2}\ell e\right)^{|q|}$ (Plummer, 1918) and thus for $e = 0.002$ it is sufficient to consider only $q = 0, \pm 1$ for all three equations. It is possible to estimate the order of magnitude of the theoretical rates of change by substituting mean values for the elements, maximum values for the inclination function and approximate values for the lumped harmonics. For the various values of γ and q, Table 3.3 illustrates the order of magnitude of terms in the equations for the theoretical changes in the inclination, mean motion and eccentricity.

	INCLINATION AND MEAN MOTION			ECCENTRICITY		
q \ γ	1	2	3	1	2	3
0	100%	2%	0.2%	0.01%	—	—
±1	1%	0.1%	—	(+1) 80% (–1) 100%	4%	0.1%

(–) indicates a value of less than $10^{-2}\%$

Table 3.3 The order of magnitude of terms in the equations for the theoretical changes in the inclination, mean motion and eccentricity at resonance, expressed as a percentage of the dominant terms.

The m–suffix of a relevant $\left(\bar{C}_{\ell m},\ \bar{S}_{\ell m}\right)$ pair is determined by the choice of γ. The values of ℓ to be taken must be such that $\ell \geq m$ and $\ell - k$ is even. Successive coefficients which arise, for a given γ and q, may be grouped into a lumped harmonic, written as

$$\bar{C}_m^{q,k} = \sum_{\ell} Q_\ell^{q,k}\, \bar{C}_{\ell m}\,,\quad \bar{S}_m^{q,k} = \sum_{\ell} Q_\ell^{q,k}\, \bar{S}_{\ell m}$$

where ℓ increases in steps of 2 from its minimum permissible value ℓ_0, and $Q_\ell^{q,k}$ are functions of inclination that can be taken as constant for a particular satellite, with $Q_\ell^{q,k} = 1$ when $\ell = \ell_0$.

Developing the resonance equation (2.38) from chapter 2, the theoretical changes in inclination of 14th order resonance as experienced by the satellite 1984–106A can be approximated by (Walker, 1979).

$$\begin{aligned}
\frac{di}{dt} = \frac{n}{\sin i}\left(\frac{a_e}{a}\right)^{14}\Bigg[& \frac{a_e}{a}(14 - \cos i)\,\bar{F}_{15,14,7}\left\{\bar{C}_{14}^{0,1}\cos\Phi + \bar{S}_{14}^{0,1}\sin\Phi\right\} \\
& + \frac{15e}{2}(14)\,\bar{F}_{14,14,7}\left\{\bar{C}_{14}^{1,0}\sin(\Phi - \omega) - \bar{S}_{14}^{1,0}\cos(\Phi - \omega)\right\} \\
& + \frac{11e}{2}(14 - 2\cos i)\,\bar{F}_{14,14,6}\left\{\bar{C}_{14}^{-1,2}\sin(\Phi + \omega) - \bar{S}_{14}^{-1,2}\cos(\Phi + \omega)\right\} \\
& + \left(\frac{a_e}{a}\right)^{14}(28 - 2\cos i)\,\bar{F}_{28,28,13}\left\{\bar{C}_{28}^{0,2}\sin 2\Phi - \bar{S}_{28}^{0,2}\cos 2\Phi\right\}\Bigg] \qquad (3.1)
\end{aligned}$$

In this equation $G_{\ell pq}(e)$ has been replaced by its expansion in powers of e (Gooding et al, 1989).

Similarly, from (2.39) and (2.40) the theoretical changes in the eccentricity and mean motion may be written

$$\frac{de}{dt} = n\left(\frac{a_e}{a}\right)^{14}\left[\frac{e}{2}\left(\frac{a_e}{a}\right)\bar{F}_{15,14,7}\left\{\bar{C}_{14}^{0,1}\cos\Phi + \bar{S}_{14}^{0,1}\sin\Phi\right\}\right.$$

$$-\frac{15}{2}\bar{F}_{14,14,7}\left\{\bar{C}_{14}^{1,0}\sin(\Phi-\omega) - \bar{S}_{14}^{1,0}\cos(\Phi-\omega)\right\}$$

$$+\frac{11}{2}\bar{F}_{14,14,6}\left\{\bar{C}_{14}^{-1,2}\sin(\Phi+\omega) - \bar{S}_{14}^{-1,2}\cos(\Phi+\omega)\right\}$$

$$-\left(\frac{a_e}{a}\right)^{15}16\,\bar{F}_{29,28,14}\left\{\bar{C}_{28}^{1,1}\cos(2\Phi-\omega) + \bar{S}_{28}^{1,1}\sin(2\Phi-\omega)\right\}$$

$$\left.+\left(\frac{a_e}{a}\right)^{15}12\bar{F}_{29,28,13}\left\{\bar{C}_{28}^{-1,3}\cos(2\Phi+\omega) + \bar{S}_{28}^{-1,3}\sin(2\Phi+\omega)\right\}\right] \quad (3.2)$$

and

$$\frac{dn}{dt} = 3n^2\left(\frac{a_e}{a}\right)^{14}\left[\frac{a_e}{a}\bar{F}_{15,14,7}\left\{\bar{C}_{14}^{0,1}\cos\Phi + \bar{S}_{14}^{0,1}\sin\Phi\right\}\right.$$

$$+\frac{15e}{2}\bar{F}_{14,14,7}\left\{\bar{C}_{14}^{1,0}\sin(\Phi-\omega) - \bar{S}_{14}^{1,0}\cos(\Phi-\omega)\right\}$$

$$+\frac{11e}{2}\bar{F}_{14,14,6}\left\{\bar{C}_{14}^{-1,2}\sin(\Phi+\omega) - \bar{S}_{14}^{-1,2}\cos(\Phi+\omega)\right\}$$

$$+2\left(\frac{a_e}{a}\right)^{14}\bar{F}_{28,28,13}\left\{\bar{C}_{28}^{0,2}\sin 2\Phi - \bar{S}_{28}^{0,2}\cos 2\Phi\right\}$$

$$+2\left(\frac{a_e}{a}\right)^{15}16e\,\bar{F}_{29,28,14}\left\{\bar{C}_{28}^{1,1}\cos(2\Phi-\omega) + \bar{S}_{28}^{1,1}\sin(2\Phi-\omega)\right\}$$

$$+2\left(\frac{a_e}{a}\right)^{15}12e\,\bar{F}_{29,28,13}\left\{\bar{C}_{28}^{-1,3}\cos(2\Phi+\omega) + \bar{S}_{28}^{-1,3}\sin(2\Phi+\omega)\right\}$$

$$\left.+3\left(\frac{a_e}{a}\right)^{29}12\bar{F}_{43,42,20}\left\{\bar{C}_{42}^{0,3}\cos 3\Phi + \bar{S}_{42}^{0,3}\sin 3\Phi\right\}\right]. \quad (3.3)$$

Since the mean motion is determined to within $2 \times 10^{-5}\%$ throughout, it is deemed possible to include the smaller resonance terms corresponding to $\gamma = 3$ and the two terms corresponding to $\gamma = 2,\ q = \pm 1$.

Since for 1984–106A $\dot{\Phi} \approx \dot{\omega}$, we will see later that there are terms in equations (3.1) to (3.3) which have almost identical frequencies. These are terms with identical k–values, $(k = \alpha\gamma - q)$, i.e. $(\gamma, q) = (1, -1)$ and $(2, 0)$ in equations (3.1) and (3.3);

$(\gamma, q) = (1, 0)$ and $(2, 1)$ in equations (3.2) and (3.3); and $(\gamma, q) = (2, -1)$ and $(3, 0)$ in equation (3.3) for feasible γ, i.e. $\gamma = 1, 2, 3 \ldots$. Consequently, the weighted least squares method will yield high correlations between the derived coefficients corresponding to identical values of k. It is therefore necessary to solve only for the dominant terms and the resulting parameters will represent the contribution of all terms with the corresponding value of k. In equation (3.2), using the results of Table 3.3, the $(\gamma, q) = (1, 0)$ term is clearly negligible compared to the $(2, -1)$ terms and therefore the parameters obtained corresponding to $(\gamma, q) = (2, -1)$ will not be corrupted by any unmodelled resonance terms.

The observed values of the inclination were cleared of the $J_{2,2}$ sectorial harmonic by PROP 6. The program PROD (Cook, 1973), based on numerical integration with a step length of 1 day, was used to remove the effects of the zonal harmonics and luni–solar perturbations for both inclination and eccentricity. The corrected elements then exhibited variation due to air–drag, resonance and secondary perturbations (e.g. solar radiation pressure, tides) with the intention to apply the RAE program THROE (Gooding, 1971) to determine the lumped harmonic values.

§3.3 SECONDARY RESONANCE

The satellite 1984 – 106A exhibits the unusual feature of being in almost exact $\Phi - \omega$ resonance for an extended time period. Since both $\dot{\Phi}$ and $\dot{\omega}$ are approximately equal at around –1.5°/day, the Φ–ω terms in the expansions for the rates of change in the orbital elements correspond to a quasi–secular variation in each of the elements. In the case of inclination and mean motion this quasi–secular resonance term is of order 'e' smaller than the dominant sinusoidal term, whereas for eccentricity the quasi–secular resonance term is dominant.

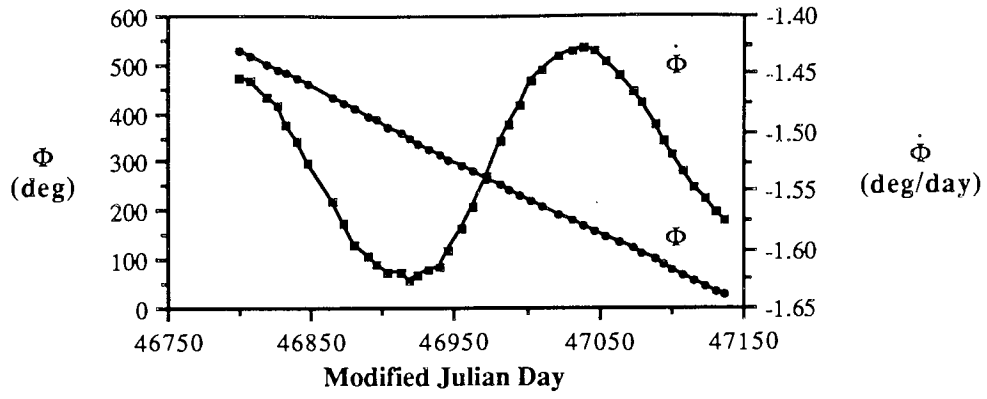

Figure 3.1 Variation of Φ and $\dot{\Phi}$.

Figure 3.1 illustrates the changes in both Φ and $\dot{\Phi}$ over the period of analysis. Φ decreases very nearly linearly with only a small sinusoidal variation superimposed due to the oscillation of $\dot{\Phi}$. From Figure 3.1 it is possible to estimate the overall increase in $\dot{\Phi}$ to be around 0.04°/day over the 338 days, which corresponds to the same overall increase observed in the mean–motion. This increase in both $\dot{\Phi}$ and the observed value for the mean motion is anticipated to be the result of the combined effect of both air–drag and the quasi–secular resonance perturbation yielded by $\dot{\Phi} - \dot{\omega} \approx 0$.

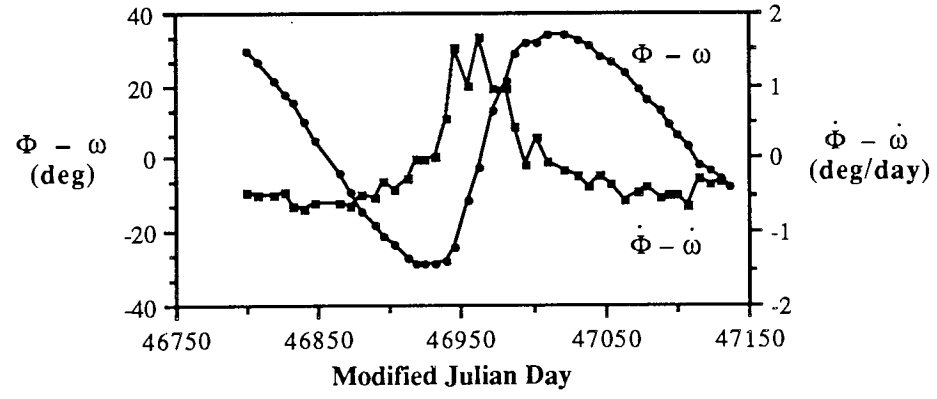

Figure 3.2 Variaton of $\Phi - \omega$ and $\dot{\Phi} - \dot{\omega}$.

Figure 3.2 illustrates the change in the secondary resonance parameter $\Phi - \omega$ and $\dot{\Phi} - \dot{\omega}$ as calculated using the elements of Table 3.2. Of particular interest is the

libration of $\Phi - \omega$ between ±35°. This is related to the near constancy of the mean motion in Table 3.2, a result of low drag effects due to the perigee height being near 840km and the low solar activity in 1987. Consequently in considering the effect of both drag and the quasi–secular resonance perturbation in the eccentricity and mean motion, air–drag can be strongly opposed by the resonance to such an extent that the resonance is dominant. For the period of the study the satellite is effectively trapped in resonance with respect to $\Phi - \omega$. Hypothetically, the satellite would remain trapped in this fashion until drag effects increase either with atmospheric density variation or with the decrease of perigee height. As seen in Figure 3.3 the perigee height, $h_p = a(1 - e) - a_e$, experiences an oscillatory motion due to the zonal harmonics (Cook, 1966) with a quasi–secular decrease due to the effect of near exact commensurability of $\Phi - \omega$ on e. In reality however, this phenomenon will be short–lived, as atmospheric density increased due to the rise in solar activity over the subsequent period. The mean monthly solar activity of 10.7cm wavelength, $\bar{F}_{10.7}$, increased from $\bar{F}_{10.7} \approx 85$ in 1987 to over 200 in 1989–1991, following the near 11–year solar cycle. Consequently, atmospheric density increases 15–fold and the satellite 1984–106A was forced through resonance in 1989.

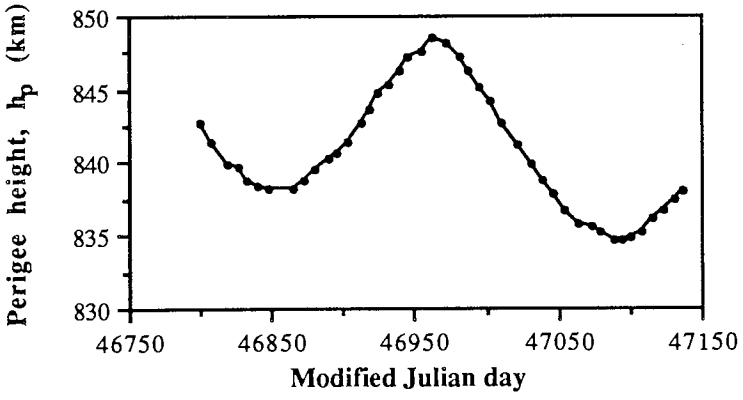

Figure 3.3 Variation in perigee height, $h_p = a(1 - e) - a_e$.

The very low drag-effect experienced by 1984–106A poses a couple of problems not normally encountered. For inclination, the program THROE models the effects of

atmospheric rotation, based on the values of the rate of change of mean motion, $2M_2$, with the assumption that the effect of air–drag is dominant. From equation (2.54) in chapter 2, the change in inclination over one revolution (for small z and e), is given by

$$\Delta i_{ROT} = -\left(\frac{a}{\mu F}\right)^{1/2} \frac{\pi a^2 w}{2} \rho_0 \frac{S}{M} C_D \exp[-z] \sin i \quad + O(e)$$

Therefore over the 338 day period of analysis, estimating ρ_0 as 4×10^{-15} Kg/m^3 (CIRA, 1972), F as 0.96, S/m as 0.01 m^2/kg, C_D as 2.2 and H as 272 km, w to be 6.3 rads/day and taking $\mu \approx 4 \times 10^8$ Nkm^2/kg, the total change in inclination due to atmospheric rotation is,

$$\Delta i_{ROT}^{TOTAL} \simeq 3 \times 10^{-6} \text{ degrees}$$

Thus the effect of air–drag is small and the values of i are dominated by the sinusoidal variation due to resonance, as seen in Figure 3.4. The dominant term seen here corresponds to $(\gamma, q) = (1, 0)$. Thus, it was necessary to run THROE (for inclination) having suppressed the facility within the program to model atmospheric rotation.

Secondly, the program THROE calculates the effect of air–drag on the change in eccentricity using M_2 with the same assumption as before, that these values change primarily as a consequence of air–drag and not resonance. Since this assumption is erroneous, it is necessary to suppress this correction to the eccentricity values. This was achieved by setting the M_2 values to zero. To justify this procedure, it is necessary to quantify the quasi–secular decrease in eccentricity due to air drag. The effects of air drag were outlined in section 2.2 and the change in eccentricity, over one revolution, may be written

$$\Delta e_{DRAG} = - a \rho_0 F \frac{S}{m} C_D \pi (z + e) \exp [-z]$$

Thus, over 338 days of the analysis, estimating as before the values for ρ_0, F, S/m, C_D and H, we obtain for the total change in e,

$$\Delta e_{DRAG}^{TOTAL} \cong - 5 \times 10^{-7} .$$

This estimated change in eccentricity is clearly negligible relative to the change observed in Figure 3.5 of approximately 7×10^{-4}. Thus it is reasonable to assume that the effects of air–drag on eccentricity are not likely to contaminate the derived lumped harmonic values corresponding to the quasi–secular rate of change.

§3.4 ANALYSIS OF THE ORBITAL INCLINATION

The Hewitt camera orbits with S.D.'s (for inclination) below 5×10^{-4}° were downgraded to an S.D. near 5×10^{-4}° as the original values were unrealistic, because several forces were not modelled in PROP, e.g. tides, solar radiation pressure. Values of the lumped harmonic coefficients derived for all four sets of parameters (γ, q), i.e. equation (3.1), were only well–determined for $(\gamma, q) = (1, 0)$. Similarly, when restricting the analysis to the first two sets of parameters, i.e. $(\gamma, q) = (1, 0)$ and $(2, 0)$, the second pair of lumped harmonic values were still undetermined. Thus it was considered necessary to reduce the number of parameters to be determined to those corresponding to $(\gamma, q) = (1, 0)$ and the initial value only. Further, four data points fitted badly, namely three Hewitt camera orbits and one orbit derived solely from U.S. Naval observations. It was anticipated that some disagreement would exist between the Hewitt camera orbits and the U.S. Naval orbits, resulting from the inherent bias of the latter. Therefore, these four orbits were downgraded, with the S.D.'s attached to their inclination values increased by a factor of two. These orbits were numbered 2, 26, 30 and 36.

As explained previously, the effect of atmospheric rotation on the rate of change of the inclination is small, but was not in any way accounted for. However, since this change is secular whilst the resonance term is sinusoidal, it is unlikely that the derived lumped harmonic values will be contaminated by these neglected effects. The program THROE was run, including the modelling of atmospheric rotation as a comparison, and no change in the final lumped harmonic values was observed.

Numerical values of the lumped harmonic coefficients for $(\gamma,\ q) = (1,\ 0)$, as given by the analysis of the change in inclination, were

$$10^9\ \bar{S}_{14}^{0,1} = -\ 20.8 \pm 1.3 \quad ; \quad 10^9\ \bar{C}_{14}^{0,1} = 5.1 \pm 1.2$$

with $\varepsilon = 1.62$.

Interpretation of the $(\gamma,\ q) = (2,\ 0)$ coefficients does not arise as these coefficients were undetermined.

Values of the inclination cleared of the effects of the zonal harmonics and luni–solar gravitational attraction are plotted in Figure 3.4 together with the theoretical fit of the resonance perturbations.

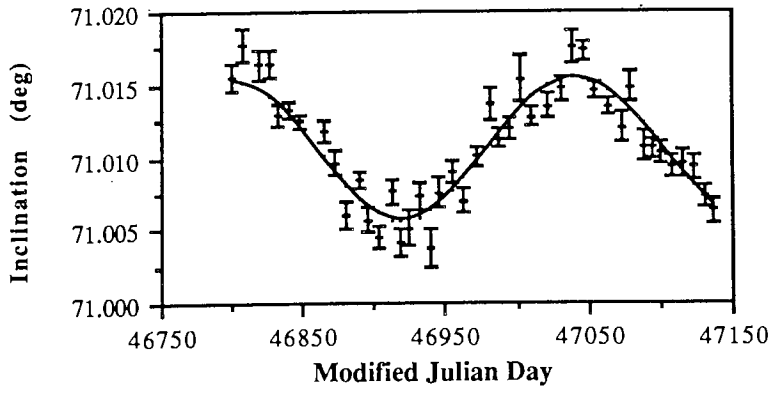

Figure 3.4 Values of the inclination cleared of other perturbations with error bars and theoretical fit.

§3.5 ANALYSIS OF THE ECCENTRICITY

Examination of Table 3.3 reveals that the contribution of the first term in equation (3.2) is negligible compared to the $(\gamma, q) = (2, 1)$ term. It was decided, therefore, to neglect the $(1, 0)$ term completely. Initial trials to determine all four remaining sets of parameters for (γ, q) yielded high correlations between several of the values. As a consequence, it was necessary to reduce the number of parameters determined by eliminating the (γ, q) terms corresponding to $(2, 1)$ and $(2, -1)$. This produced a good fit with $\varepsilon = 1.34$. A further two runs were investigated. In each case only one of the the two pairs of coefficients corresponding to $\gamma = 2$ was reintroduced. The trial incorporating the $(\gamma, q) = (2, 1)$ term yielded undetermined values and no improvement on the degree of fit, whilst the run incorporating the $(\gamma, q) = (2, -1)$ term gave reasonable values and an improved fit with $\varepsilon = 1.26$. Given the compatibility of the results with and without the $(2, -1)$ term and the large S.D.'s for the $(2, -1)$ term, the values from the trial with only two pairs of lumped harmonic coefficients were preferred.

The preferred lumped harmonic values derived were,

$$10^9\ \bar{S}_{14}^{1,0} = 61.8 \pm 1.6 \quad ; \quad 10^9\ \bar{C}_{14}^{1,0} = -20.6 \pm 9.9$$

$$10^9\ \bar{S}_{14}^{-1,2} = 8.0 \pm 6.3 \quad ; \quad 10^9\ \bar{C}_{14}^{-1,2} = -59.2 \pm 8.1$$

Values of the eccentricity cleared of the effects of the zonal harmonics and luni–solar gravitational attraction together with the theoretical variation at 14th order resonance, as given by the above coefficients, are plotted in Figure 3.5.

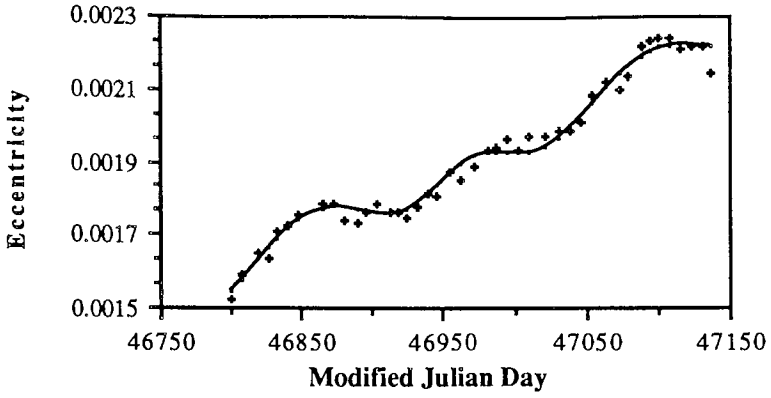

Figure 3.5 Values of the eccentricity cleared of other perturbations with theoretical fit.

For comparison, the values derived by including the $(\gamma, q) = (2, -1)$ term were,

$$10^9\ \bar{S}_{14}^{1,0} = 60.7 \pm 1.6 \quad ; \quad 10^9\ \bar{C}_{14}^{1,0} = -27.7 \pm 9.8$$

$$10^9\ \bar{S}_{14}^{-1,2} = 5.5 \pm 6.3 \quad ; \quad 10^9\ \bar{C}_{14}^{-1,2} = -50.7 \pm 8.4$$

$$10^9\ \bar{S}_{14}^{-1,3} = -92.2 \pm 36.7 \quad ; \quad 10^9\ \bar{C}_{14}^{-1,3} = -25.0 \pm 37.2$$

§3.6 ANALYSIS OF THE MEAN MOTION

This is the first orbital analysis in which the mean motion has been analysed for resonance parameters. In previous studies it has been impossible to separate air–drag effects from resonance perturbations with any degree of reliability. However, the coincidence of 14th order resonance of 1984 – 106A and the low solar activity during 1987, combined to yield a signature in the mean motion, as seen in Figure 3.6, clearly dominated by resonance effects.

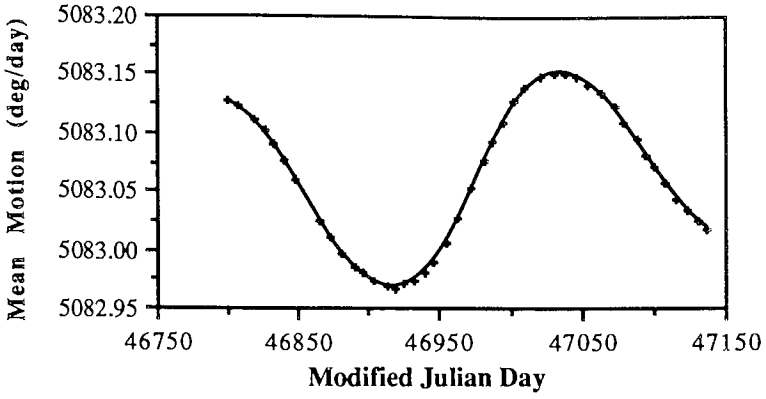

Figure 3.6 Values of the observed mean motion with theoretical fit.

The effect of air–drag can be estimated in a similar analysis to that outlined for the eccentricity. By using the change in the semi–major axis in section 2.2, the corresponding change in n over one revolution is given by

$$\Delta n = \frac{-3}{2}\frac{n}{a}\Delta a = 3na\,\rho_0 F \frac{S}{m} C_D \pi \exp[-z]$$

Over the 338 days of the analysis, estimating as before the values for ρ_0, F, S/m, C_D and H, the total change in n due to air–drag is

$$\Delta n_{DRAG}^{TOTAL} \equiv 0.13°/\text{day} .$$

This value seemed at first quite large compared to the observed overall change of approximately 0.04°/day in the observed values of the mean motion as seen in Figure 3.6. It is important to realise, however, that this estimate was derived from several approximations, particularly the value for S/m. Very little is known about the satellite so a typical value was assumed, but this may be in error by a factor of two or more.

Comparison of equations (3.2) and (3.3) yields a relationship between the quasi–secular resonance terms $(\gamma, q) = (1, 1)$ of both eccentricity and mean motion which may be written as,

$$\Delta n_{(1,1)}^{TOTAL} = -3ne\Delta e_{(1,1)}^{TOTAL}$$

From Figure 3.5, it is clear that the total overall change in eccentricity due to the $(\gamma,q) = (1, 1)$ resonance is approximately 7 x 10^{-4}. Thus, the total change in mean motion due to the quasi–secular resonance term over 338 days is

$$\Delta n_{(1,1)}^{TOTAL} = -0.02 \text{ deg/day}.$$

It is possible therefore that an over–estimation has been made in one of the parameters, e.g. area to mass ratio and that the true value for the change in n due to air–drag is around 0.06°/day. Thus combining this perturbation with that of the quasi–secular resonance, an overall change in mean motion of 0.04°/day is observed.

Solar activity gradually increased during 1987, to a maximum in November. This can be seen in the monthly average EUV index, $\overline{F}_{10.7}$, listed in Table 3.4 (CIRA).

A first approximation of Jacchia's model, as given by equation (2.44), yields

$$T_c = 379 + 3.24\,\overline{F}_{10.7} \qquad K \tag{3.4}$$

As discussed in chapter 2, the average daily temperature, $T_{(av)}$ is calculated from (3.4) by multiplying T_c by 1.15. Upon utilizing Fig. 2.3 it is possible to obtain approximate values for the air–density at the height of 840km. These values are given in Table 3.4. The variation of atmospheric density, throughout 1987, is shown graphically in Figure 3.7. The straight line through the data set represents the best linear fit (with regression coefficient of 0.76). Although the linear fit does not accurately model the density changes, it nevertheless indicates an increase in air–drag during the period of analysis.

MONTH	$\bar{F}_{10.7}$ 10^{-22} W/m^2/Hz	T_{av} (Kelvin)	$\rho(x10^{-15})$ (kg/m^3)
JAN	72.5	706.0	2.096
FEB	71.5	702.2	2.078
MAR	74.0	711.6	2.126
APR	84.9	752.2	2.418
MAY	87.8	763.0	2.518
JUN	77.6	725.0	2.207
JUL	84.2	749.6	2.395
AUG	90.0	771.2	2.600
SEP	86.1	756.7	2.458
OCT	98.1	801.4	2.948
NOV	101.2	812.9	3.101
DEC	94.4	787.6	2.779

Table 3.4 Monthly average EUV index, temperatures and the estimated air–density at perigee height of 840km during 1987.

Since the rate of change of the mean motion, $\dot{n}$, is directly proportional to air–drag it was anticipated that n would vary non linearly with time. Hence, both air–drag and the quasi–secular resonance, corresponding to $(\gamma, q) = (1, 1)$ in equation (3.3) were modelled by solving for a linear and a quadratic coefficient in n, i.e. $n^{(1,1)}_{air-drag} = n_0 + at + bt^2$, where n_0 is the initial value of n at MJD 46799; t being measured from this epoch.

Due to the near identical frequencies of the $(\gamma, q) = (1, 0)$ and $(2, 1)$ terms, only the parameters corresponding to the dominant term were sought. The $(2, 1)$ term contributes as little as 0.1% of that of the $(1, 0)$ terms, hence the parameters of only the latter were solved for and the results are considered to be wholly representative of

the lumped harmonic coefficients corresponding to $(\gamma, q) = (1, 0)$. The $(\gamma, q) = (2, 0)$ and $(1, -1)$ terms and the $(\gamma, q) = (3, 0)$ and $(2, -1)$ terms also have near identical frequencies of approximately $2\dot{\Phi}$ and $3\dot{\Phi}$, respectively. However, in both instances, the contribution of the dominant term is only twice that of the smaller term, as seen in Table 3.3. The phase difference between terms of similar frequency is not constant, but varies between ±35°. Consequently, all pairs of parameters were solved for, with the initial aim of seeking independent solutions for all the lumped harmonic coefficients.

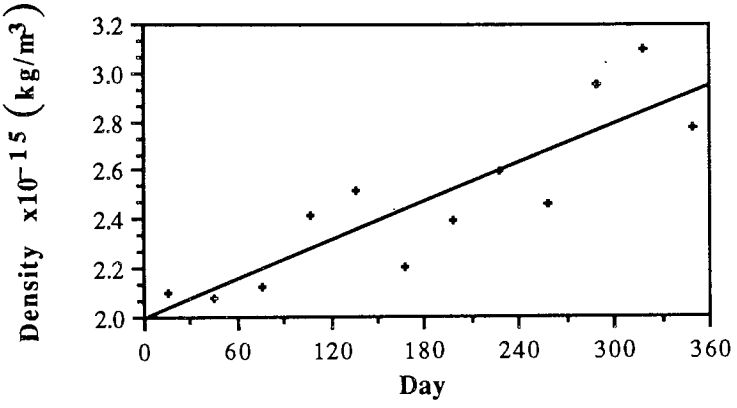

Figure 3.7 Variation of density at perigee height 840km during 1987 and linear fit.

Solar radiation pressure (SRP) was a further uncertainty and although this was initially modelled using the theory of Aksnes (1976), it contributed nothing to the degree of fit, with the SRP multiplicative parameter undetermined. In addition, there were high correlations between this parameter and the linear and quadratic terms. Consequently the coefficient for SRP was suppressed and its effects absorbed within the linear and quadratic terms, together with air-drag and other unmodelled resonances.

Thus, up to 5 pairs of lumped harmonic values, the initial value and the linear and quadratic coefficients were sought by a weighted least squares fit of the 43 PROP 6 values of the mean motion and their S.D.'s. It was pertinent, however, to increase the

PROP 6 S.D.'s by a factor of three as they were considered to be over optimistic given the uncertainties within the analysis.

When the 13 parameters were derived the linear coefficient was undetermined, as too were half of the lumped harmonic coefficients corresponding to $\gamma = 2$ and 3. Further, there were high correlations between the linear and quadratic terms, and between all the lumped harmonic coefficients associated with terms having nearly identical frequencies. Several trials were then made, suppressing one of the pairs of correlated lumped harmonic coefficients, and the linear and quadratic coefficients in turn. Suppressing the quadratic term yielded determined values only for the lumped harmonic coefficients with $(\gamma, q) = (1, 0)$ and $(2, 0)$, with the degree of fit parameter $\varepsilon = 3.48$. On suppressing the linear term, however, the quadratic term and all pairs of lumped harmonic coefficients corresponding to $q = 0$ were well–determined, with the degree of fit improved to $\varepsilon = 0.99$. Throughout these trials there remained consistency for the derived lumped harmonic values corresponding to $(\gamma, q) = (1, 0)$.

The lumped harmonic values determined from this analysis of the change in mean motion with their formal SD's quoted at the 3 sigma level are given for reference,

$$10^9\ \bar{S}^{0,1}_{14} = -\ 20.7 \pm 0.1 \quad ; \quad 10^9\ \bar{C}^{0,1}_{14} = -\ 2.2 \pm 0.1$$

$$10^9\ \bar{S}^{0,2}_{28} = \ 12.2 \pm 1.8 \quad ; \quad 10^9\ \bar{C}^{0,2}_{28} = \ 9.3 \pm 1.6$$

$$10^9\ \bar{S}^{0,3}_{42} = \ 30.5 \pm 7.7 \quad ; \quad 10^9\ \bar{C}^{0,3}_{42} = \ 11.7 \pm 8.0$$

The quadratic coefficient derived was $(3.96 \pm 0.04) \times 10^{-7}$ °/day^3 with initial value given as (5083.1281 ± 0.0003) °/day.

As discussed previously it was considered that the above coefficients corresponding to $\gamma = 2$ and 3 are contaminated by the unmodelled resonances, whilst the trials showed that it was not possible to separate the coefficients of terms with similar frequencies.

Consequently, the contribution of the less dominant terms, namely those for which $(\gamma, q) = (1, -1)$ and $(2, -1)$, were evaluated and subtracted from the observed values of the mean motion. Estimates for the lumped harmonic coefficients for $(\gamma, q) = (1, -1)$ were taken from those derived from the rate of change of the eccentricity in section 3.5. Values for coefficients corresponding to $(\gamma, q) = (2, -1)$ were evaluated from the GEM–T1 gravity field (Marsh, et al, 1988), namely $10^9 \bar{S}_{28}^{-1,3} = 5.2$ and $10^9 \bar{C}_{28}^{-1,3} = 19.2$. By this technique the lumped harmonic values for $(\gamma, q) = (2, 0)$ and $(3, 0)$ were cleared of the secondary contributions. On removing these effects, the degree of fit improved slightly to $\varepsilon = 0.98$ with small changes to the derived values.

The preferred lumped harmonic values determined from analysis of the change in mean motion are,

$$10^9 \bar{S}_{14}^{0,1} = -20.7 \pm 0.1 \quad ; \quad 10^9 \bar{C}_{14}^{0,1} = -2.0 \pm 0.1$$

$$10^9 \bar{S}_{28}^{0,2} = 12.1 \pm 1.8 \quad ; \quad 10^9 \bar{C}_{28}^{0,2} = 13.6 \pm 1.6$$

$$10^9 \bar{S}_{42}^{0,3} = 30.2 \pm 7.6 \quad ; \quad 10^9 \bar{C}_{42}^{0,3} = 15.2 \pm 8.0$$

The quadratic coefficient is $(3.99 \pm 0.04) \times 10^{-7}$ °/day^3 with initial value given as (5083.1282 ± 0.0003) °/day.

The first pair of values are in good agreement with those previously derived from the changes in inclination. However, due to the greater accuracy in the data for the mean motion the values derived here are favoured. The smaller terms corresponding to $\gamma = 2$ and 3 may be contaminated by absorbing effects due to uncertainties in air–drag, the quasi–secular secondary resonance and SRP as well as errors in the $(\gamma, q) = (1, -1)$ and $(2, -1)$ lumped harmonics. Further tests revealed sensitivity of the solution to the $(\gamma, q) = (1, -1)$ harmonics but little variation

with $(\gamma, q) = (2, -1)$. In view of the accuracy of the $(1, -1)$ lumped harmonics, as derived from the eccentricity, it is deemed unlikely that the $(\gamma, q) = (2, 0)$ and $(3, 0)$ harmonics are contaminated by secondary resonance harmonics.

§3.7 COMPARISONS WITH OTHER SATELLITES OF SIMILAR INCLINATION AND THE GEM MODELS

The lumped harmonic values obtained from analysis of the change in inclination and mean motion for 1984 – 106A are in reasonable agreement with those derived previously. A summary of these and some earlier results (King–Hele et al, 1979) for 1965-16G, a satellite of nearly identical orbital inclination are listed in Table 3.5, along with the computed values given by GEM–T1 (Marsh et al, 1988), GEM–T2 (Marsh et al, 1989) and PGS–3337 (Marsh et al, 1990).

For eccentricity, the derived lumped harmonic values are a considerable improvement on those obtained previously for the terms $\gamma = 1$, $q = \pm 1$. This is primarily a consequence of the satellite being in almost exact $\Phi - \omega$ resonance whilst experiencing very little air–drag. Table 3.6 summarizes the values for $\gamma = 1$, $q = \pm 1$ derived here and the comparable values from a previous study (King–Hele et al, 1986) along with the computed values of both GEM and the PGS 3337 gravity models.

Values of lumped harmonics derived in this and analogous studies are useful as an independent check on global gravity fields such as the GEM models. Overall, the agreement for the 14^{th} order harmonics is excellent, whereas, the 28^{th} and 42^{nd} order terms differ from the global gravity field solution. However, this is not unexpected as the GEM–T1 and GEM–T2 high order coefficients may be in error by up to 100%, and disagree with each other, whilst the values derived in this study for order 28 and 42 may be contaminated by aforementioned effects. (The values for order 42 are probably numerically too large.)

Source	i (deg)		$10^9 \bar{S}^{0,1}_{14}$	$10^9 \bar{C}^{0,1}_{14}$	$10^9 \bar{S}^{0,2}_{28}$	$10^9 \bar{C}^{0,2}_{28}$	$10^9 \bar{S}^{0,3}_{42}$	$10^9 \bar{C}^{0,3}_{42}$
1984 – 106A	71.0	(a)	–20.7 ± 0.1	–2.0 ± 0.1	12.5 ± 1.8	13.4 ± 1.6	29.6 ± 7.6	15.0 ± 7.9
		(b)	–20.8 ± 1.3	5.1 ± 1.2	–	–	–	–
1971 – 10B	69.9		–2 ± 20	32 ± 44 †	–	–	–	–
1965 – 16G	70.1		–16.6 ± 0.9	–2.1 ± 0.3	–	–	–	–
GEM–T1			–22.2	–0.8	8.8	26.0	–	–
GEM–T2			–21.4	–0.9	–5.7	4.7	4.5	–0.7
PGS–3337			–22.2	–2.0	4.9	16.1	11.1	–1.0

† PROP derived S.D. x 4 : in solving for individual harmonics (King–Hele et al, 1986), the original S.D. was downgraded by a factor of four.

(a) derived from mean motion (b) derived from inclination

Table 3.5 A summary of the lumped harmonic values obtained from analysis of the changes in inclination and mean motion for 1984–106A along with some earlier results (King–Hele et al., 1979) and the computed values given by GEM–T1 (Marsh et al., 1988), GEM–T2 (Marsh et al., 1989) and PGS–3337 (Marsh et al., 1990)

Source	i (deg)	$10^9 \bar{S}_{14}^{1,0}$	$10^9 \bar{C}_{14}^{1,0}$	$10^9 \bar{S}_{14}^{-1,2}$	$10^9 \bar{C}_{14}^{-1,2}$
1984 – 106A	71.0	61.8 ± 1.6	–20.6 ± 9.9	8.0 ± 6.3	–59.2 ± 8.1
1965 – 16G	70.1	68 ± 51	17 ± 31*	–11 ± 43	–38 ± 25
GEM–T1		61.0	–19.3	9.3	–49.0
GEM–T2		61.0	–19.1	12.9	–49.7
PGS–3337		60.8	–19.2	12.0	–50.6

* PROP derived S.D. × 2 : in solving for individual harmonics (King–Hele et al, 1986), the original S.D. was downgraded by a factor of two. In their solution the residual for $10^9 \bar{C}_{14}^{1,0}$ was 33; so the solution gave a value of – 16 at inclination 70.1° .

Table 3.6 A summary of the lumped harmonic values obtained from analysis of the change in eccentricity for 1984–106A along with some earlier results (King–Hele et al, 1979) and the computed values given by GEM–T1 (Marsh et al., 1988), GEM–T2 (Marsh et al., 1989) and PGS–3337 (Marsh et al., 1990).

CHAPTER IV

THE RESONANCE ANGLE

This chapter exploits the phenomenon of very low air–drag (as experienced by the satellite 1984–106A) and looks at the development of the resonance parameter within this constraint. Expressions are obtained for the resonance angle that lead to the determination of lumped harmonic coefficients – this being the first time coefficients have been evaluated from the resonance angle. Usually, drag–effects dominate other perturbations, such as resonance, making it impossible to arrive at any reliable solutions.

§4.1 EXPLICIT TIME DEPENDENCE OF THE RESONANCE ANGLE

From the definition of the resonance angle, (2.35), we may write

$$\ddot{\Phi}_{\alpha\beta} = \alpha\left(\ddot{M} + \ddot{\omega}\right) + \beta\ddot{\Omega} .$$

Now from Lagrange's planetary equations, (2.24), substitution for $\ddot{M}$, $\ddot{\omega}$ and $\ddot{\Omega}$ yields

$$\begin{aligned}\ddot{\Phi}_{\alpha\beta} = \alpha \frac{d}{dt}\Bigg[n - \frac{\left(1-e^2\right)}{e}\left\{\frac{1}{na^2}\frac{\partial R}{\partial e}\right\} - 2a\left\{\frac{1}{na^2}\frac{\partial R}{\partial a}\right\} + \\ + \frac{\left(1-e^2\right)^{1/2}}{e}\left\{\frac{1}{na^2}\frac{\partial R}{\partial e}\right\} - \frac{\cot i}{\left(1-e^2\right)^{1/2}}\left\{\frac{1}{na^2}\frac{\partial R}{\partial i}\right\}\Bigg] \\ + \beta \frac{d}{dt}\left[\frac{\operatorname{cosec} i}{\left(1-e^2\right)^{1/2}}\left\{\frac{1}{na^2}\frac{\partial R}{\partial i}\right\}\right] .\end{aligned} \tag{4.1}$$

By neglecting terms of O(e) inside the square brackets then equation (4.1) may be written

$$\ddot{\Phi}_{\alpha\beta} = \alpha\frac{dn}{dt} - \frac{d}{dt}\left[2\alpha a\left\{\frac{1}{na^2}\frac{\partial R}{\partial a}\right\} + (\alpha\cot i - \beta\,\mathrm{cosec}\, i)\left\{\frac{1}{na^2}\frac{\partial R}{\partial i}\right\}\right]$$

$$= \alpha\frac{dn}{dt} - \frac{d}{d\Phi_{\alpha\beta}}\left[2\alpha a\left\{\frac{1}{na^2}\frac{\partial R}{\partial a}\right\} + (\alpha\cot i - \beta\,\mathrm{cosec}\, i)\left\{\frac{1}{na^2}\frac{\partial R}{\partial i}\right\}\right]\dot{\Phi}_{\alpha\beta}\,, \tag{4.2}$$

where from equation (2.32), following the notation developed in chapter 2,

$$\frac{1}{na^2}\frac{\partial R}{\partial a} = -\sum\frac{(\ell+1)}{a}\left(\frac{\mu}{a^3}\right)^{1/2}\left(\frac{a_e}{a}\right)^{\ell}\bar{F}_{\ell m\frac{1}{2}(\ell-\alpha\gamma)}(i)\,\phi^{B}_{\ell m}$$

$$\frac{1}{na^2}\frac{\partial R}{\partial i} = \sum\left(\frac{\mu}{a^3}\right)^{1/2}\left(\frac{a_e}{a}\right)^{\ell}\bar{F}'_{\ell m\frac{1}{2}(\ell-\alpha\gamma)}(i)\,\phi^{B}_{\ell m}\,;$$

the summation being over the appropriate ranges for ℓ and γ, subject to the usual resonance conditions, (2.36).

Now

$$\frac{d}{d\Phi_{\alpha\beta}}\left[\frac{1}{na^2}\frac{\partial R}{\partial a}\right] = \gamma\sum\frac{(\ell+1)}{a}\left(\frac{\mu}{a^3}\right)^{1/2}\left(\frac{a_e}{a}\right)^{\ell}\bar{F}_{\ell m\frac{1}{2}(\ell-\alpha\gamma)}(i)\,\phi^{A}_{\ell m} \tag{4.3}$$

and

$$\frac{d}{d\Phi_{\alpha\beta}}\left[\frac{1}{na^2}\frac{\partial R}{\partial i}\right] = -\gamma\sum\left(\frac{\mu}{a^3}\right)^{1/2}\left(\frac{a_e}{a}\right)^{\ell}\bar{F}'_{\ell m\frac{1}{2}(\ell-\alpha\gamma)}(i)\,\phi^{A}_{\ell m}\,. \tag{4.4}$$

Equations (4.3) and (4.4) are $O(J_{\ell m})$, therefore, provided $\dot{\Phi}_{\alpha\beta}$ is of $O(J_{\ell m}{}^{1/2})$, (which is true even for shallow resonance) then the second term in (4.2) is $O(J_{\ell m}{}^{3/2})$ and is thus small compared with $\dot{n}$, which is $O(J_{\ell m})$. Hence the second time derivative of the resonance angle may be approximated by

$$\ddot{\Phi}_{\alpha\beta} = \alpha \frac{dn}{dt} \ . \tag{4.5}$$

Both resonance and drag contribute to the along–track perturbations, $\frac{dn}{dt}$. However, the theory will be developed initially as if drag is negligible. Later, drag will be examined in more detail and incorporated analytically as a small correction. This is not unreasonable as it has already been shown in chapter 3 that drag had very little effect on the change in mean motion for the satellite 1984–106A. Nevertheless, drag must eventually be incorporated for any theoretical or numerical evaluations to be substantiated.

The rate of change of the mean motion is given by

$$\frac{dn}{dt} = -\frac{3n}{2a}\frac{da}{dt} = -3\left(\frac{\mu}{a^3}\right)^{1/2}\left\{\frac{1}{na^2}\frac{\partial R}{\partial M}\right\} . \tag{4.6}$$

By utilizing (2.32) and (4.5), then equation (4.6) yields

$$\dot{n}_{\ell mpq} = 3\left(\frac{\mu}{a^3}\right)\left(\frac{a_e}{a}\right)^{\ell} \bar{F}_{\ell mp}(i)\, G_{\ell pq}(e)\left[\ell - 2p + q\right] \varphi^{A}_{\ell mpq}$$

and hence applying the resonance conditions (2.36), equation (4.5) becomes to O(e)

$$\ddot{\Phi}_{\alpha\beta} = \sum 3\alpha^2\gamma \left(\frac{\mu}{a^3}\right)\left(\frac{a_e}{a}\right)^{\ell} \bar{F}_{\ell m\frac{1}{2}(\ell-\alpha\gamma)}(i)\, \phi^{A}_{\ell m} , \tag{4.7}$$

where summation is over all permissible ℓ and γ values.

Examining the dominant term in (4.7), i.e. $\gamma = 1$ and summing over all permissible ℓ–values (using the usual notation for lumped harmonic coefficients as given in chapter 3),

$$\ddot{\Phi}_{\alpha\beta} = 3n^2\alpha^2 \left(\frac{a_e}{a}\right)^L \bar{F}_{L\beta\frac{1}{2}(L-\alpha)(i)} \left\{ \begin{bmatrix} \bar{C}_\beta^{0,\alpha} \\ -\bar{S}_\beta^{0,\alpha} \end{bmatrix}_{\alpha\ \text{odd}}^{\alpha\ \text{even}} \sin \Phi_{\alpha\beta} - \begin{bmatrix} \bar{S}_\beta^{0,\alpha} \\ \bar{C}_\beta^{0,\alpha} \end{bmatrix}_{\alpha\ \text{odd}}^{\alpha\ \text{even}} \cos \Phi_{\alpha\beta} \right\},$$

which upon dropping the subscripts α and β on Φ for brevity, may be written as

$$\ddot{\Phi} = -\frac{A}{2} \sin\left(\Phi - \lambda\right) \tag{4.8}$$

where

$$A = 6n^2\alpha^2 \left(\frac{a_e}{a}\right)^L \left|\bar{F}_{L\beta\frac{1}{2}(L-\alpha)(i)}\right| \sqrt{\left(\bar{C}_\beta^{0,\alpha}\right)^2 + \left(\bar{S}_\beta^{0,\alpha}\right)^2}$$

$$\lambda = \begin{bmatrix} \arctan\left(-\bar{S}_\beta^{0,\alpha}\ \bar{F},\ -\bar{C}_\beta^{0,\alpha}\ \bar{F}\right) \\ \arctan\left(-\bar{C}_\beta^{0,\alpha}\ \bar{F},\ \bar{S}_\beta^{0,\alpha}\ \bar{F}\right) \end{bmatrix}_{\alpha\ \text{odd}}^{\alpha\ \text{even}}$$

and $$L = \beta + \begin{bmatrix} 0 \\ 1 \end{bmatrix}_{\alpha\ \text{odd}}^{\alpha\ \text{even}}$$

Equation (4.8) readily integrates to

$$\left(\dot{\Phi}\right)^2 = \tilde{C} + A \cos\left(\Phi - \lambda\right), \tag{4.9}$$

where $\tilde{C}$ is a constant depending on the initial conditions. For $\tilde{C} \gg A$, i.e. for shallow resonance, equation (4.9) yields a first approximation

$$\Phi \simeq \Phi_0 + \sigma t, \tag{4.10}$$

where Φ_0 is the initial value of Φ at $t = 0$ and σ is a constant, related to $\tilde{C}$ via the equation

$$\sigma \simeq \pm\sqrt{\tilde{C}};$$

the sign depending on whether the resonance angle is approaching (–) or receding (+) from exact commensurability. (A more accurate definition of σ is given by equation (4.21) later in this chapter.) The resonance parameter thus appears to vary linearly with time.

Equation (4.10) is only an approximation. We may use this form whenever $\tilde{C} \gg A$ and we need only the dominant secular variation in Φ. If the magnitude of A is comparable to that of $\tilde{C}$ or in circumstances where Φ is required more accurately, it is necessary to develop the resonance angle retaining the oscillatory part. This can be achieved by using elliptic integral theory.

Elliptic Integrals of the first kind

An *elliptic integral of the first kind,* denoted u or $F(\phi, \kappa)$, is usually written (Abramowitz and Stegun, p589).

$$u = F(\phi, \kappa) = \int_0^{\phi} \frac{d\phi}{(1 - \kappa^2 \sin^2 \phi)^{1/2}}$$

where κ is the *modulus* $(\kappa^2 < 1)$ and ϕ is the *amplitude* corresponding to the *argument* u. A *complete elliptic integral of the first kind,* denoted K, is an elliptic integral whose upper limit is $\pi/2$, i.e.

$$K(\kappa^2) = F(\pi/2, \kappa) = \int_0^{\pi/2} \frac{d\phi}{(1 - \kappa^2 \sin^2 \phi)^{1/2}}$$

Conversion of the resonance parameter

Making the substitution $\phi = \frac{\Phi - \lambda}{2}$ and denoting $\dot{\Phi}$ at $t = 0$ by $\dot{\Phi}_0$, equation (4.9) becomes

$$(\dot{\Phi})^2 = (\dot{\Phi}_0)^2 - A\cos(\Phi_0-\lambda) + A\cos(\Phi-\lambda) = v_0^2(1 - \kappa^2 \sin^2\phi)$$

(4.11)

where

$$v_0^2 = (\dot{\Phi}_0)^2 + A[1 - \cos(\Phi_0-\lambda)] \qquad (4.12)$$

and $\kappa^2 = \frac{2A}{v_0^2}$ with v_0, κ chosen to be positive.

For the case $\kappa^2 > 1$, the resonance angle *librates*, i.e. Φ is continually changing direction and oscillates between two extreme values, at which $\dot{\Phi}$ vanishes. For $\kappa^2 < 1$, the solution is within the *circulation* region of Φ, where Φ is unrestricted.

§4.2 LIBRATION

Libration of the resonance parameter, Φ, is examined here for completeness, but is not applicable to Cosmos 1603 during the period of orbital analysis. We denote the amplitude of libration of ϕ by the positive constant, α. As previously stated, $\dot{\phi} = 0$ when $\phi = \alpha$, hence from equation (4.11)

$$\sin^2\alpha = 1/\kappa^2 .$$

We now make a change of variable, given by

$$\sin\varphi = \frac{\sin\phi}{\sin\alpha} ,$$

which reduces equation (4.11) to

$$(\dot{\varphi})^2 = \frac{A}{2}(1 - \tilde{\kappa}^2 \sin^2\varphi) \qquad (4.13)$$

where $\tilde{\kappa} = \sin\alpha = 1/\kappa$. Equation (4.13) may be integrated to give

$$\int_{\varphi_0}^{\varphi} \frac{\pm\, d\varphi}{\left(1 - \tilde{\kappa}^2 \sin^2 \varphi\right)^{1/2}} = \int_0^t \frac{\kappa v_0}{2}\, dt = \left(\frac{\kappa v_0}{2}\right) t\,. \qquad (4.14)$$

The sign is chosen such that time is positive and increasing with respect to integration over the parameter φ. Because ϕ librates between $\pm\alpha$, Φ librates between $\lambda \pm 2\alpha$ and φ also librates, but due to the choice of variable change, the limits for φ are $\pm \pi/2$. It is thus possible to express the left integral in (4.14) in terms of complete elliptic integrals $\left(\text{since } \tilde{\kappa}^2 < 1\right)$.

An initial value and direction, φ_0 and $\dot{\varphi}_0$, will dictate the initial choice of sign within the integrand. φ will then continue to vary until its magnitude is equal to $\pi/2$, at which point the sign in the integrand changes in order to maintain positively increasing time, whilst φ (hence Φ) changes direction. There are effectively four quadrants to the phases of φ, namely, 0 to $\pi/2$, $\pi/2$ to 0, 0 to $-\pi/2$ and $-\pi/2$ to 0. The period, T, of libration is given by the total time for φ to complete each quadrant and return to its initial value. Therefore, T is the sum total of four complete elliptic integrals with respect to the modulus $\tilde{\kappa} = 1/\kappa$ and may be written

$$T = \frac{8}{\kappa v_0} K\left(1/\kappa^2\right)$$

§4.3 CIRCULATION

Cosmos 1603 experienced circulation of its resonance parameter Φ, during the one year of orbital analysis. Thus the subsequent development of the resonance angle is directly applicable to Cosmos 1603 and some important results obtained here are later used in further development of orbital theories.

Returning to equation (4.11), further integration is permissible. On using the definition of an elliptic integral, we may write

$$u = \Lambda \pm \frac{v_0}{2} t, \tag{4.15}$$

where the choice of sign is dictated by $\dot{\Phi}_0$ and does not alter thereafter. The constant Λ is a function of the initial conditions, namely

$$\Lambda = F\left(\frac{\Phi_0 - \lambda}{2}, \kappa\right). \tag{4.16}$$

Without loss of generality, we may choose $\Phi_0 = \lambda$ and equation (4.12) reveals $v_0^2 \equiv (\dot{\Phi}_0)^2$ and equation (4.16) yields $\Lambda \equiv 0$. Thus, we eradicate the problem of choice of the sign by writing $u = \frac{\dot{\Phi}_0}{2} t$.

From the theory of elliptic integrals (Abramowitz and Stegun, p591) the argument, ϕ, can be written in terms of the amplitude of u, denoted *am u*, where

$$\phi = \text{am}\, u = \frac{\pi u}{2K} + \sum_{n=1}^{\infty} \frac{2q^n \sin\left(\frac{n\pi u}{K}\right)}{n(1 + q^{2n})} \tag{4.17}$$

and for $|\kappa^2| < 1$

$$q = \exp\left[\frac{-\pi K'}{K}\right] = \frac{\kappa^2}{16} + 8\left(\frac{\kappa^2}{16}\right)^2 + 84\left(\frac{\kappa^2}{16}\right)^3 + O(\kappa^8) \tag{4.18}$$

where $K' = K(1-\kappa^2)$.

For our purpose it is sufficient to examine the theory to $O(\kappa^4)$ since for even relatively large values of κ^2, (0.3 say), terms containing κ^6 contribute less than 3% of the dominant term.

Expanding terms in equations (4.17) and (4.18), the parameter ϕ may be written

$$\phi = \frac{\pi u}{2K} + \left[\frac{\kappa^2}{8} + \frac{\kappa^4}{16}\right] \sin\left(\frac{\pi u}{K}\right) + \frac{\kappa^4}{256} \sin\left(\frac{2\pi u}{K}\right) + O(\kappa^6)$$

where u is given by equation (4.15).

The resonance angle can now be expressed explicitly in terms of time, thus to $O(\kappa^4)$

$$\Phi = \lambda + 2\phi = \lambda + p + \sigma t + \left[\frac{\kappa^2}{4} + \frac{\kappa^4}{8}\right] \sin(p+\sigma t) + \frac{\kappa^4}{128} \sin 2(p+\sigma t) \tag{4.19}$$

where

$$p = \frac{\pi \Lambda}{K} \tag{4.20}$$

and

$$\sigma = \pm \frac{\pi v_0}{2K} ; \tag{4.21}$$

the choice of sign depending on the sign of $\dot{\Phi}_0$.

Again, putting $\dot{\Phi}_0 = \lambda$ (hence $p = 0$) and denoting $\frac{\kappa^2}{4}$ by z, equation (4.19) becomes

$$\Phi = \lambda + \sigma t + z(1 + 2z) \sin \sigma t + \frac{z^2}{8} \sin 2\sigma t + O(z^3) \tag{4.22}$$

where now $\sigma = \frac{\pi \dot{\Phi}_0}{2K}$.

Comparing equation (4.22) with equation (4.10), it is apparent that, to $O(\kappa^4)$, the oscillations superimposed on the linear variation of Φ are sinusoidal with frequencies σ and 2σ.

§4.4 THE EFFECT OF AIR–DRAG ON THE RESONANCE ANGLE

It was shown in section 4.1 that the acceleration of the resonance angle is proportional to the rate of change of the mean motion, which is directly related to the air–density, ρ. Summarizing the relationship between Φ, n and ρ, we write

$$\ddot{\Phi}_{DRAG} \alpha \dot{n}_{DRAG} \alpha \rho_h$$

where ρ_h is the atmospheric density at a fixed height, h, say. As shown in chapter 2, air–density varies with time, predominantly as a consequence of changing solar activity. In Fig. 3.7, a simple model for $\rho(t)$ was proposed in the form, $\rho(t) = a + bt$, where a and b are constants. We may thus consider the equation,

$$\ddot{\Phi}_{DRAG} = Q''(t)$$

where $Q''(t)$ is a polynomial in time whose coefficients are constant for a fixed height. It will be seen later that $Q''(t)$ need only be a function of time that can be integrated twice.

Combining drag and resonance

$$\ddot{\Phi} = -\frac{A}{2} \sin(\Phi - \lambda) + Q''(t)$$

which has a first integral

$$(\dot{\Phi})^2 = \tilde{C} + A \cos(\Phi - \lambda) + 2 \int_0^t \dot{\Phi}(s)\, Q''(s)\, ds \qquad (4.23)$$

where $\tilde{C}$ is a constant and without loss of generality, t_0 is taken as zero.

Restricting ourselves to the circulation region of Φ, we consider the situation of resonance perturbations dominating the effect of air–drag on the rate of change of the mean–motion, as experienced by Cosmos 1603 during 1987. Given these criteria, the integration term in (4.23) is much smaller than the pure periodic term which in turn is dominated by the constant, $\tilde{C}$. Thus, utilizing equation (4.10) and writing

$$\dot{\Phi}(t) \simeq \sigma,$$

equation (4.23) simplifies to

$$\dot{\Phi} = \left[\tilde{C} + A\cos(\Phi-\lambda) + 2\sigma Q'(t)\right]^{1/2} \simeq \left[\tilde{C} + A\cos(\Phi-\lambda)\right]^{1/2}\left[1 + \frac{Q'(t)}{\sigma}\right] \tag{4.24}$$

where $Q'(t) = \int_0^t Q''(s)\, ds.$

Again using the substitution $\phi = \frac{\Phi - \lambda}{2}$, equation (4.24) can be written

$$u = \Lambda \pm \frac{v_0}{2}\left[t + \frac{1}{\sigma}Q(t)\right] \tag{4.25}$$

where v_0 is the positive constant as defined by equation (4.12) and $Q(t)$ is given by

$$Q(t) = \int_0^t Q'(s)\, ds = \int_0^t \int_0^s Q''(u)\, du\, ds.$$

The difference between equations (4.15) and (4.25) is the term containing $Q(t)$, which acts as a small correction to the drag–free result. If $Q''(t)$ is any twice–integrable function of time, $Q(t)$ can be evaluated analytically. Specifically if $Q''(t)$ is a

polynomial in time of degree n, say, then Q(t) is a polynomial in time of degree $n + 2$ with the zero and first order terms absent.

The equation for Φ may thus be written

$$\Phi(t) = \lambda + p + \bar{Q}(t) + z(1 + 2z) \sin\left(p+\bar{Q}(t)\right) + \frac{z^2}{8} \sin 2\left(p+\bar{Q}(t)\right) + O(z^3) \tag{4.26}$$

where p is given by (4.20) and $\bar{Q}(t) = \sigma t + Q(t)$.

Again, choosing $\Phi_0 = \lambda$, (4.26) simplifies to

$$\Phi = \Phi_0 + \bar{Q}(t) + z(1 + 2z) \sin \bar{Q}(t) + \frac{z^2}{8} \sin 2\bar{Q}(t). \tag{4.27}$$

§4.5 DETERMINATION OF LUMPED HARMONIC VALUES FROM THE RESONANCE ANGLE

Equation (4.27) is analytically the easiest form in which to express the changes in Φ. However, in determination of parameters by numerical means, it is impossible to quantify λ and hence specify Φ_0 accurately in advance. It is therefore necessary to develop the general expression (4.26) and write

$$\Phi = \Phi_0 + \bar{Q}(t) + z(1+2z)\left[\sin\left(p+\bar{Q}(t)\right) - \sin p\right] + \frac{z^2}{8}\left[\sin 2\left(p+\bar{Q}(t)\right) - \sin 2p\right]. \tag{4.28}$$

Equation (4.28) was incorporated into a least–squares–fit procedure with the aim of evaluating the four parameters $\{\Phi_0, \sigma, \kappa^2, p\}$ and the two drag parameters $\{D_2, D_3\}$, where $Q(t) = D_2t^2 + D_3t^3$, from the orbital data of Cosmos 1603 for the duration of 1987. The first four parameters can be easily converted to yield λ and

hence the two lumped harmonics $\bar{S}_{14}^{01}$ and $\bar{C}_{14}^{01}$, using the relationships given previously. Although not directly solved for, these parameters are listed along with the main parameters in Table 4.1, with corresponding S.D.'s. (Once again, it was deemed pertinent to quote all formal S.D.'s at the 3 sigma level.)

Initially all six parameters were sought by least–squares–fit, yielding high correlation between σ and D_2 and between D_2 and D_3. The drag coefficients had large S.D.'s and were not well determined. Subsequently, each drag coefficient was suppressed in turn, which gave a better fit with no high correlations. A run with drag totally suppressed was also made and the comparison of these results is seen in Table 4.1.

Run	ε	κ^2	σ	D_2	D_3	$\bar{S}_{14}^{01}$	$\bar{C}_{14}^{01}$
1	1.3	0.221 5	–1.5108 84	4.78 6.15	0.0031 120	–22.44 69	–2.99 95
2	1.2	0.220 5	–1.5042 12	–	0.0123 9	–22.26 57	–2.35 31
3	1.1	0.221 4	–1.5129 15	6.35 46	–	–22.52 51	–3.20 29
4	7.5	0.254 20	–1.4910 21	–	–	–25.71 2.72	–2.93 1.93

Table 4.1 The results of a least–squares–fit procedure determining parameters from the resonance angle, Φ.

There appears to be a slight advantage with inclusion of the cubic drag term, provided the quadratic term is suppressed. This parameter corresponds to a linear variation in atmospheric density as expected. Although crude, this model illustrates that drag effects are significant but small. The preferred solution is thus taken with D_2 suppressed and

D_3 included. The residuals of the preferred run are shown in Figure 4.1. It should be noted that the residuals for each run exhibit a common signature, namely an oscillation of frequency 2Φ, which is clearly seen in Figure 4.1. This observation lends weight to further investigations with the resonance angle, incorporating the 28^{th}–order harmonics.

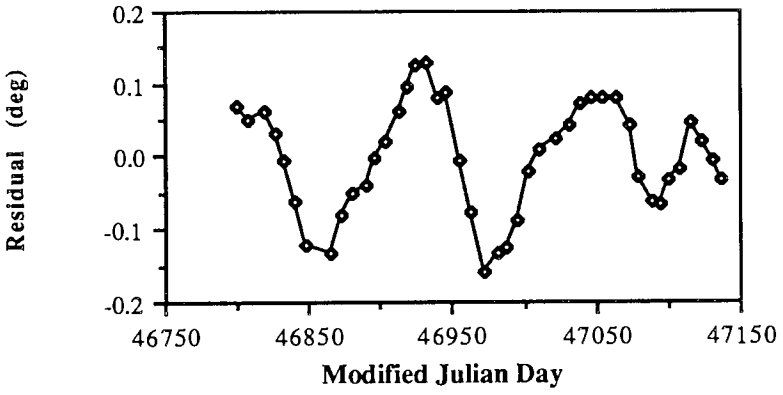

Figure 4.1 The residuals of a least–squares–fit procedure applied to equation (4.28) for Φ (incorporating a cubic time coefficient in the drag model).

§4.6 2nd ORDER RESONANCE EFFECTS

Including $(\gamma = 2)$ terms in the equation for $\ddot{\Phi}$, we have

$$\ddot{\Phi} = -3n^2\left(\frac{a_e}{a}\right)^{14}\left[\left(\frac{a_e}{a}\right)\overline{F}_{15,14,7}\left\{\overline{S}^{0,1}_{14}\sin\Phi + \overline{C}^{0,1}_{14}\cos\Phi\right\} - 2\left(\frac{a_e}{a}\right)^{14}\overline{F}_{28,28,13}\left\{\overline{C}^{0,2}_{28}\sin 2\Phi - \overline{S}^{0,2}_{28}\cos 2\Phi\right\}\right]$$

which integrates to give

$$(\dot{\Phi})^2 = \tilde{C} + A_1\sin\Phi + B_1\cos\Phi + A_2\sin 2\Phi + B_2\cos 2\Phi = X(\Phi), \qquad (4.29)$$

thus defining $X(\Phi)$, where

$$\left.\begin{matrix} A_1 \\ B_1 \end{matrix}\right\} = -6n^2\left(\frac{a_e}{a}\right)^{15} \bar{F}_{15,14,7}(i) \begin{cases} \bar{C}_{14}^{0,1} \\ -\bar{S}_{14}^{0,1} \end{cases}$$

and

$$\left.\begin{matrix} A_2 \\ B_2 \end{matrix}\right\} = -6n^2\left(\frac{a_e}{a}\right)^{28} \bar{F}_{28,28,13}(i) \begin{cases} \bar{S}_{28}^{0,2} \\ \bar{C}_{28}^{0,2} \end{cases}$$

$\tilde{C}$ is a positive constant depending on the initial conditions. On integrating equation (4.29) it is found that

$$t = \pm \int_{\Phi_0}^{\Phi} \frac{d\Phi}{\sqrt{X(\Phi)}} \tag{4.30}$$

where Φ_0 represents Φ at $t = 0$, and the sign is chosen such that time is positive and increasing.

Using the change of variable

$$x = \tan \Phi/2 \tag{4.31}$$

equation (4.30) may be reduced to the quartic form

$$t = \pm 2 \int_{x_0}^{x} \frac{dx}{\sqrt{a_0x^4 + a_1x^3 + a_2x^2 + a_3x + a_4}} \tag{4.32}$$

where

$a_0 = \tilde{C}-B_1+B_2$; $a_1 = 2A_1-4A_2$; $a_2 = 2\tilde{C}-6B_2$; $a_3 = 2A_1+4A_2$; $a_4 = \tilde{C}+B_1+B_2$.

For shallow resonance a_0, a_2 and a_4 are positive and of greater magnitude than a_1 and a_3. These criteria give rise to four complex roots of the polynomial $a_0x^4 + a_1x^3 + a_2x^2 + a_3x + a_4$, which permits the quartic to be expressed as a product of the two quadratics

$$\begin{aligned} Q_1(x) &= x^2 + 2b_1x + c_1 \\ Q_2(x) &= x^2 + 2b_2x + c_2 \end{aligned} \tag{4.33}$$

where c_1 and c_2 are positive (i.e. the product of the roots with their complex conjugates) and without loss of generality we choose $c_1 > c_2$. Hence, equation (4.32) becomes

$$t = \pm \frac{2}{a_0^{1/2}} \int_{x_0}^{x} \frac{dx}{\sqrt{Q_1(x)\, Q_2(x)}}. \tag{4.34}$$

We now introduce a new variable, s, defined by

$$s^2 = \frac{Q_1(x)}{Q_2(x)}$$

which may be alternatively written as

$$Q_1 - Q_2 s^2 = 0 = (1 - s^2)x^2 + 2(b_1 - b_2\, s^2)x + (c_1 - c_2\, s^2). \tag{4.35}$$

Changing the variable of integration to s, the integral I in (4.34) becomes

$$\pm \int_{x_0}^{x} \frac{dx}{\sqrt{Q_1\, Q_2}} = I = \pm \int_{s_0}^{s} \frac{2ds}{\sqrt{Q'_1 - Q'_2\, s^2}}$$

where the prime denotes differentiation with respect to the parameter x.

From equation (4.33)

$$Q'_1 - Q'_2 s^2 = 2(1 - s^2)x + 2(b_1 - b_2 s^2), \qquad (4.36)$$

which is non–zero $(\text{for } b_1 \neq b_2 \text{ and } c_1 \neq c_2)$. Thus squaring equation (4.36) and utilizing (4.35), we obtain

$$(Q'_1 - Q'_2 s^2)^2 = 4(b_1 - b_2 s^2)^2 - 4(1 - s^2)(b_1 - b_2 s^2) > 0. \qquad (4.37)$$

The right–hand side of (4.37) is the discriminant of (4.35), denoted $4S^2$, say. Because $4S^2 > 0$ equation (4.35) has real roots.

We write

$$S^2 = \left(\frac{Q'_1 - Q'_2 s^2}{2}\right)^2 = As^4 + Bs^2 + C \qquad (4.38)$$

where $A = b_2^2 - c_2 < 0$, $B = c_1 + c_2 - 2b_1 b_2 > 0$, and $C = b_1^2 - c_1 < 0$.

The roots of (4.38) are given by

$$s^2 = \frac{-B \pm \sqrt{B^2 - 4AC}}{2A}$$

which we denote by α^2 and β^2. Choosing $\alpha^2 > \beta^2$, we may write

$$S^2 = |A|(\alpha^2 - s^2)(s^2 - \beta^2),$$

since $A < 0$.

The integral I is now

$$I = \pm \int_{s_0}^{s} S^{-1}\, ds = \pm \int_{s_0}^{s} \frac{ds}{\sqrt{|A|(\alpha^2 - s^2)(s^2 - \beta^2)}}. \qquad (4.39)$$

Equations (4.39) can be evaluated by means of elliptic integral theory (Abramowitz and Stegun, p596).

The substitution required is

$$s = \beta\, nd(u|\kappa^2)$$
$$\kappa^2 = \frac{\alpha^2 - \beta^2}{\alpha^2}$$

where

$$nd(u|\kappa^2) = \frac{1}{dn(u|\kappa^2)} = \frac{1}{(1 - \kappa^2 \sin^2\phi)^{1/2}}$$

and the formal result only is quoted here, that is

$$\int_{\beta}^{s} \frac{ds}{\sqrt{(\alpha^2 - s^2)(s^2 - \beta^2)}} = \frac{1}{\alpha}\, nd^{-1}\left(\frac{s}{\beta}\middle|\frac{\alpha^2 - \beta^2}{\alpha^2}\right).$$

Then equation (4.32) yields

$$t = \frac{\pm 2}{a_0^{1/2}\, |A|^{1/2}} \int_{s_0}^{s} \frac{ds}{\sqrt{(\alpha^2 - s^2)(s^2 - \beta^2)}} = \frac{2\,\varepsilon}{\alpha\, a_0^{1/2}\, |A|^{1/2}} \left[nd^{-1}\left(\frac{s}{\beta}\middle|\kappa^2\right) - nd^{-1}\left(\frac{s_0}{\beta}\middle|\kappa^2\right)\right] \qquad (4.40)$$

where $\varepsilon = \pm 1$, the sign chosen such that time is positive and increasing.

Drag

It was shown in section 4.4, that drag can be incorporated by modelling air–density through the function $Q''(t)$ which yields the additional term $\frac{Q(t)}{\sigma}$. Equation (4.30) thus becomes

$$\int_{\Phi_0}^{\Phi} \frac{d\Phi}{\sqrt{X(\Phi)}} = t + \frac{Q(t)}{\sigma}$$

and similarly in equations (4.32) and (4.40), whence

$$s = \beta\, nd\left(n_0 + \chi t + \frac{\chi}{\sigma} Q(t) \middle| \kappa^2\right)$$

where

$$n_0 = nd^{-1}\left(\frac{s_0}{\beta} \middle| \kappa^2\right)$$

$$\chi = \frac{\alpha\, a_0^{1/2}\, |A|^{1/2}}{2\varepsilon} .$$

Expanding $nd(u|\kappa^2)$ in terms of powers of q, as defined by (4.18), we have (Abramowitz and Stegun, p575)

$$nd(u|\kappa^2) = \frac{\pi}{2K(1-\kappa^2)^{1/2}}\left[1 + 4\sum_{n=1}^{\infty}(-1)^n \frac{q^n}{1+q^{2n}} \cos\left(\frac{n\pi u}{K}\right)\right]$$

which eventually leads to

$$s^2 = \beta^2\left(\frac{\pi}{2K}\right)^2 \frac{1}{1-\kappa^2}\left[1 - \frac{\kappa^2}{2}\cos\bar{P}(t) + \frac{\kappa^4}{32}\left(1 - 8\cos\bar{P}(t) + 2\cos 2\bar{P}(t)\right)\right] + O(\kappa^6) \tag{4.41}$$

where $\bar{P}(t)$ is given by

$$\bar{P}(t) = \frac{\pi}{K}\left[n_0 + \chi t + \frac{\chi}{\sigma} Q(t)\right] = P_0 + P_1 t + P_2 t^2 + P_3 t^3$$

Utilizing equations (4.31), (4.35) and (4.41) it is possible to express the resonance angle as a function of time. Writing $s^2 = s^2(t)$, we have

$$\Phi = 2\tan^{-1} \frac{-\left[b_1 - b_2\, s^2(t)\right] \pm \sqrt{\left[b_1 - b_2\, s^2(t)\right]^2 - \left[1 - s^2(t)\right]\left[c_1 - c_2\, s^2(t)\right]}}{\left[1 - s^2(t)\right]} \qquad (4.42)$$

This expression does not lend itself to a least–squares–fit procedure as readily as (4.41). It was intended that equation (4.41), for s^2, would be used to determine the eight parameters $\{ b_1, b_2, c_1, c_2, P_0, P_1, P_2, P_3 \}$. Even after several trials, suppressing in turn one or more of the coefficients, it was deemed highly unlikely that convergence would be achieved. This is because the solution always tended towards the trivial result of $b_1 \equiv b_2$ and $c_1 \equiv c_2$, at which point the theory has no meaning and the application of the least–squares procedure breaks down. It seemed that the desired solution to the problem represented a *local* minimum upon a manifold that *sloped* towards a *global* minimum $(\text{i.e. } b_1 \equiv b_2 \text{ and } c_1 \equiv c_2)$ and that the required local minimum was stable only for values very close to the solution. Despite several attempts to improve the accuracy of the initial values, the method always moved away from the desired solution and thus failed. Consequently it was decided to approach the problem directly, using equation (4.42), which removes the occurrence of a trivial solution.

Trials putting $b_1 = 0$ and $c_1 = 1$ (equivalent to seeking a solution for the lumped harmonic coefficients corresponding to $\gamma = 1$ only) were made, suppressing in turn the drag coefficients P_2 and P_3. Again there was little difference between the two solutions and the run which incorporated the cubic term was favoured. The preferred values obtained in this manner were

$$10^9\, \overline{S}_{14}^{0,1} = -21.9 \pm 0.7 \;\; ; \;\; 10^9\, \overline{C}_{14}^{0,1} = -2.3 \pm 0.8$$

with $\varepsilon = 1.4$. These values are in good agreement with those obtained in section 4.5. The residuals are plotted in Figure 4.2 and clearly show the 2Φ signature.

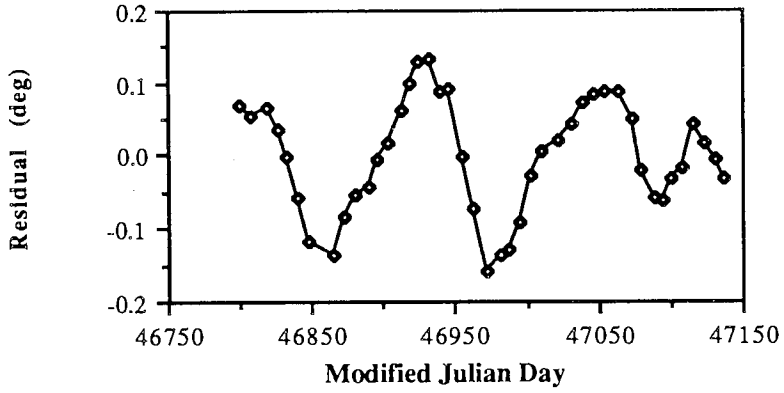

Figure 4.2 The residuals of a least–squares–fit procedure applied to equation (4.42) for Φ, suppressing the determination of 28^{th}–order harmonics.

The rate of change of the resonance parameter is proportional to the rate of change of the mean motion. In chapter 3, Table 3.3 shows the relative contribution of the resonance terms for the rate of change for the mean motion. It is apparent that the contribution corresponding to the $\Phi + \omega$ term is almost 50% that of the 2Φ term. Due to the near identical frequencies of these two terms, it was necessary to remove the effects of the $\Phi + \omega$ contribution before solving for the 2Φ parameters. The results for the mean motion indicated that the lumped harmonic values change little due to the $\Phi + \omega$ term. Consequently, the 2Φ values sought using equation (4.42) are considered to be reasonable and only minimally corrupted by the effects of the $\Phi + \omega$ terms.

Runs incorporating the 28^{th}–order lumped harmonic coefficients were made and the trial including the cubic drag coefficient was favoured.

The derived values were

$$10^9\ \bar{S}_{14}^{0,1} = -22.4 \pm 0.2 \quad ; \quad 10^9\ \bar{C}_{14}^{0,1} = -2.6 \pm 0.2$$

$$10^9\ \bar{S}_{28}^{0,2} = 13.3 \pm 4.2 \quad ; \quad 10^9\ \bar{C}_{28}^{0,2} = 12.4 \pm 4.0$$

with the corresponding degree of fit given by $\varepsilon = 0.6$. The residuals are plotted in Figure 4.3 and show a signature with a period of approximately 55 days. This periodicity is not readily explained by unmodelled resonances as it corresponds to a frequency of 4Φ and such terms would be negligible in their contribution.

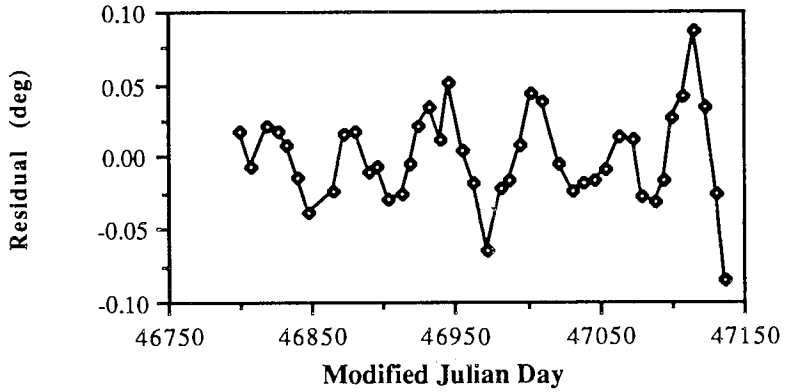

Figure 4.3 The residuals of a least–squares–fit procedure applied to equation (4.42) for Φ.

The 27 day Solar cycle was investigated briefly by examination of the daily $F_{10.7}$ index. The values were very static for the first three months and thus could not in any way account for the necessary changes in atmospheric density to yield the oscillation seen in Figure 4.3.

A possible explanation that requires further investigation is that the effect is a result of day–to–night variation in air–density. This creates the diurnal bulge which moves around the Earth, lagging behind the position of the sun in the sky by around 2 hours. The right ascension of the Sun advances daily by approximately 1 degree, whilst for Cosmos 1603 the right ascension of the ascending node recedes by around 2 deg/day.

Combining these two effects, the orbital plane precesses relative to the diurnal bulge at a rate of 3 deg/day. Since the orbit is near–circular the coincidence of the orbital plane with the bulge gives rise to increased air–drag effects with a period of around 60 days.

It is probably appropriate to remove the $\Phi + \omega$ resonance contribution before a solution is sought and to model the drag effects of the diurnal bulge, through the parameter $\dot{\theta} - \dot{\Omega}$. However, this is not detailed here and is left for future work.

CHAPTER V

PERTURBATIONS OF NEAR-CIRCULAR ORBITS

Cosmos 1603 had a near–circular orbit during the period of analysis. It is for this reason that we examine orbital theory pertaining to small eccentricity. The usual six osculating elements $\{a, e, i, \Omega, \omega, M\}$ are not suitable for defining an orbit of small eccentricity since the time derivatives of ω and M contain singularities at $e = 0$. We introduce the transformation (Cook, 1966)

$$\begin{aligned} \xi &= e \cos \omega \\ \eta &= e \sin \omega \end{aligned} \tag{5.1}$$

with time derivatives

$$\begin{aligned} \dot{\xi} &= \dot{e} \cos \omega - e\dot{\omega} \sin \omega \\ \dot{\eta} &= \dot{e} \sin \omega + e\dot{\omega} \cos \omega . \end{aligned} \tag{5.2}$$

Evaluating the perturbation in $\omega + M$, (instead of ω and M separately) we remove these singularities (Allan, 1967). In this chapter the long periodic development of a near–circular orbit is examined. The variation of $\omega + M$ is not required for our purpose and will not be discussed.

§5.1 THE ZONAL HARMONICS

From Lagrange's planetary equations the rates of changes of e and ω due to a disturbing function R are given by equation (2.24)

$$\dot{e} = \frac{(1 - e^2)^{1/2}}{na^2 e} \left[(1 - e^2)^{1/2} \frac{\partial R}{\partial M} - \frac{\partial R}{\partial \omega} \right]$$

(5.3)

$$\dot{\omega} = \frac{(1 - e^2)^{1/2}}{na^2 e}\left[\frac{\partial R}{\partial e} - \frac{e \cot i}{(1 - e^2)}\frac{\partial R}{\partial i}\right].$$

Combining (5.2) and (5.3) thus gives

$$\dot{\xi} = \frac{1}{na^2}\left[\frac{1}{e}\left\{(1 - e^2)\frac{\partial R}{\partial M} - (1 - e^2)^{1/2}\frac{\partial R}{\partial \omega}\right\}\cos\omega - \left\{(1 - e^2)^{1/2}\frac{\partial R}{\partial e} - \frac{e \cot i}{(1 - e^2)^{1/2}}\frac{\partial R}{\partial i}\right\}\sin\omega\right]$$

$$\dot{\eta} = \frac{1}{na^2}\left[\frac{1}{e}\left\{(1 - e^2)\frac{\partial R}{\partial M} - (1 - e^2)^{1/2}\frac{\partial R}{\partial \omega}\right\}\sin\omega + \left\{(1 - e^2)^{1/2}\frac{\partial R}{\partial e} - \frac{e \cot i}{(1 - e^2)^{1/2}}\frac{\partial R}{\partial i}\right\}\cos\omega\right].$$

(5.4)

On neglecting the central part and the longitude dependent contribution of the Earth's gravitational potential V in (2.26) the axi–symmetric component may be written as

$$R = -\left(\frac{\mu}{r}\right)\sum_{n=2}^{\infty} J_n \left(\frac{a_e}{r}\right)^n P_n(\sin\phi). \qquad (5.5)$$

We examine separately the effects of the even zonals and the odd zonals on the disturbing function, R, retaining dominant long–periodic terms only.

Even harmonics

Given that J_2 is $O(10^{-3})$ whilst all higher zonal harmonics are $O(10^{-6})$, it is sufficient to retain only J_2 from the even harmonics. Thus, from (2.33), the contribution in (5.5) from the even zonals may be written explicitly as

$$R_2 = J_2\left(\frac{\mu}{a_e}\right)\left(\frac{a_e}{a}\right)^3 (1 - e^2)^{-3/2}\left(3/4\cos^2 i - 1/4\right).$$

From (5.4), the effect of the even zonals is summarised by

$$\dot{\xi}_{EVEN} = -3J_2 n \left(\frac{a_e}{a}\right)^2 \left(1 - 5/4 \sin^2 i\right) \eta$$

$$\dot{\eta}_{EVEN} = 3J_2 n \left(\frac{a_e}{a}\right)^2 \left(1 - 5/4 \sin^2 i\right) \xi \qquad (5.6)$$

on neglecting terms of $O(e^2)$.

Odd harmonics

The Legendre polynomials in (5.5) may be expanded using the addition theorem for zonal harmonics (Jeffreys and Jeffreys, 1956)

$$P_n(\sin \phi) = P_n(\cos i) P_n\left(\cos \frac{\pi}{2}\right) + 2\sum_{s=1}^{n} \frac{(n-s)!}{(n+s)!} P_n^s(\cos i) P_n^s\left(\cos \pi/2\right) \cos s\left(u - \pi/2\right)$$

where P_n^s are associated Legendre functions of degree n and order s; and u is the argument of latitude $\omega + \theta$ (θ being the true anomaly). Thus, for a general term R_n in the disturbing potential

$$R_n = -J_n\left(\frac{\mu}{a_e}\right)\left(\frac{a_e}{r}\right)^{n+1}\left[P_n(\cos i)\, P_n(0) + 2\sum_{s=1}^{n} \frac{(n-s)!}{(n+s)!} P_n^s(\cos i)\, P_n^s(0) \cos s\left(u - \pi/2\right)\right]. \qquad (5.7)$$

Upon expansion of the true anomaly in terms of the eccentricity function, $G_{\ell pq}(e)$ (given in chapter 2), denoting ℓ by n, neglecting short periodic terms and for n odd, equation (5.7) becomes

$$R_n \cong -2J_n\left(\frac{\mu}{a_e}\right)\left(\frac{a_e}{r}\right)^{n+1} \sum_{\substack{s=1 \\ (odd)}}^{n} \frac{(n-s)!}{(n+s)!} P_n^s(\cos i) P_n^s(0) G_{n,\frac{1}{2}(n+s),s}(e) \cos s\left(\omega - \pi/2\right).$$

Since $G_{npq}(e)$ is $O(e^{|q|})$, only the first term in the summation is retained, yielding to $O(e^2)$

$$R_n = -J_n \left(\frac{\mu}{a_e}\right)\left(\frac{a_e}{r}\right)^{n+1} \left\{\frac{(n-1)}{n(n+1)} P_n^1(\cos i)\, P_n^1(0)\, e \sin \omega \qquad \text{(n odd)}\right.$$

whence, from equations (5.4), the contribution to $\dot{\xi}$ and $\dot{\eta}$ by the odd harmonics may be written

$$\dot{\xi}_{ODD} = \sum_{n_{ODD} \geq 3} J_n \left(\frac{\mu}{a^3}\right)^{1/2} \left(\frac{a_e}{a}\right)^n \left\{\frac{(n-1)}{n(n+1)} P_n^1(\cos i)\, P_n^1(0)\right\} + O(e^2)$$

$$\dot{\eta}_{ODD} = O(e^2)\,. \qquad (5.8)$$

The associated Legendre functions appearing in equation (5.8) may be written as

$$P_n^1(\cos i) = \frac{\sin i}{2^n} \sum_{t=0}^{(n-1)/2} \frac{(2n-2t)!\,(-1)^t}{(n-1-2t)!\,(n-t)!\,t!} (\cos i)^{n-1-2t}\,.$$

Equations of motion

Combining equations (5.6) and (5.8), the rates of change $\dot{\xi}$ and $\dot{\eta}$ due to the even and odd harmonics is summarised by

$$\begin{aligned} \dot{\xi} &= -k\eta + C \\ \dot{\eta} &= k\xi \end{aligned} \qquad (5.9)$$

where

$$k = 3J_2 \left(\frac{\mu}{a^3}\right)^{1/2} \left(\frac{a_e}{a}\right)^2 \left(1 - \frac{5}{4}\sin^2 i\right)$$

and

$$C = \left(\frac{\mu}{a^3}\right)^{1/2} \sum_{n_{ODD} \geq 3} J_n \left(\frac{a_e}{a}\right)^n \frac{(n-1)}{n(n+1)} P_n^1(0)\, P_n^1(\cos i).$$

The solution to equation (5.9) is given by (Cook, 1966)

$$\Psi(t) = \begin{pmatrix} -\eta_0 + C/k & \xi_0 \\ \xi_0 & \eta_0 - C/k \end{pmatrix} \begin{bmatrix} \sin kt \\ \cos kt \end{bmatrix} + \begin{bmatrix} 0 \\ C/k \end{bmatrix}, \qquad (5.10)$$

where $\underline{\psi}(t) = (\xi(t), \eta(t))^T$; or alternatively

$$\xi = A\cos(kt + \alpha)$$
$$\eta = A\sin(kt + \alpha) + C/k$$

where A and α are constants of integration depending on the initial conditions, ξ_0 and η_0 at $t = 0$, and may be written as

$$A^2 = (\eta_0 - C/k)^2 + \xi_0^2 , \qquad \alpha = \tan^{-1}\left(\frac{\eta_0 - C/k}{\xi_0}\right).$$

The conventional elements may thus be recovered from

$$e = (\xi^2 + \eta^2)^{1/2}$$

and

$$\omega = \tan^{-1}(\eta/\xi) .$$

It is apparent that e^2 varies sinusoidally with time. The motion may be represented diagrammatically in the (ξ, η) plane by a circle, radius A centred on $(0, C/k)$. The argument of perigee is then represented by the angular distance of the radius vector from the positive ξ–axis. (see Figure 5.1).

If $A > |C/k|$ the radial arm rotates with period $2\pi/|k|$ and the eccentricity oscillates between $A - C/k$ and $A + C/k$. Since the motion around the circle is at a uniform rate, ω may vary rapidly if A exceeds $|C/k|$ by only a small amount. Although ω is ill–defined as $e \to 0$, there is a corresponding variation in M and $\omega + M$ remains finite. When $A \gg |C/k|$, e varies approximately sinusoidally with ω.

If $A < |C/k|$, the radial arm oscillates about $|\omega| = \pi/2$, with amplitude $\sin^{-1}(|Ak/C|)$ and period $2\pi/|k|$, while the eccentricity oscillates between $|C/k| - A$ and $|C/k| + A$.

For an orbit with initial conditions $(\xi_0, \eta_0) = (0, C/k)$, the eccentricity and the argument of perigee do not change. This *frozen orbit* has particular significance for certain altimeter satellites.

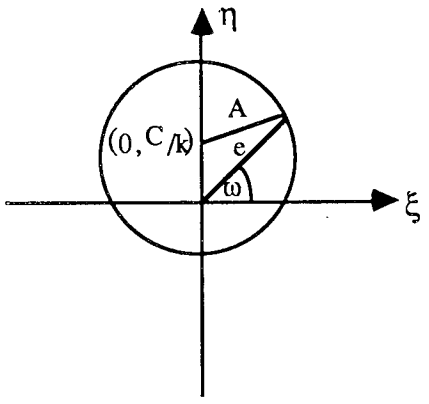

(a) $A > C/k$

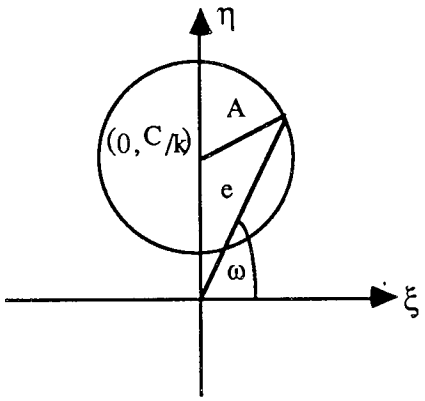

(b) $A < C/k$

Figure 5.1 (a) and (b) representing orbital motion in the (ξ, η) plane.

§5.2 RESONANCE

We seek the rates of change of the variables ξ and η, solely due to the resonance. This is achieved by substituting the disturbing function R, in normalized form, into (5.3), which in turn is substituted into (5.2). Since R may be differentiated term by term, it is possible to interchange the order of summation and differentiation. When resonance occurs, only a certain number of terms need to be retained in the analysis, subject to the resonance conditions (2.34). Therefore, we consider a general term

$R_{\ell mpq}$, of the disturbing potential R, and whenever the subscripts ℓ, m, p and q appear, summation over the appropriate ranges is assumed. When it becomes desirable to introduce a particular constraint into an equation, the corresponding subscript/s will be dropped and the constraint will be incorporated within the equation.

Utilizing equations (2.30) and (2.32), a general term in (5.3) may be written as

$$\dot{e}_{\ell mpq} = -\left[\frac{(1-e^2)}{e}(\ell-2p+q) - \frac{(1-e^2)^{1/2}}{e}(\ell-2p)\right] n \left(\frac{a_e}{a}\right)^{\ell} \bar{F}_{\ell mp}(i)\, G_{\ell pq}(e)\, \varphi^{A}_{\ell mpq}$$

$$\dot{\omega}_{\ell mpq} = \left[\frac{(1-e^2)^{1/2}}{e} \bar{F}_{\ell mp}(i)\, G'_{\ell pq}(e) - \frac{\cot i}{(1-e^2)^{1/2}} \bar{F}'_{\ell mp}(i)\, G_{\ell pq}\right] n \left(\frac{a_e}{a}\right)^{\ell} \varphi^{B}_{\ell mpq} \,. \tag{5.11}$$

Since $G_{\ell pq}(e)$ is $O(e^{|q|})$ it is sufficient to restrict q to take the values $q = 0, \pm 1$ only. Using Kaula's (1966) expression for $G_{\ell p0}(e)$, namely

$$G_{\ell p0}(e) = (1+\beta^2)^{\ell} \sum_{k=0}^{\infty} \left\{ \sum_{r=0}^{k} \binom{2p-2\ell}{k-r} \frac{(-1)^r}{r!} \left(\frac{e}{2\beta}\right)^r (\ell-2p)^r \right\} * \left\{ \sum_{r=0}^{k} \binom{-2p}{k-r} \frac{1}{r!} \left(\frac{e}{2\beta}\right)^r (\ell-2p)^r \right\} \beta^{2k}$$

where $\beta = \dfrac{e}{1 + (1-e^2)^{1/2}} = O(e/2)$ and Allan's expression for $G_{\ell pq}(e)$ $q \neq 0$, given by

$$G_{\ell pq}(e) = \begin{cases} \left(-\frac{e}{2}\right)^{q} \sum_{z=0}^{q} \frac{(2p-\ell-q)^z}{z!} \binom{2p-2\ell}{q-z} + O(e^{q+2}) \,, & q > 0 \\ \left(-\frac{e}{2}\right)^{-q} \sum_{z=0}^{-q} \frac{(\ell-2p+q)^z}{z!} \binom{-2p}{-q-z} + O(e^{-q+2}) \,, & q < 0 \end{cases}$$

then for $\ell-2p+q = \alpha\gamma$, i.e. $p = \dfrac{\ell + q - \alpha\gamma}{2}$

$$G_{\ell,\frac{1}{2}(\ell-\alpha\gamma),0}(e) = 1 + e^2\left[\frac{\ell}{4}(\ell+1)-\alpha^2\gamma^2\right] + O(e^4)$$
$$G_{\ell,\frac{1}{2}(\ell-\alpha\gamma\pm1),\pm1}(e) = \frac{e}{2}\left[\ell-1\pm2\alpha\gamma\right] + O(e^3) \qquad (5.12)$$

and consequently

$$G'_{\ell,\frac{1}{2}(\ell-\alpha\gamma),0}(e) = 2e\left[\frac{\ell}{4}(\ell+1)-\alpha^2\gamma^2\right] + O(e^3);$$
$$G'_{\ell,\frac{1}{2}(\ell-\alpha\gamma\pm1),\pm1}(e) = \frac{1}{2}\left[\ell-1\pm2\alpha\gamma\right] + O(e^2). \qquad (5.13)$$

Applying the resonance constraint $\ell-\alpha\gamma+q = 0$, restricting $q = 0, \pm 1$ and utilizing (5.12) and (5.13), equation (5.11) becomes

$$\dot{e}_{\ell m} = \frac{e}{2}\alpha\gamma\left(\frac{\mu}{a^3}\right)^{1/2}\left(\frac{a_e}{a}\right)^{\ell}\overline{F}_{\ell m,\frac{1}{2}(\ell-\alpha\gamma)}\,\varphi^{A}_{\ell m,\frac{1}{2}(\ell-\alpha\gamma),0}$$
$$-\left(\frac{\mu}{a^3}\right)^{1/2}\left(\frac{a_e}{a}\right)^{\ell}\overline{F}_{\ell m,\frac{1}{2}(\ell-\alpha\gamma+1)}\frac{1}{2}\left[\ell-1+2\alpha\gamma\right]\varphi^{A}_{\ell m,\frac{1}{2}(\ell-\alpha\gamma+1),1}$$
$$+\left(\frac{\mu}{a^3}\right)^{1/2}\left(\frac{a_e}{a}\right)^{\ell}\overline{F}_{\ell m,\frac{1}{2}(\ell-\alpha\gamma-1)}\frac{1}{2}\left[\ell-1-2\alpha\gamma\right]\varphi^{A}_{\ell m,\frac{1}{2}(\ell-\alpha\gamma-1),-1} + \text{terms } O(e^2)$$
$$e\dot{\omega}_{\ell mpq} = e\left(\frac{\mu}{a^3}\right)^{1/2}\left(\frac{a_e}{a}\right)^{\ell}\left[\overline{F}_{\ell m,\frac{1}{2}(\ell-\alpha\gamma)}\,2\left[\frac{\ell}{4}(\ell+1)-\alpha^2\gamma^2\right] - \cot i\,\overline{F}'_{\ell m,\frac{1}{2}(\ell-\alpha\gamma)}\right]\varphi^{B}_{\ell m,\frac{1}{2}(\ell-\alpha\gamma),0}$$
$$+\left(\frac{\mu}{a^3}\right)^{1/2}\left(\frac{a_e}{a}\right)^{\ell}\overline{F}_{\ell m,\frac{1}{2}(\ell-\alpha\gamma+1)}\frac{1}{2}\left[\ell-1+2\alpha\gamma\right]\varphi^{B}_{\ell m,\frac{1}{2}(\ell-\alpha\gamma+1),1}$$
$$+\left(\frac{\mu}{a^3}\right)^{1/2}\left(\frac{a_e}{a}\right)^{\ell}\overline{F}_{\ell m,\frac{1}{2}(\ell-\alpha\gamma-1)}\frac{1}{2}\left[\ell-1-2\alpha\gamma\right]\varphi^{B}_{\ell m,\frac{1}{2}(\ell-\alpha\gamma-1),-1} + \text{terms } O(e^2). \qquad (5.14)$$

Upon utilizing the relationship between $\psi_{\ell mpq}$ and $\Phi_{\alpha\beta}$ and assuming the resonance constraints, basic trigonometric identities give

$$\sin \psi_{\ell m,\frac{1}{2}(\ell-\alpha\gamma),0} = \sin \gamma\Phi_{\alpha\beta}$$

$$\cos \psi_{\ell m,\frac{1}{2}(\ell-\alpha\gamma),0} = \cos \gamma\Phi_{\alpha\beta}$$

$$\sin \psi_{\ell m,\frac{1}{2}(\ell-\alpha\gamma\pm1),\pm1} = \sin \gamma\Phi_{\alpha\beta} \cos \omega \mp \cos \gamma\Phi_{\alpha\beta} \sin \omega$$

$$\cos \psi_{\ell m,\frac{1}{2}(\ell-\alpha\gamma\pm1),\pm1} = \cos \gamma\Phi_{\alpha\beta} \cos \omega \pm \sin \gamma\Phi_{\alpha\beta} \sin \omega .$$

Hence the substitution of (5.14) into equation (5.11) yields

$$\begin{aligned}
\dot{\xi}_{\ell m} &= e \cos \omega \left[\frac{\alpha\gamma}{2}\right] \left(\frac{\mu}{a^3}\right)^{1/2} \left(\frac{a_e}{a}\right)^{\ell} \bar{F}_{\ell m,\frac{1}{2}(\ell-\alpha\gamma)} \phi^{A}_{\ell m} \\
&- \frac{1}{2}(\ell-1+2\alpha\gamma) \bar{F}_{\ell m,\frac{1}{2}(\ell-\alpha\gamma+1)} \left(\frac{\mu}{a^3}\right)^{1/2} \left(\frac{a_e}{a}\right)^{\ell} \phi^{A}_{\ell m} \\
&+ \frac{1}{2}(\ell-1-2\alpha\gamma) \bar{F}_{\ell m,\frac{1}{2}(\ell-\alpha\gamma-1)} \left(\frac{\mu}{a^3}\right)^{1/2} \left(\frac{a_e}{a}\right)^{\ell} \phi^{A}_{\ell m} \\
&+ e \sin \omega \left[\bar{F}_{\ell m,\frac{1}{2}(\ell-\alpha\gamma)} 2\left[\frac{\ell}{4}(\ell+1)-\alpha^2\gamma^2\right] - \cot i \, \bar{F}_{\ell m,\frac{1}{2}(\ell-\alpha\gamma)}\right] \left(\frac{\mu}{a^3}\right)^{1/2} \left(\frac{a_e}{a}\right)^{\ell} \phi^{B}_{\ell m}
\end{aligned} \tag{5.15}$$

and

$$\begin{aligned}
\dot{\eta}_{\ell m} &= e \sin \omega \left[\frac{\alpha\gamma}{2}\right] \left(\frac{\mu}{a^3}\right)^{1/2} \left(\frac{a_e}{a}\right)^{\ell} \bar{F}_{\ell m,\frac{1}{2}(\ell-\alpha\gamma)} \phi^{A}_{\ell m} \\
&+ \frac{1}{2}(\ell-1+2\alpha\gamma) \bar{F}_{\ell m,\frac{1}{2}(\ell-\alpha\gamma+1)} \left(\frac{\mu}{a^3}\right)^{1/2} \left(\frac{a_e}{a}\right)^{\ell} \phi^{B}_{\ell m} \\
&+ \frac{1}{2}(\ell-1-2\alpha\gamma) \bar{F}_{\ell m,\frac{1}{2}(\ell-\alpha\gamma-1)} \left(\frac{\mu}{a^3}\right)^{1/2} \left(\frac{a_e}{a}\right)^{\ell} \phi^{B}_{\ell m} \\
&+ e \sin \omega \left[\bar{F}_{\ell m,\frac{1}{2}(\ell-\alpha\gamma)} 2\left[\frac{\ell}{4}(\ell+1)-\alpha^2\gamma^2\right] - \cot i \, \bar{F}_{\ell m,\frac{1}{2}(\ell-\alpha\gamma)}\right] \left(\frac{\mu}{a^3}\right)^{1/2} \left(\frac{a_e}{a}\right)^{\ell} \phi^{B}_{\ell m}
\end{aligned} \tag{5.16}$$

where $\phi^{A}_{\ell m}$ and $\phi^{B}_{\ell m}$ are given by (2.37).

It is only to O(e) that the expressions in (5.15) and (5.16), for which $q = \pm 1$, have similar coefficients. Without these conditions the following analysis would not be possible.

Thus, summing over all permissible ℓ and m (hence γ), subject to the constraints given by equation (2.34), the rates of change may be written

$$\begin{aligned} \dot{\xi} &= V(\Phi)\xi - W(\Phi)\eta + G(\Phi) \\ \dot{\eta} &= W(\Phi)\xi + V(\Phi)\eta + H(\Phi) \end{aligned} \tag{5.17}$$

where, in the interests of brevity, the subscripts α and β on Φ have been suppressed and

$$V(\Phi) = \sum_{\ell,m} \frac{\alpha\gamma}{2} \left(\frac{\mu}{a^3}\right)^{1/2} \left(\frac{a_e}{a}\right)^{\ell} \overline{F}_{\ell m,\frac{1}{2}(\ell-\alpha\gamma)}\, \phi^{A}_{\ell m}$$

$$W(\Phi) = \sum_{\ell,\,m} \left[\overline{F}_{\ell m,\frac{1}{2}(\ell-\alpha\gamma)}\, 2\left[\frac{\ell}{4}(\ell+1)-\alpha^2\gamma^2\right] - \cot i\, \overline{F}'_{\ell m,\frac{1}{2}(\ell-\alpha\gamma)}\right]\left(\frac{\mu}{a^3}\right)^{1/2}\left(\frac{a_e}{a}\right)^{\ell} \phi^{B}_{\ell m}$$

$$G(\Phi) = \sum_{\ell,\,m} \left[\frac{1}{2}(\ell-1-2\alpha\gamma)\, \overline{F}_{\ell m,\frac{1}{2}(\ell-\alpha\gamma-1)} - \frac{1}{2}(\ell-1+2\alpha\gamma)\, \overline{F}_{\ell m,\frac{1}{2}(\ell-\alpha\gamma+1)}\right]\left(\frac{\mu}{a^3}\right)^{1/2}\left(\frac{a_e}{a}\right)^{\ell} \phi^{A}_{\ell m}$$

$$H(\Phi) = \sum_{\ell,\,m} \left[\frac{1}{2}(\ell-1-2\alpha\gamma)\, \overline{F}_{\ell m,\frac{1}{2}(\ell-\alpha\gamma-1)} + \frac{1}{2}(\ell-1+2\alpha\gamma)\, \overline{F}_{\ell m,\frac{1}{2}(\ell-\alpha\gamma+1)}\right]\left(\frac{\mu}{a^3}\right)^{1/2}\left(\frac{a_e}{a}\right)^{\ell} \phi^{B}_{\ell m}$$

(5.18)

In matrix form (5.17) becomes

$$\dot{\Psi}(t) = \begin{pmatrix} V(\Phi) & -W(\Phi) \\ W(\Phi) & V(\Phi) \end{pmatrix} \Psi(t) + \begin{bmatrix} G(\Phi) \\ H(\Phi) \end{bmatrix} \tag{5.19}$$

where again $\underline{\Psi}(t) = (\xi, \eta)^T$.

The expressions within the summations of (5.18) may be written in terms of lumped harmonic coefficients.

§5.3 ATMOSPHERIC DRAG

We now examine the effect of air–drag on a near–circular orbit. Utilizing the expressions for air–density derived in section 2.2, the resulting changes in the semi–major axis and eccentricity, over one revolution, may be written (Cook and King–Hele, 1966)

$$\begin{aligned} \Delta a &= -2a_0^2 \rho_0 \delta\pi \left(1 + 2\beta a_0 e^2\right) \exp\left[\beta\left(a_0 - a - x_0\right)\right] \\ \Delta e &= -a_0 \rho_0 \delta\pi e \left(\beta a_0 + 1\right) \exp\left[\beta\left(a_0 - a - x_0\right)\right] \end{aligned} \qquad (5.20)$$

where δ is a constant and depends upon the properties of a particular satellite (detailed in chapter 2), $\beta = 1/H$ and $x_0 = a_0 e$ (a_0 being the initial value of a).

The orbital period, T, is the change in time over one revolution

$$\Delta t = T = 2\pi\left(a_0^3/\mu\right)^{1/2}$$

and dividing Δa and Δe by Δt, yields the rates of change of a and e, to O(e), as

$$\dot{a} = -\left(\mu a_0\right)^{1/2} \rho_0 \delta \exp\left[\beta\left(a_0 - a - x_0\right)\right] \qquad (5.21)$$

and

$$\dot{e} = -\frac{1}{2H}\left(\mu a_0\right)^{1/2} \rho_0 \delta e \exp\left[\beta\left(a_0 - a - x_0\right)\right] . \qquad (5.22)$$

Since $e_0 \ll 1$, x_0 may be neglected and as a first approximation (5.21) integrates to

$$t \simeq \frac{H}{\left(\mu a_0\right)^{1/2} \delta \rho_0} \left\{1 - \exp\left[-\beta\left(a_0 - a\right)\right]\right\}$$

which may be rewritten as

$$\exp\left[\beta\left(a_0 - a\right)\right] \simeq \frac{1}{1 - Gt} \tag{5.23}$$

where

$$G = \frac{\left(\mu a_0\right)^{1/2} \rho_0 \delta}{H} \ . \tag{5.24}$$

Substitution of (5.23) and (5.24) into (5.22) gives rise to the differential equation

$$\dot{e} = -\frac{G}{2}\left(1 - Gt\right)^{-1} e \exp\left[-\beta x_0\right] \tag{5.25}$$

which may be integrated, yielding

$$\ln e = \frac{1}{2}\exp\left[-\beta x_0\right] \ln\left(1 - Gt\right) + \ln e_0 \tag{5.26}$$

and since $\beta x_0 \ll 1$, (5.26) gives as a first approximation

$$e \simeq e_0 \left(1 - Gt\right)^{1/2} . \tag{5.27}$$

Alternatively $\Delta\xi$ and $\Delta\eta$ may be written as

$$\begin{aligned} \Delta\xi &= \Delta e \cos\omega - e\,\Delta\omega \sin\omega \\ \Delta\eta &= \Delta e \sin\omega + e\,\Delta\omega \cos\omega \end{aligned} \ . \tag{5.28}$$

For a spherically symmetric atmosphere $\Delta\omega = 0$ (King–Hele, 1989), hence (5.20) and (5.28) lead to

$$\begin{aligned} \Delta\xi &= -a_0 \rho_0 \delta\pi \left(\beta a_0 + 1\right) \exp\left[\beta\left(a_0 - a - x_0\right)\right] \xi \\ \Delta\eta &= -a_0 \rho_0 \delta\pi \left(\beta a_0 + 1\right) \exp\left[\beta\left(a_0 - a - x_0\right)\right] \eta \ . \end{aligned} \tag{5.29}$$

Again, dividing through by $\Delta t = T$ and utilizing (5.23) and (5.24), equation (5.29) becomes

$$\begin{aligned} \dot{\xi} &= -\frac{G}{2}(1 - Gt)^{-1} \exp\left[-\beta x_0\right] \xi \\ \dot{\eta} &= -\frac{G}{2}(1 - Gt)^{-1} \exp\left[-\beta x_0\right] \eta \end{aligned} \tag{5.30}$$

and putting $\exp\left[-\beta x_0\right] \approx 1$, (5.30) reduces to the matrix expression

$$\dot{\underline{\Psi}}(t) = \begin{pmatrix} -\frac{G}{2}(1 - Gt)^{-1} & 0 \\ 0 & -\frac{G}{2}(1 - Gt)^{-1} \end{pmatrix} \underline{\Psi}(t) \tag{5.31}$$

which, after comparison with (5.25)–(5.27), yields

$$\underline{\Psi}(t) = (1 - Gt)^{1/2}\, \underline{\Psi}_0 \ .$$

CHAPTER VI

ZONALS AND RESONANCE PERTURBATIONS ON A NEAR-CIRCULAR ORBIT

§6.1 EQUATIONS OF MOTION

The perturbation of ξ and η due to the zonals has been discussed previously in chapter 5 and may be summarized as

$$\dot{\xi} = -k\eta + C$$
$$\dot{\eta} = k\xi$$

where

$$k = 3\left(\frac{\mu}{a^3}\right)^{1/2} J_2 \left(\frac{a_e}{a}\right)^2 \left(1 - \frac{5}{4}\sin^2 i\right)$$

$$C = \left(\frac{\mu}{a^3}\right)^{1/2} \sum_{n_{odd} \geq 3} J_n \left(\frac{a_e}{a}\right)^n \frac{n-1}{n(n+1)} P_n^1(0)\, P_n^1(\cos i).$$

The perturbation due to the tesserals at $\beta : \alpha$ resonance is developed from the longitude–dependent part of the geopotential, which after substitution into Lagrange's planetary equations (2.24) for $\dot{e}$ and $\dot{\omega}$ and utilizing equation (5.2) yields to O(e) equation (5.17), namely

$$\dot{\xi} = V(\Phi_{\alpha\beta})\xi - W(\Phi_{\alpha\beta})\eta + G(\Phi_{\alpha\beta})$$
$$\dot{\eta} = W(\Phi_{\alpha\beta})\xi + V(\Phi_{\alpha\beta})\eta + H(\Phi_{\alpha\beta})$$

Combining the effects of the zonals and the resonant tesserals on the perturbation of $\dot{\xi}$ and $\dot{\eta}$ gives rise to differential equations which can be represented in matrix form by

$$\dot{\psi}(t) = \begin{pmatrix} V(\Phi) & -W(\Phi)-k \\ W(\Phi)+k & V(\Phi) \end{pmatrix} \psi(t) + \begin{pmatrix} G(\Phi) + C \\ H(\Phi) \end{pmatrix} \qquad (6.1)$$

where $\underline{\psi} = (\xi, \eta)^T$ and for brevity the subscripts α and β on Φ have been suppressed.

Equation (6.1) is a non–homogeneous linear differential equation which may be expressed in the form

$$\dot{\underline{X}}(t) = \underline{A}(t)\,\underline{X}(t) + \underline{P}(t) \tag{6.2}$$

where $\underline{X} = (x_1, x_2)^T$; $A_{ij} = A_{ij}(t)$ $(i, j = 1, 2)$ and $P(t) = (p_1(t), p_2(t))^T$; and t lies in an interval J, which in this instance is $(-\infty, \infty)$. If $\underline{A}(t)$ and $\underline{P}(t)$ are continuous on J, the solution to (6.2) may be written (Wilson, 1971)

$$\underline{X}(t) = \underline{M}(t)\,\underline{M}^{-1}(t_0)\,\underline{X}_0 + \int_{t_0}^{t} \underline{M}(t)\,\underline{M}^{-1}(s)\,\underline{P}(s)\,ds \qquad \forall\ t, t_0 \in J \tag{6.3}$$

where $\underline{M}(t)$ is called a *fundamental matrix,* whose columns satisfy the homogeneous linear differential equation

$$\dot{\underline{X}}(t) = \underline{A}(t)\,\underline{X}(t) \tag{6.4}$$

and is non–singular. $\underline{M}(t)$ is not unique, but is defined to within a scalar multiplication or a constant matrix multiplication. Thus, a $\underline{M}(t)$ and $\underline{M}(t)\underline{C}$ are also fundamental matrices of the homogeneous linear differential equation (6.4), where 'a' is an arbitrary constant and $\underline{C}$ is a non–singular constant matrix. (Equation (6.3) is often recognised as the formula for the variation of parameters.)

If the matrix $\underline{A}(t)$ is written in the form

$$\underline{A}(t) = \begin{pmatrix} a_1(t) & -a_2(t) \\ a_2(t) & a_1(t) \end{pmatrix}, \tag{6.5}$$

then by inspection, the general solution for $\underline{M}(t)$ is given by

$$\underline{M}(t) = \begin{pmatrix} \cos\theta(t) & \sin\theta(t) \\ \sin\theta(t) & -\cos\theta(t) \end{pmatrix} \exp\varphi(t) \tag{6.6}$$

where $\theta(t)$ and $\varphi(t)$ are indefinite integrals of the form

$$\theta(t) = \int^{t} a_2(t)\,dt \;; \qquad \varphi(t) = \int^{t} a_1(t)\,dt \tag{6.7}$$

where the constants of integration may be neglected.

In equation (6.1), $V(\Phi)$ and $W(\Phi)$ are $O(J_{\ell m})$, where $J_{\ell m} = \sqrt{C_{\ell m}^2 + S_{\ell m}^2}$ and oscillatory (except at exact commensurability), whereas k is $O(J_2)$ (except at critical inclinations). Thus, by an order of magnitude study, V and W can be neglected since $J_{\ell m} = O(J_2^2)$ and equation (6.1) simplifies to

$$\dot{\underline{\Psi}}(t) = \begin{pmatrix} 0 & -k \\ k & 0 \end{pmatrix} \underline{\Psi}(t) + \begin{pmatrix} G + C \\ H \end{pmatrix}. \tag{6.8}$$

A *fundamental matrix* for the non–homogeneous linear differential equation (6.8) may, by equations (6.5) through to (6.7), be written in the form

$$\underline{M}(t) = \begin{pmatrix} \cos kt & \sin kt \\ \sin kt & -\cos kt \end{pmatrix}$$

with the property $\underline{M}^{-1}(t) = \underline{M}(t)$.

The Complementary Solution

The *complementary solution* of (6.8) is given by equation (6.3) with $\underline{P}(s) \equiv \underline{0}$; thus

$$\Psi_c(t) = \begin{pmatrix} \cos kt & \sin kt \\ \sin kt & -\cos kt \end{pmatrix} \begin{pmatrix} \cos kt_0 & \sin kt_0 \\ \sin kt_0 & -\cos kt_0 \end{pmatrix} \Psi_0$$
$$= \begin{pmatrix} \cos k(t-t_0) & -\sin k(t-t_0) \\ \sin k(t-t_0) & \cos k(t-t_0) \end{pmatrix} \begin{pmatrix} \xi_0 \\ \eta_0 \end{pmatrix}. \qquad (6.9)$$

On putting $t_0 = 0$, equation (6.9) becomes

$$\Psi_c(t) = \begin{pmatrix} -\eta_0 & \xi_0 \\ \xi_0 & \eta_0 \end{pmatrix} \begin{pmatrix} \sin kt \\ \cos kt \end{pmatrix}. \qquad (6.10)$$

In order to evaluate the *particular solution,* it is necessary to use an expression for the resonance angle that is explicitly given in terms of time.

Development of the Particular Solution

For general $\beta : \alpha$ resonance, $G(\Phi)$ and $H(\Phi)$ from equations (2.37) and (5.18) may be written

$$G(\Phi) = \sum_{\gamma} \left\{ \begin{bmatrix} A_{c\gamma} - B_{c\gamma} \\ -A_{s\gamma} + B_{s\gamma} \end{bmatrix}_{\alpha\gamma \text{ even}}^{\alpha\gamma \text{ odd}} \sin \gamma\Phi - \begin{bmatrix} A_{s\gamma} - B_{s\gamma} \\ A_{c\gamma} - B_{c\gamma} \end{bmatrix}_{\alpha\gamma \text{ even}}^{\alpha\gamma \text{ odd}} \cos \gamma\Phi \right\}$$
$$H(\Phi) = \sum_{\gamma} \left\{ \begin{bmatrix} A_{c\gamma} + B_{c\gamma} \\ -A_{s\gamma} - B_{s\gamma} \end{bmatrix}_{\alpha\gamma \text{ even}}^{\alpha\gamma \text{ odd}} \cos \gamma\Phi + \begin{bmatrix} A_{s\gamma} + B_{s\gamma} \\ A_{c\gamma} + B_{c\gamma} \end{bmatrix}_{\alpha\gamma \text{ even}}^{\alpha\gamma \text{ odd}} \sin \gamma\Phi \right\} \qquad (6.11)$$

where the coefficients $A_{c\gamma}$, $A_{s\gamma}$, $B_{s\gamma}$, $B_{s\gamma}$ are functions of inclination and the lumped harmonics and may be taken as constant for a particular satellite. In detail

$$\left.\begin{matrix} A_{c\gamma} \\ A_{s\gamma} \end{matrix}\right\} = \left(\frac{\mu}{a^3}\right)^{1/2} \left(\frac{a_e}{a}\right)^L \frac{1}{2} (L-1-2\alpha\gamma)\, \bar{F}_{L,\beta\alpha,\frac{1}{2}(L-\alpha\gamma-1)} \begin{Bmatrix} \bar{C}_{\beta\gamma}^{-1,\alpha\gamma+1} \\ \bar{S}_{\beta\gamma}^{-1,\alpha\gamma+1} \end{Bmatrix}$$

and

$$\left.\begin{matrix} B_{c\gamma} \\ \\ B_{s\gamma} \end{matrix}\right\} = \left(\frac{\mu}{a^3}\right)^{1/2} \left(\frac{a_e}{a}\right)^{L} \frac{1}{2}\left(L-1+2\alpha\gamma\right) \bar{F}_{L,\beta\alpha,\frac{1}{2}(L-\alpha\gamma+1)} \left\{\begin{matrix} \bar{C}^{1,\alpha\gamma-1}_{\beta\gamma} \\ \\ \bar{S}^{1,\alpha\gamma-1}_{\beta\gamma} \end{matrix}\right.$$

where

$$L = \beta\gamma + \begin{bmatrix} 0 \\ 1 \end{bmatrix}_{\alpha\gamma \text{ even}}^{\alpha\gamma \text{ odd}} .$$

For a satellite experiencing 14:1 resonance, as for instance Cosmos 1603, equations (6.11) become

$$\begin{aligned} G(\Phi) &= (A_c - B_c)\sin\Phi - (A_s - B_s)\cos\Phi \\ H(\Phi) &= (A_c + B_c)\cos\Phi + (A_s + B_s)\sin\Phi \end{aligned}$$

on taking the dominant $\gamma = 1$ terms only and dropping the γ subscript. The coefficients are given by

$$\left.\begin{matrix} A_c \\ \\ A_s \end{matrix}\right\} = \left(\frac{\mu}{a^3}\right)^{1/2} \left(\frac{a_e}{a}\right)^{14} \frac{11}{2} \bar{F}_{14,14,6} \left\{\begin{matrix} \bar{C}^{-1,2}_{14} \\ \\ \bar{S}^{-1,2}_{14} \end{matrix}\right.$$

$$\left.\begin{matrix} B_c \\ \\ B_s \end{matrix}\right\} = \left(\frac{\mu}{a^3}\right)^{1/2} \left(\frac{a_e}{a}\right)^{14} \frac{15}{2} \bar{F}_{14,14,7} \left\{\begin{matrix} \bar{C}^{1,0}_{14} \\ \\ \bar{S}^{1,0}_{14} \end{matrix}\right. .$$

To obtain the *particular solution* it is necessary to integrate $\underline{M}^{-1}(t)\,\underline{P}(t)$ between t_0 and t, where $\underline{M}^{-1}(t)$ is the same *fundamental matrix* as defined in section 6.1. Without loss of generality we take $t_0 = 0$ and denote

$$\underline{\aleph}(t) = \int_0^t \underline{M}^{-1}(s)\,\underline{P}(s)\,ds = \int_0^t \begin{pmatrix} \cos ks & \sin ks \\ \sin ks & -\cos ks \end{pmatrix} \begin{bmatrix} G(\Phi(s)) + C \\ H(\Phi(s)) \end{bmatrix} ds. \qquad (6.12)$$

Expanding terms we may write

$$\underline{\aleph}(t) = \int_0^t \begin{bmatrix} C\cos ks + G(s)\cos ks + H(s)\sin ks \\ C\sin ks + G(s)\sin ks - H(s)\cos ks \end{bmatrix} ds.$$

Now

$$\begin{aligned} G(s)\cos ks + H(s)\sin ks = {} & (A_c - B_c)\sin\Phi\cos ks - (A_s - B_s)\cos\Phi\cos ks \\ & + (A_c + B_c)\cos\Phi\sin ks + (A_s + B_s)\sin\Phi\sin ks \\ = {} & A_c\sin(\Phi + ks) - B_c\sin(\Phi - ks) \\ & - A_s\cos(\Phi + ks) + B_s\cos(\Phi - ks) \end{aligned}$$

and

$$\begin{aligned} G(s)\sin ks - H(s)\cos ks = {} & (A_c - B_c)\sin\Phi\sin ks - (A_s - B_s)\cos\Phi\sin ks \\ & - (A_c + B_c)\cos\Phi\cos ks - (A_s + B_s)\sin\Phi\cos ks \\ = {} & -A_c\cos(\Phi + ks) - B_c\cos(\Phi - ks) \\ & - A_s\sin(\Phi + ks) - B_s\sin(\Phi - ks). \end{aligned}$$

Thus we may write

$$\underline{\aleph}(t) = \underline{A}(t) + \underline{B}(t) + \underline{C}(t)$$

where

$$\underline{A}(t) = \int_0^t \begin{bmatrix} A_c\sin\{\Phi(s) + ks\} - A_s\cos\{\Phi(s) + ks\} \\ -A_c\cos\{\Phi(s) + ks\} - A_s\sin\{\Phi(s) + ks\} \end{bmatrix} ds$$

$$\underline{B}(t) = \int_0^t \begin{bmatrix} -B_c\sin\{\Phi(s) - ks\} + B_s\cos\{\Phi(s) - ks\} \\ -B_c\cos\{\Phi(s) - ks\} - B_s\sin\{\Phi(s) - ks\} \end{bmatrix} ds \qquad (6.13)$$

and

$$\underline{C}(t) = C\int_0^t \begin{bmatrix} \cos ks \\ \sin ks \end{bmatrix} ds = \frac{C}{k}\begin{bmatrix} \sin kt \\ 1 - \cos kt \end{bmatrix}. \qquad (6.14)$$

For shallow Φ resonance, the resonance angle changes quasi–secularly, as discussed in chapter 4. In this instance Φ may be assumed to have the form (4.10), i.e.

$$\Phi(t) \cong \Phi_0 + \sigma t \tag{6.15}$$

where σ is a constant and Φ_0 the value of Φ at $t = 0$.

When $\sigma \approx \pm k$ we observe the unusual phenomenon of deep resonance of a secondary resonance parameter, $\Phi \mp \omega$. The integration in the evaluation of $\underline{A}(t)$ or $\underline{B}(t)$, but not both, is invalidated as a consequence of small divisors. As previously discussed in chapter 4, the neglected small oscillations superimposed on the linear variation of Φ become significant and may dominate. Equation (6.15) is therefore an inadequate expression for the resonance angle and the linear perturbation techniques fail for the evaluation of one of the expressions in equation (6.13). However, the other expression remains valid. The same integration approach is employed whenever $\sigma = +k$ or $\sigma = -k$.

§6.2 SHALLOW $\Phi \pm \omega$ RESONANCE

Proceeding with the integration of equation (6.13), given $|\sigma| \neq |k|$, it is found that

$$\underline{A}(t) = \frac{1}{\sigma+k}\begin{bmatrix} A_c \cos\Phi_0 + A_s \sin\Phi_0 - A_c \cos\{\Phi_0+(\sigma+k)t\} - A_s \sin\{\Phi_0+(\sigma+k)t\} \\ A_c \sin\Phi_0 - A_s \cos\Phi_0 - A_c \sin\{\Phi_0+(\sigma+k)t\} + A_s \cos\{\Phi_0+(\sigma+k)t\} \end{bmatrix}$$

$$\underline{B}(t) = \frac{1}{\sigma-k}\begin{bmatrix} -B_c \cos\Phi_0 - B_s \sin\Phi_0 + B_c \cos\{\Phi_0+(\sigma-k)t\} + B_s \sin\{\Phi_0+(\sigma-k)t\} \\ B_c \sin\Phi_0 - B_s \cos\Phi_0 - B_c \sin\{\Phi_0+(\sigma-k)t\} + B_s \cos\{\Phi_0+(\sigma-k)t\} \end{bmatrix}.$$

(6.16)

To evaluate $\underline{M}(t)\,\underline{\aleph}(t)$, we require

$$\underline{M}(t)\,\underline{A}(t) = \begin{pmatrix} \alpha^{(-)} & -\alpha^{(+)} \\ \alpha^{(+)} & \alpha^{(-)} \end{pmatrix}\begin{bmatrix} \sin\sigma t + \sin kt \\ \cos\sigma t - \cos kt \end{bmatrix}$$

$$\underline{M}(t)\,\underline{B}(t) = \begin{pmatrix} -\beta^{(-)} & \alpha^{(+)} \\ \beta^{(+)} & \beta^{(-)} \end{pmatrix} \begin{bmatrix} \sin \sigma t - \sin kt \\ \cos \sigma t - \cos kt \end{bmatrix} \tag{6.17}$$

and
$$\underline{M}(t)\,\underline{C}(t) = \underline{C}(t) = \frac{C}{k}\begin{bmatrix} \sin kt \\ 1 - \cos kt \end{bmatrix} \tag{6.18}$$

where

$$\begin{aligned} \alpha^{(+)} &= \frac{A_c}{\sigma+k}\cos\Phi_0 + \frac{A_s}{\sigma+k}\sin\Phi_0 \\ \alpha^{(-)} &= \frac{A_c}{\sigma+k}\sin\Phi_0 - \frac{A_s}{\sigma+k}\cos\Phi_0 \\ \beta^{(+)} &= \frac{B_c}{\sigma-k}\cos\Phi_0 + \frac{B_s}{\sigma-k}\sin\Phi_0 \\ \beta^{(-)} &= \frac{B_c}{\sigma-k}\sin\Phi_0 - \frac{B_s}{\sigma-k}\cos\Phi_0 . \end{aligned} \tag{6.19}$$

Thus, from equations (6.17) and (6.18), our particular solution to equation (6.1) may be written

$$\underline{\Psi}_p(t) = \begin{pmatrix} \hat{S}^{(+)} & \hat{C}^{(-)} \\ \hat{C}^{(-)} & -\hat{S}^{(+)} \end{pmatrix}\begin{bmatrix} \sin kt \\ \cos kt \end{bmatrix} + \begin{pmatrix} \hat{S}^{(-)} & -\hat{C}^{(-)} \\ \hat{C}^{(+)} & \hat{S}^{(+)} \end{pmatrix}\begin{bmatrix} \sin \sigma t \\ \cos \sigma t \end{bmatrix} \tag{6.20}$$

where
$$\hat{S}^{(\pm)} = \alpha^{(-)} \pm \beta^{(-)} \quad \text{and} \quad \hat{C}^{(\pm)} = \alpha^{(+)} \pm \beta^{(+)} . \tag{6.21}$$

Combining the *particular solution* (6.20) and the *complementary solution* (6.10) the equations of motion in the (ξ, η) plane are given by

$$\underline{\Psi}(t) = \begin{pmatrix} -\eta_0 + C/k + \hat{S}^{(+)} & \xi_0 + \hat{C}^{(-)} \\ \xi_0 + \hat{C}^{(-)} & \eta_0 - C/k - \hat{S}^{(+)} \end{pmatrix}\begin{bmatrix} \sin kt \\ \cos kt \end{bmatrix} + \begin{pmatrix} \hat{S}^{(-)} & -\hat{C}^{(-)} \\ \hat{C}^{(+)} & \hat{S}^{(+)} \end{pmatrix}\begin{bmatrix} \sin \sigma t \\ \cos \sigma t \end{bmatrix} + \begin{bmatrix} 0 \\ C/k \end{bmatrix} . \tag{6.22}$$

§6.3 DEEP $\Phi - \omega$ RESONANCE

During the one year of orbital analysis Cosmos 1603 exhibited deep resonance of the secondary resonance parameter $\Phi - \omega$. For this reason we examine the theory pertaining to $\sigma \simeq k$.

The expression for the main resonance parameter, Φ, as given by equation (6.15), does not give a true and accurate description of this variable and its explicit time–dependence. In chapter 4 equation (4.22) revealed that this parameter could be written

$$\Phi = \lambda + \sigma t + z(1+2z)\sin\sigma t + \frac{z^2}{8}\sin 2\sigma t + 0(z^3) \qquad (6.23)$$

where again without loss of generality Φ_0 (the initial value of Φ) is taken to be λ at $t = 0$ and σ and z are constants ($z \ll 1$ due to criteria discussed in chapter 4).

Let us write

$$\Phi - kt = \Phi_0 + F(t) \qquad (6.24)$$

where Φ_0 remains arbitrary and $F(t)$ is explicit in terms of time and represents the true and accurate variation of $\Phi - kt$ from the initial value Φ_0, i.e. $F(0) = 0$.

Returning to the second term in equation (6.13), substitution of equation (6.24) yields

$$\underline{B}(t) = \int_0^t \begin{bmatrix} -B_c \sin\Phi_0 \cos F(s) - B_c \cos\Phi_0 \sin F(s) + B_s \cos\Phi_0 \cos F(s) - B_s \sin\Phi_0 \sin F(s) \\ -B_c \cos\Phi_0 \cos F(s) + B_c \sin\Phi_0 \sin F(s) - B_s \sin\Phi_0 \cos F(s) - B_s \cos\Phi_0 \sin F(s) \end{bmatrix} ds$$

$$= \begin{pmatrix} -\hat{\beta}^{(+)} & -\hat{\beta}^{(-)} \\ \hat{\beta}^{(-)} & -\hat{\beta}^{(+)} \end{pmatrix} \int_0^t \begin{bmatrix} \sin F(s) \\ \cos F(s) \end{bmatrix} ds$$

where $\hat{\beta}^{(+)} = B_c \cos\Phi_0 + B_s \sin\Phi_0$; $\hat{\beta}^{(-)} = B_c \sin\Phi_0 - B_s \cos\Phi_0$. (6.25)

Now $\underline{M}(t)\,\underline{B}(t)$ is given by

$$\underline{M}(t)\,\underline{B}(t) = \begin{pmatrix} \cos kt & \sin kt \\ \sin kt & -\cos kt \end{pmatrix} \begin{pmatrix} -\hat{\beta}^{(+)} & -\hat{\beta}^{(-)} \\ \hat{\beta}^{(-)} & -\hat{\beta}^{(+)} \end{pmatrix} \begin{bmatrix} R_s \\ R_c \end{bmatrix}$$

$$= \begin{pmatrix} -\hat{\beta}^{(+)} & \hat{\beta}^{(-)} \\ -\hat{\beta}^{(-)} & -\hat{\beta}^{(+)} \end{pmatrix} \begin{bmatrix} R_s \cos kt + R_c \sin kt \\ R_s \sin kt - R_c \cos kt \end{bmatrix} \qquad (6.26)$$

where $$R_s = \int_0^t \sin F(s)\, ds \quad \text{and} \quad R_c = \int_0^t \cos F(s)\, ds.$$

From equations (6.23) and (6.24), on setting $\Phi_0 = \lambda$, F(t) can be approximated by

$$F(t) \simeq \bar{\omega}t + z(1 + 2z) \sin \sigma t + \frac{z^2}{8} \sin 2\sigma t \qquad (6.27)$$

where $\bar{\omega} = \sigma - k$.

The $\frac{z^2}{8} \sin 2\sigma t$ term contributes less than 1% to the variation of F(t), whilst the $2z^2 \sin \sigma t$ term contributes around 10%. Hence, the smaller term may be neglected and equation (6.27) becomes

$$F(t) \simeq \bar{\omega}t + Z \sin \sigma t$$

where $$Z = z(1 + 2z).$$

Expanding the sine and cosine of F(t) gives

$$\begin{aligned} \sin(\bar{\omega}t + Z \sin \sigma t) &= \sin \bar{\omega}t \cos(Z \sin \sigma t) + \cos \bar{\omega}t \sin(Z \sin \sigma t) \\ \cos(\bar{\omega}t + Z \sin \sigma t) &= \cos \bar{\omega}t \cos(Z \sin \sigma t) - \sin \bar{\omega}t \sin(Z \sin \sigma t) \end{aligned} \qquad (6.28)$$

and upon utilizing the expressions (Abramowitz and Stegun, p361)

$$\sin(Z \sin b) = 2 \sum_{\nu = 0}^{\infty} J_{2\nu+1}(Z) \sin(2\nu+1)b$$

and

$$\cos(Z \sin b) = J_0(Z) + 2\sum_{\nu=1}^{\infty} J_{2\nu}(Z) \cos 2\nu b$$

where $J_\nu(Z)$ are Bessel functions (Abramowitz and Stegun, p360) which for $|Z| < 2$ can be written

$$J_\nu(Z) = (Z/2)^\nu \sum_{k=0}^{\infty} \frac{(-Z^2/4)^k}{k!(\nu + k)!}\ , \tag{6.29}$$

we obtain

$$\sin F(t) = J_0(Z) \sin\bar{\omega}t + 2\sum_{\nu=1}^{\infty} J_{2\nu}(Z) \sin\bar{\omega}t \cos 2\nu\sigma t + 2\sum_{\nu=0}^{\infty} J_{2\nu+1}(Z) \cos\bar{\omega}t \sin(2\nu+1)\sigma t$$

$$\cos F(t) = J_0(Z) \cos\bar{\omega}t + 2\sum_{\nu=1}^{\infty} J_{2\nu}(Z) \cos\bar{\omega}t \cos 2\nu\sigma t - 2\sum_{\nu=0}^{\infty} J_{2\nu+1}(Z) \sin\bar{\omega}t \sin(2\nu+1)\sigma t\ . \tag{6.30}$$

It may be of interest to observe that equations (6.28) and (6.30) are valid for $\bar{\omega} = \sigma \pm k$. Although it is assumed that $\bar{\omega} = \sigma - k$, the following equations are also valid for $\bar{\omega} = \sigma + k$, with the appropriate change of sign for 'k'. Expanding equation (6.30) leads to

$$\sin F(t) = J_0(Z) \sin(\sigma - k)t + \sum_{\nu=1}^{\infty} J_{2\nu}(Z)\{\sin[\sigma(2\nu+1) - k]t - \sin[\sigma(2\nu-1) + k]t\}$$

$$+ \sum_{\nu=0}^{\infty} J_{2\nu+1}(Z)\{\sin[\sigma(2\nu+2) - k]t + \sin[\sigma(2\nu) + k]t\}$$

$$= \sum_{\nu=0}^{\infty} J_\nu(Z) \sin[\sigma(\nu+1) - k]t - \sum_{\nu=1}^{\infty} (-1)^\nu J_\nu(Z) \sin[\sigma(\nu-1) + k]t$$

and

$$\cos F(t) = J_0(Z)\cos(\sigma-k)t + \sum_{\nu=1}^{\infty} J_{2\nu}(Z)\{\cos[\sigma(2\nu+1)-k]t + \cos[\sigma(2\nu-1)+k]t\}$$

$$+ \sum_{\nu=0}^{\infty} J_{2\nu+1}(Z)\{\cos[\sigma(2\nu+2)-k]t - \cos[\sigma(2\nu)+k]t\}$$

$$= \sum_{\nu=0}^{\infty} J_\nu(Z)\cos[\sigma(\nu+1)-k]t + \sum_{\nu=1}^{\infty}(-1)^\nu J_\nu(Z)\cos[\sigma(\nu-1)+k]t\,. \tag{6.31}$$

The summations in equation (6.31) are convergent, enabling term by term integration. Thus, we have

$$R_s^{(\pm)} = \int_0^t \sin F(s)\,ds = \sum_{\nu=0}^{\infty} \frac{J_\nu(Z)\{1-\cos[\sigma(\nu+1)\pm k]t\}}{[\sigma(\nu+1)\pm k]} -$$

$$- \sum_{\nu=1}^{\infty} \frac{(-1)^\nu J_\nu(Z)\{1-\cos[\sigma(\nu-1)\mp k]t\}}{[\sigma(\nu-1)\mp k]}$$

$$R_c^{(\pm)} = \int_0^t \cos F(s)\,ds = \sum_{\nu=0}^{\infty} \frac{J_\nu(Z)\sin[\sigma(\nu+1)\pm k]t}{[\sigma(\nu+1)\pm k]} +$$

$$+ \sum_{\nu=1}^{\infty} \frac{(-1)^\nu J_\nu(Z)\sin[\sigma(\nu-1)\mp k]t}{[\sigma(\nu-1)\mp k]} \tag{6.32}$$

where (±) denotes the choice of sign for k. For Cosmos 1603 the negative sign is applicable.

It is now possible to accumulate components of the *particular solution* from equations (6.14), (6.17), (6.26) and (6.32), yielding

$$\Psi_p(t) = \begin{pmatrix} \alpha^{(-)} & -\alpha^{(+)} \\ \alpha^{(+)} & \alpha^{(-)} \end{pmatrix} \begin{bmatrix} \sin \sigma t \\ \cos \sigma t \end{bmatrix} + \begin{pmatrix} C/k + \alpha^{(-)} & \alpha^{(+)} \\ \alpha^{(+)} & -C/k - \alpha^{(-)} \end{pmatrix} \begin{bmatrix} \sin kt \\ \cos kt \end{bmatrix}$$

$$- \begin{pmatrix} \hat{\beta}^{(+)} & -\hat{\beta}^{(-)} \\ \hat{\beta}^{(-)} & \hat{\beta}^{(+)} \end{pmatrix} \begin{bmatrix} R_s^{(-)} \cos kt + R_c^{(-)} \sin kt \\ R_s^{(-)} \sin kt - R_c^{(-)} \cos kt \end{bmatrix} + \begin{bmatrix} 0 \\ C/k \end{bmatrix}.$$

Hence the final solution to the equations of motion in the (ξ, η) plane, where $\sigma \simeq k$, is

$$\Psi(t) = \begin{pmatrix} -\eta_0 + C/k + \alpha^{(-)} & \xi_0 + \alpha^{(+)} \\ \xi_0 + \alpha^{(+)} & \eta_0 - C/k - \alpha^{(-)} \end{pmatrix} \begin{bmatrix} \sin kt \\ \cos kt \end{bmatrix} + \begin{pmatrix} \alpha^{(-)} & -\alpha^{(+)} \\ \alpha^{(+)} & \alpha^{(-)} \end{pmatrix} \begin{bmatrix} \sin \sigma t \\ \cos \sigma t \end{bmatrix}$$

$$- \begin{pmatrix} \hat{\beta}^{(+)} & -\hat{\beta}^{(-)} \\ \hat{\beta}^{(-)} & \hat{\beta}^{(+)} \end{pmatrix} \begin{bmatrix} R_s^{(-)} \cos kt + R_c^{(-)} \sin kt \\ R_s^{(-)} \sin kt - R_c^{(-)} \cos kt \end{bmatrix} + \begin{bmatrix} 0 \\ C/k \end{bmatrix}. \qquad (6.33)$$

§6.4 DETERMINATION OF LUMPED HARMONICS FROM e cos ω AND e sin ω

In chapter 3, lumped harmonic coefficients were obtained from analysis of the orbital eccentricity of Cosmos 1603. The program PROD removed the effects of the zonal harmonic and luni–solar perturbations. Resonance was modelled in the program THROE, which determined the lumped harmonic coefficients. In this section we estimate the same coefficients via the orbital parameters ξ and η which are related to the eccentricity through equation (5.1), namely

$$\xi = e \cos \omega$$

$$\eta = e \sin \omega.$$

This approach is considered reasonable given the low eccentricity of Cosmos 1603 during the period of analysis ($e < 0.003$). However, it is a much more demanding problem as we attempt to fit two independent variables, hence increasing the number of points to be fitted by a factor of two. Furthermore, after luni–solar perturbations are removed, the intention is to model simultaneously the zonal harmonic perturbations, the resonance perturbations and their interactions.

Equation (6.33) was incorporated in a weighted least–squares–fit of the parameters ξ and η, utilizing the Bessel function expansions of equations (6.29) and (6.32). (The weights were calculated from the PROP 6 S.D.'s for e and ω). The aim was to determine a maximum of four lumped harmonic coefficients and two initial values, ξ_0 and η_0. Drag was not modelled, but was absorbed within the quasi–secular secondary resonance corresponding to the lumped harmonics $\overline{S}_{14}^{1,0}$ and $\overline{C}_{14}^{1,0}$. PROD was run to evaluate luni–solar perturbations to e and ω before ξ and η were evaluated. The adjustment to e on a few epochs was as large as 2×10^{-6} but generally less than 1×10^{-6}, whilst the adjustment to ω approached 0.12 degrees on a small number of epochs, but for the majority was less than 0.02 degrees.

The three parameters $\{\lambda, \sigma, z\}$ were obtained from the least–squares–fit of the resonance angle, in section 4.5, the results of which are given in Table 4.1. Runs 1 to 3, in section 4.5, included either a quadratic coefficient in time (Q), a cubic coefficient (C) or both (B), whilst run 4 had neither (–). Four runs to determine lumped harmonics from ξ and η were made, corresponding to the four sets of $\{\lambda, \sigma, z\}$ available from Table 4.1. The values obtained, along with their S.D.'s and the degree of fit, ε, are given in Table 6.1. Runs 1 to 3 in this section are favoured since drag is in someway accounted for in the parameters $\{\lambda, \sigma, z\}$, even though it is not modelled directly. It must be realised, therefore, that the lumped harmonic coefficients, corresponding to the quasi–secular resonance, may be corrupted by inadequate modelling of air–drag effects. Indeed all parameters absorb other unmodelled effects,

such as resonance effects of other frequencies and SRP, etc. However, as outlined in chapter 3, these unmodelled perturbations are small (including drag) and the results are therefore considered to be highly accurate.

Run	ε	$10^9\,\bar{S}_{14}^{1,0}$	$10^9\,\bar{C}_{14}^{1,0}$	$10^9\,\bar{S}_{14}^{-1,2}$	$10^9\,\bar{C}_{14}^{-1,2}$
1(B)	0.76	60.6 1.5	–27.6 1.3	6.8 7.6	–64.4 7.5
2(C)	0.76	59.5 1.4	–30.3 1.3	3.5 7.5	–64.7 7.4
3(Q)	0.76	61.0 1.5	–26.8 1.3	7.8 7.6	–64.3 7.5
4(–)	0.75	59.0 1.4	–31.8 1.3	0.7 7.5	–65.1 7.2

Table 6.1 The results of a least–squares–fit procedure determining lumped harmonic coefficients from e cos ω and e sin ω.

Despite the slightly improved fit, run 4 is considered less favourable than the other three for the reasons already stated concerning drag. To remain consistent with section 4.5 and in view of the consistency between runs 1 to 3, the preferred values are taken from run 2. A comparison of the preferred values against previously evaluated values is given in Table 6.2.

Table 6.2 A summary of the lumped harmonic values obtained from analysis of the eccentricity and analysis of e cos ω and e sin ω along with the computed values by PGS–3337 (Marsh et al., 1990).

The eccentricity and argument of perigee, recovered from the fitted values of ξ and η, are plotted in Figures 6.1 and 6.2, along with the observed values (adjusted for luni–solar perturbations).

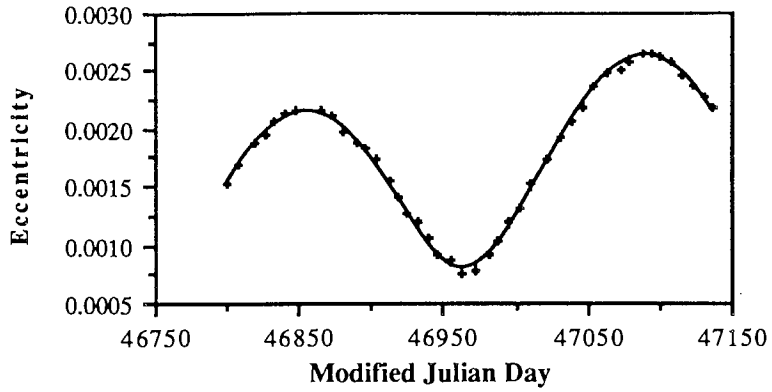

Figure 6.1 Observed values of the eccentricity cleared of luni–solar perturbations, with theoretical fit.

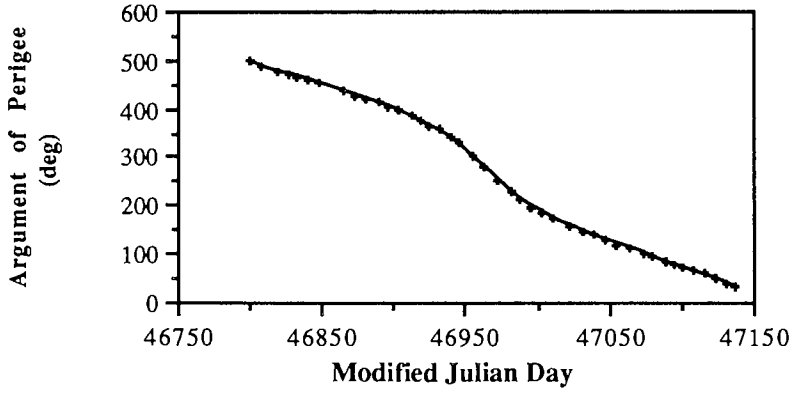

Figure 6.2 Observed values of the argument of perigee cleared of luni–solar perturbations, with theoretical fit.

As would be expected the agreement is good. A better view of the accuracy of this method can be obtained by examination of the residuals. The residuals for the eccentricity and argument of perigee are plotted against time in Figures 6.3 and 6.4.

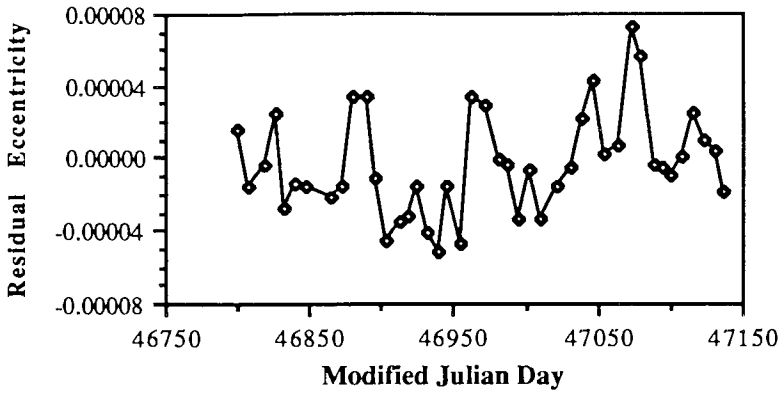

Figure 6.3 The residuals between the calculated and the observed values of the eccentricity.

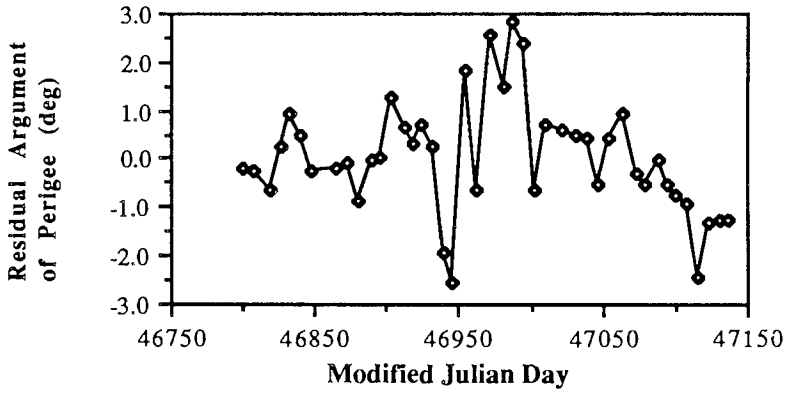

Figure 6.4 The residuals between the calculated and the observed values of the argument of perigee.

On the other hand residuals in ξ and η are given by Figures 6.5 and 6.6.

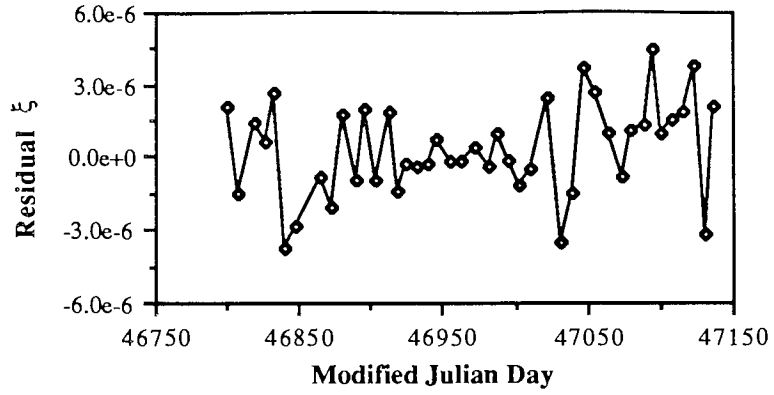

Figure 6.5 The residuals between the calculated and the observed values of e cos ω.

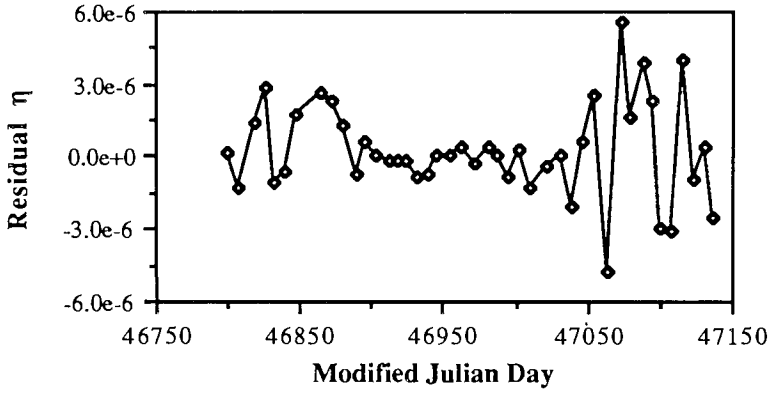

Figure 6.6 The residuals between the calculated and the observed values of e sin ω.

The residuals for ξ and η, in Figures 6.5 and 6.6, diminish in magnitude from their initial values over the first quarter of 1987. They are minimal over the central epochs and increase for the final quarter of 1987. This suggests that unmodelled long–period effects are present and cannot be compensated for by the least–squares–fit procedure. However, the residuals are small relative to the determined values and in all four Figures the even distribution of the residuals indicates a good fit with smaller perturbation effects creating only a background *noise*.

§6.5 FROZEN ORBITS

A *frozen orbit* is one where e and ω are invariant under the influence of zonal harmonic perturbations. In this section we examine the criteria that yield minimal rates of change in the parameters ξ and η, as used to represent near–circular motion. By exploiting frozen orbits, otherwise dominant perturbations are removed and it becomes possible to obtain a better perspective of the remaining perturbations. Further, we explore the possibility of removing or reducing these remaining perturbations, mainly resonances, to yield a *more* frozen orbit.

Φ resonance

It was briefly mentioned in section 5.1 that the solution to the equations of motion for ξ and η, under the influence of the zonals, yielded a *frozen orbit* given the initial condition

$$\begin{bmatrix}\xi_0\\ \eta_0\end{bmatrix} = \Psi_0 = \begin{bmatrix}0\\ C/k\end{bmatrix}. \tag{6.34}$$

When the effects of shallow resonance are incorporated, equation (6.22) gives the remaining small periodic perturbations in ξ and η, namely

$$\Psi(t) = \begin{pmatrix}\hat{S}^{(+)} & \hat{C}^{(-)}\\ \hat{C}^{(-)} & -\hat{S}^{(+)}\end{pmatrix}\begin{bmatrix}\sin kt\\ \cos kt\end{bmatrix} + \begin{pmatrix}\hat{S}^{(-)} & -\hat{C}^{(-)}\\ \hat{C}^{(+)} & \hat{S}^{(+)}\end{pmatrix}\begin{bmatrix}\sin \sigma t\\ \cos \sigma t\end{bmatrix} + \begin{bmatrix}0\\ C/k\end{bmatrix} \tag{6.35}$$

where $\hat{S}^{(\pm)}$ and $\hat{C}^{(\pm)}$ are functions of lumped harmonic coefficients, given by equations (6.21) and (6.19). Motion in the (ξ, η) plane is described in equation (6.35) by the superposition of a circle (kt terms) and an ellipse (σt terms). If $p|k| \simeq q|\sigma|$, where p and q are two mutually prime integers, $\Psi(t)$ returns near to the initial point Ψ_0, with a period $T = \dfrac{2\pi pq}{|k|\,|\sigma|}$.

Upon modifying the initial condition (6.34) to

$$\Psi_0 = \begin{bmatrix} -\hat{C}^{(-)} \\ C/k - \hat{S}^{(+)} \end{bmatrix}, \tag{6.36}$$

the first term in (6.22) vanishes yielding elliptical motion in the (ξ, η) plane, centred on $(0, C/k)$ and with period $T = \frac{2\pi}{|\sigma|}$. When linear perturbation techniques are applicable the initial condition (6.36) represents the best approximation to a frozen orbit for a satellite perturbed by the zonal harmonics and $\beta : \alpha$ resonance.

Exact commensurability of Φ resonance

In the case of exact commensurability, $V(\Phi)$, $W(\Phi)$, $G(\Phi)$ and $H(\Phi)$ in equation (6.1) are invariant and no longer oscillatory. The solution then becomes

$$\Psi(t) = \begin{pmatrix} -\eta_0 + (G+C)/k & \xi_0 + H/k \\ \xi_0 + H/k & \eta_0 - (G+C)/k \end{pmatrix} \begin{bmatrix} \sin kt \\ \cos kt \end{bmatrix} + \frac{1}{k} \begin{bmatrix} -H \\ G + C \end{bmatrix} + \text{terms } O\left(J_{\ell m}^2\right),$$

and thus for the initial condition

$$\Psi_0 = \frac{1}{k} \begin{bmatrix} -H \\ G + C \end{bmatrix}$$

the eccentricity and argument of perigee are frozen.

Deep Φ–ω resonance

Let $\Psi_{(\Phi-\omega)}$ denote the variation in Ψ due to the secondary resonance parameter, $\Phi - \omega$. Examination of the solution to the equations of motion for deep $\Phi - \omega$ resonance, (6.33), reveals

$$\Psi_{(\Phi-\omega)} = -\begin{pmatrix} \hat{\beta}^{(+)} & -\hat{\beta}^{(-)} \\ \hat{\beta}^{(-)} & \hat{\beta}^{(+)} \end{pmatrix} \begin{bmatrix} R_s^{(-)} \cos kt + R_c^{(-)} \sin kt \\ R_s^{(-)} \sin kt - R_c^{(-)} \cos kt \end{bmatrix} \tag{6.37}$$

where $R_s^{(-)}$, $R_c^{(-)}$ and $\hat{\beta}^{(\pm)}$ are given by equations (6.32) and (6.25). Truncating the series expansion for $R_s^{(-)}$, $R_c^{(-)}$ (which is permissible for small z), i.e. taking the first term only, we may write

$$R_s^{(-)} \simeq \frac{1}{\bar{\omega}} \left[1 - \cos \bar{\omega} t\right] \; ; \; R_c^{(-)} \simeq \frac{1}{\bar{\omega}} \sin \bar{\omega} t. \tag{6.38}$$

Recovering the eccentricity, using the relationship $e^2 = \xi^2 + \eta^2$, equations (6.37) and (6.38) yield

$$e^2 \simeq -\frac{2}{\bar{\omega}^2} \left[\left(\hat{\beta}^{(+)}\right)^2 + \left(\hat{\beta}^{(-)}\right)^2\right] \cos \bar{\omega} t \, .$$

Thus taking the derivative with respect to time, we have

$$\dot{e} \simeq \frac{1}{e\bar{\omega}} \left[\left(\hat{\beta}^{(+)}\right)^2 + \left(\hat{\beta}^{(-)}\right)^2\right] \sin \bar{\omega} t,$$

illustrating the quasi–secular increase in the eccentricity that results from deep $\Phi - \omega$ resonance. It follows, therefore, that an orbit in deep $\Phi \pm \omega$ resonance cannot be frozen.

CHAPTER VII

AIR–DRAG PERTURBATIONS ON A NEAR–CIRCULAR ORBIT IN RESONANCE WITH THE EARTH'S GRAVITY

So far we have considered the effects of the zonal and tesseral harmonics on a near–circular orbit, under the assumption that air–drag is minimal. Although drag was considered in the development of the equations of motion for the resonance angle, we have yet to extend the general theory for a resonant orbit. With respect to ξ and η, as used to describe the changes of a near–circular orbit, we initially examined the effects of air–drag neglecting all other perturbations. The theory is now developed combining the effects of zonal harmonics and air–drag with the ultimate intention of incorporating resonance, thus yielding a unified solution for all three perturbations.

§7.1 COMBINING ZONAL HARMONIC PERTURBATIONS WITH AIR–DRAG

Combining the effects of the zonal harmonics and drag on the changes in ξ and η, as given by (5.9) and (5.31), the equations of motion may be written in matrix form as

$$\dot{\underline{\Psi}}(t) = \begin{pmatrix} -\frac{G}{2}(1-Gt)^{-1} & -k \\ k & -\frac{G}{2}(1-Gt)^{-1} \end{pmatrix} \underline{\Psi}(t) + \begin{bmatrix} C \\ 0 \end{bmatrix}. \tag{7.1}$$

Using results from section 6.1, a *fundamental matrix* $\underline{M}(t)$, for equation (7.1) may be written as

$$\underline{M}(t) = (1-Gt)^{1/2}\, \underline{\Theta}(kt) \tag{7.2}$$

where

$$\underline{\Theta}(kt) = \begin{pmatrix} \cos kt & \sin kt \\ \sin kt & -\cos kt \end{pmatrix}.$$

Hence, taking as before the initial value of time to be zero, the *complementary solution* to equation (7.1) is given by, c.f. (6.3)

$$\Psi_c(t) = (1-Gt)^{1/2} \begin{pmatrix} -\eta_0 & \xi_0 \\ \xi_0 & \eta_0 \end{pmatrix} \begin{bmatrix} \sin kt \\ \cos kt \end{bmatrix}, \tag{7.3}$$

and from (6.3) the *particular solution* may be written as

$$\Psi_p(t) = (1-Gt)^{1/2}\, \underline{\Theta}(kt)\, C \int_0^t \begin{bmatrix} \cos ks \\ \sin ks \end{bmatrix} \frac{ds}{(1-Gs)^{1/2}} . \tag{7.4}$$

Upon making the substitution $x = \frac{k}{G}(1-Gs)$, equation (7.4) may be expanded in terms of Fresnel integrals (Abramowitz and Stegun, p300), given by

$$C_1(x) = \frac{1}{\sqrt{2\pi}} \int^x \frac{\cos x}{x^{1/2}}\, dx \quad ; \quad S_1(x) = \frac{1}{\sqrt{2\pi}} \int^x \frac{\sin x}{x^{1/2}}\, dx.$$

Thus defining

$$\begin{aligned} \mathcal{C}(kt) &= C_1\left(k/G\right) - C_1\left(k/G - kt\right) \\ \mathcal{S}(kt) &= S_1\left(k/G\right) - S_1\left(k/G - kt\right), \end{aligned}$$

equation (7.4) yields

$$\Psi_p(t) = C\left(\frac{2\pi}{kG}\right)^{1/2} \underline{\Theta}(kt)\, \underline{\Theta}\left(k/G\right) (1-Gt)^{1/2} \begin{bmatrix} \mathcal{C}(kt) \\ \mathcal{S}(kt) \end{bmatrix}. \tag{7.5}$$

Hence, combining (7.3) and (7.5), the final solution to (7.1) may be written as

$$\Psi(t) = (1-Gt)^{1/2} \begin{pmatrix} -\eta_0 & \xi_0 \\ \xi_0 & \eta_0 \end{pmatrix} \begin{bmatrix} \sin kt \\ \cos kt \end{bmatrix} + (1-Gt)^{1/2} \begin{pmatrix} \theta_s & -\theta_c \\ \theta_c & \theta_s \end{pmatrix} \begin{bmatrix} \mathcal{C}(kt) \cos kt + \mathcal{S}(kt) \sin kt \\ \mathcal{C}(kt) \sin kt - \mathcal{S}(kt) \cos kt \end{bmatrix} \tag{7.6}$$

where $\theta_c = C\left(\frac{2\pi}{kG}\right)^{1/2} \cos {}^{k}/_{G}$ and $\theta_s = C\left(\frac{2\pi}{kG}\right)^{1/2} \sin {}^{k}/_{G}$.

Equation (7.6) does not lend itself to a simple interpolation of the resultant motion of the (ξ, η) parameters. A simplification of the preceding analysis is developed in the next section.

§7.2 EARLY STAGES IN THE LIFE OF THE SATELLITE

Since G is small ($^{1}/_{G} \simeq$ life time of satellite), for a satellite in the early stages of life, Gt remains small. Simplifications are therefore made within the fundamental matrix, which to O(Gt), can be approximated by

$$\underline{M}(t) = \left(1-{}^{Gt}/_{2}\right) \underline{\Theta}(t). \tag{7.7}$$

The *particular solution* thus becomes

$$\begin{aligned} \underline{\Psi}_p(t) &= C\,\underline{\Theta}(kt)\left(1-{}^{Gt}/_{2}\right) \int_0^t \begin{bmatrix} \cos ks \\ \sin ks \end{bmatrix} \left(1+{}^{Gs}/_{2}\right) ds \\ &= {}^{C}/_{k}\left(1-{}^{Gt}/_{2}\right) \begin{pmatrix} 1 & {}^{G}/_{2k} \\ -{}^{G}/_{2k} & 1 \end{pmatrix} \begin{bmatrix} \sin kt \\ 1-\cos kt \end{bmatrix} + Ct \begin{bmatrix} 0 \\ {}^{G}/_{2k} \end{bmatrix}, \end{aligned} \tag{7.8}$$

whence

$$\begin{aligned} \underline{\Psi}(t) = &\begin{pmatrix} -\eta_0 + {}^{C}/_{k} & \xi_0 - \left({}^{G}/_{2k}\right)\left({}^{C}/_{k}\right) \\ \xi_0 - \left({}^{G}/_{2k}\right)\left({}^{C}/_{k}\right) & \eta_0 - {}^{C}/_{k} \end{pmatrix} \left(1-{}^{Gt}/_{2}\right) \begin{bmatrix} \sin kt \\ \cos kt \end{bmatrix} + \\ &+ {}^{C}/_{k} \begin{bmatrix} {}^{G}/_{2k} \\ 1 + {}^{G}/_{2t} \end{bmatrix} \left(1-{}^{Gt}/_{2}\right). \end{aligned} \tag{7.9}$$

In comparison with (5.10), the drag–free result reveals the additional effects of a small linear perturbation, an even smaller quadratic perturbation in η and further periodic variations. The principal difference is, however, the gradual *decay* of the orbit as

$e \to 0$. This is a consequence of the $(1-Gt/2)$ term that appears as a factor throughout in (7.9).

§7.3 INCORPORATING RESONANCE

As in the previous studies for ξ and η under resonant conditions, we neglect $V(\Phi)$ and $W(\Phi)$ in the equations of motion with the tesseral harmonic contribution to the perturbation retained in the vector quantity $\underline{P}(t)$, (see section 6.1)

$$\underline{P}(t) = \begin{bmatrix} C + G(\Phi(t)) \\ H(\Phi(t)) \end{bmatrix}.$$

The fundamental matrix therefore remains as in equation (7.2) and only the particular solution changes, with the integration in (7.8), now written as

$$\underline{\tilde{x}}(t) = \int_0^t \begin{pmatrix} \cos ks & \sin ks \\ \sin ks & -\cos ks \end{pmatrix} \begin{bmatrix} C + G(s) \\ H(s) \end{bmatrix} \frac{ds}{(1-Gs)^{1/2}}, \qquad (7.10)$$

which differs from equation (6.12) for $\underline{x}(t)$ by the term $(1-Gs)^{-1/2}$ in the integrand.

Clearly a similar process to that of section 7.1 is possible, whereby expansion of all terms in (7.10) yields a solution in terms of Fresnel integrals. Alternatively, since G is small in the early stages, we may proceed as in section 7.2 by simplifying the fundamental matrix as given by equation (7.7). Writing

$$\underline{x}'(t) = \underline{A}'(t) + \underline{B}'(t) + \underline{C}'(t), \qquad (7.11)$$

where the prime denotes the derivative with respect to time, then $\underline{\tilde{x}}(t)$ may be written as

$$\underline{\tilde{\aleph}}(t) = \int_0^t \underline{\aleph}'(s)\left[1 + {}^{G}s/2\right] ds = \underline{\aleph}(t) + {}^{G}/2\left[\underline{\tilde{A}}(t) + \underline{\tilde{B}}(t) + \underline{\tilde{C}}(t)\right], \qquad (7.12)$$

where $\underline{\tilde{A}}(t)$, $\underline{\tilde{B}}(t)$ and $\underline{\tilde{C}}(t)$ are defined by equations (7.10) and (7.12) and differ from equations (6.13) and (6.14) through the extra term 's' in the integrand. All three integrals in (7.12) may be evaluated by parts. Each is premultiplied by $\underline{M}(t)$ to contribute small additional terms to the solution (7.9). The development is not straightforward but lengthy and is not detailed here, although the result is summarized. The extra term, denoted $\underline{E}(t)$, is given by

$$\underline{E}(t) = {}^{G}/2\left(1-{}^{Gt}/2\right)\left\{(1+t)\,\underline{Y}\begin{bmatrix}\sin\sigma t\\ \cos\sigma t\end{bmatrix} + \underline{Z}\begin{bmatrix}\sin kt\\ \cos kt\end{bmatrix} + {}^{C}/k\begin{bmatrix}{}^{1}/k\\ t\end{bmatrix}\right\}, \qquad (7.13)$$

where $\underline{Y}$ and $\underline{Z}$ are constant 2×2 matrices. $\underline{Y}$ involves expressions $\alpha^{(\pm)}$ and $\beta^{(\pm)}$, as defined by (6.19), and $\underline{Z}$ involves the parameters C, k and σ, given explicitly by (7.14). The first term involving $\underline{Y}$ is not only O(G) but is also oscillatory. For a first approximation this term may be neglected. The second term, involving $\underline{Z}$, is oscillatory but the coefficients of this matrix are of greater magnitude than those in $\underline{Y}$. The contribution for this term may therefore be retained. In full, $\underline{Z}$ may be written

$$\underline{Z} = \begin{pmatrix} {}^{2k}/(\sigma^2-k^2) & -{}^{C}/k^2 \\ -{}^{C}/k^2 & -{}^{2\sigma}/(\sigma^2-k^2) \end{pmatrix}. \qquad (7.14)$$

The $-{}^{C}/k^2$ contribution is identical to that seen in (7.9) and is clearly a consequence of zonal–drag interaction, whereas the other two terms in $\underline{Z}$ are due to the combined interaction of all three perturbations. The most important contribution in (7.13) is the final term and again is seen in (7.9), thus arising from zonal–drag interactions. This term is of greatest magnitude and dominates for large values of t. Neglecting the first term in (7.13), but retaining the other two, the final solution to the combined

perturbations of zonals, tesserals and air–drag on a near–circular orbit in resonance may be written, for ξ and η, as

$$\underline{\Psi}(t) = \left(1-Gt/2\right)\begin{pmatrix} -\eta_0+C/k+\hat{S}^{(+)}+Gk/\left(\sigma^2-k^2\right) & \xi_0+\hat{C}^{(-)}-GC/2k^2 \\ \xi_0+\hat{C}^{(-)}-GC/2k^2 & \eta_0-C/k-\hat{S}^{(+)}-G\sigma/\left(\sigma^2-k^2\right) \end{pmatrix}\begin{bmatrix}\sin kt \\ \cos kt\end{bmatrix}$$
$$+ \left(1-Gt/2\right)\begin{pmatrix} \hat{S}^{(-)} & -\hat{C}^{(-)} \\ \hat{C}^{(+)} & \hat{S}^{(+)} \end{pmatrix}\begin{bmatrix}\sin \sigma t \\ \cos \sigma t\end{bmatrix} + C/k\left(1-Gt/2\right)\begin{bmatrix} G/2k \\ 1+Gt/2\end{bmatrix}.$$

CHAPTER VIII

CONCLUSIONS

The orbital elements of 1984–106A have been determined at 43 epochs between January and December 1987 using over 2900 observations. Analysis of the eccentricity and mean motion yielded 3 pairs of lumped harmonic coefficients of order 14, given in Tables 8.1 and 8.2. Further pairs of lumped harmonic values of order 28 and 42 were obtained from the analysis of the mean motion and are presented in Table 8.2. Comparison against the NASA Goddard Space Flight Centre global gravity field models, GEM–T1, GEM–T2 and PGS-3337 yielded good agreement at order 14. The two values of 14^{th} order harmonics derived here from analysis of the mean motion are nominally much more accurate than either the GEM values, or previous values obtained from resonance. In view of possible errors of up to 100% in the higher order coefficients of the gravity models, there is reasonable agreement of the 28^{th}–order lumped harmonics. The values for 42^{nd} order lumped harmonic coefficients are probably numerically too large as a result of contamination from unmodelled perturbations.

The satellite was temporarily 'trapped' in secondary resonance as a direct consequence of low air-drag and the near commensurability of the satellite with respect to the secondary resonance parameter Φ–ω. For the USSR satellite the resonance effects were sufficiently large to dominate the low drag effects, with the result that Φ–ω exhibited libration about its mean value, yielding a quasi–secular increase in the eccentricity whilst the perigee height decreased.

An extended examination of the resonance angle was prompted by the secondary resonance phenomenon observed for Cosmos 1603, in conjunction with minimal drag effects. The theory was developed for the resonance parameter incorporating initially the dominant resonance terms and later the smaller resonance terms were introduced. Drag was introduced through a small correction term which modelled air-density variation.

The resulting expressions were used in a least-squares procedure to evaluate lumped harmonic coefficients. The derived values were in good agreement with those obtained from the eccentricity and the mean motion and are given in Table 8.1 for comparison. Lumped harmonic values were obtained using the secondary resonance parameter via the parameters $\xi = e \cos \omega$ and $\eta = e \sin \omega$, as used for near-circular orbits. This more demanding approach yielded good values and gave credence to the analytical techniques employed. The values obtained from this method are given in Table 8.2.

The equations of motion described by ξ and η were examined at great length. Analytical solutions were obtained for shallow Φ resonance and for both deep and shallow $\Phi - \omega$ resonance. The occurrence of deep secondary resonance as experienced by Cosmos 1603 provided an excellent opportunity to verify the developed theory against observed results. The equations of motion proved to be highly accurate.

Frozen orbits were examined, showing that modification of the initial conditions could in some instances reduce the rates of change of e and ω for a near-circular orbit that experienced significant resonance perturbations. However, for the situation of deep $\Phi - \omega$ resonance, the resulting quasi-secular increase in the eccentricity removes any possibility of the orbit being frozen.

Finally, air-drag was introduced analytically to the equations of motion for ξ and η, which were developed to yield a unified solution combining gravity and air-drag. It was revealed that the effect of even minimal air-drag is to reduce the eccentricity to zero.

Table 8.1 A summary of the lumped harmonic values obtained from analysis of the changes in inclination, mean motion and the resonance parameter Φ for 1984–106A along with the computed values given by GEM–T1 (Marsh et al., 1988), GEM–T2 (Marsh et al., 1989) and PGS–3337 (Marsh et al., 1990)

Table 8.2 A summary of the lumped harmonic values obtained from analysis of the change in eccentricity and the parameters ξ and η for 1984–106A along with the computed values given by GEM–T1 (Marsh et al., 1988), GEM–T2 (Marsh et al., 1989) and PGS–3337 (Marsh et al., 1990).

REFERENCES

Abramowitz, M. and Stegun, I.A. (1965) *Handbook of Mathematical Functions,* Dover, New York.

Aksnes, K. (1976) *Short–period and long–period perturbations of a spherical satellite due to direct solar radiation.* Celest. Mech. 13, 89.

Allan, R.R. (1967) *Resonance effects due to the Longitude–dependence of the gravitational field of the rotary primary,* Planet. Space Sci. 15, 53.

Allan, R.R. (1967) *Satellite resonance with longitude–dependent gravity – II. Effects involving the eccentricity.* RAE Technical Report, 67172.

Allan, R.R. (1973) *Satellite Resonance with Longitude – Dependent Gravity – III. Inclination Changes for Close Satellites.* Planet. Space Sci. 21, 205.

Brouwer, D. and Clemence, G.M. (1961) *Methods of Celestial Mechanics.* Academic Press, New York and London.

Cook, G.E. (1966) *Pertrbations of Near–Circular Orbits by the Earth's Gravitational Potential.* Planet Space Sci. 14, 433.

Cook, G.E. and King–Hele, D.G. (1968) *The contraction of satellite orbits under the influence of air–drag. VI Near–Circular orbits with day–to–night variation in air density.* Proc. R. Soc. A 303, 17.

Cook, G.E. (1973) *Basic theory for PROD, a program for computing the development of satellite orbits.* Celest. Mech. 7, 301.

COSPAR, Working Group 4 (1972) *Cospar International Reference Atmosphere 1972.* Akademie–Verlag, Berlin.

Gedeon, G.S. (1969) *Tesseral resonance effects on satellite orbits.* Celest. Mech., 1, 167.

Gooding, R.H. and Taylor, R.J. (1968) *A PROP 3 users' manual.* RAE Technical Report, 68299.

Gooding, R.H. (1971) *Lumped geopotential coefficients* $\bar{C}_{15,15}$ *and* $\bar{S}_{15,15}$ *obtained from resonant variation in the orbit Ariel 3.* RAE Technical Report, 71068.

Gooding, R.H. (1974)*The evolution of the PROP 6 Orbit Determination Program and related topics.* RAE Technical Report, 74164.

Gooding, R.H. and King–Hele, D.G. (1989) *Explicit forms of some functions arising in the analysis of resonant satellite orbits.* Proc. R. Soc. A 422, 241.

Kaula, W.M. (1966) *Theory of Satellite Geodesy.* Blaisdell, Waltham, Mass., USA.

King–Hele, D.G., Walker, D.M.C. and Gooding, R.H. (1979) *Evaluation of* 14^{th} *Order Harmonics in the Geopotential.* Planet. Space Sci. 27, 1.

King–Hele, D.G., Pilkington, J.A., Hiller, H. and Walker, D.M.C. (1981) *The RAE Table of Earth Satellites 1975–1980.* Macmillan Press, London.

King–Hele, D.G. (1985) *Lumped geopotential harmonics of order 14, from the orbit of 1967–11G.* Planet. Space Sci., 33, 1145.

King–Hele, D.G. and Walker, D.M.C. (1986) 14^{th} *order harmonics in the geopotential from the analysis of satellite orbits at resonance.* Planet. Space Sci., 34, 183.

King–Hele, D.G. (1987) *Satellite Orbits in an Atmosphere, Theory and Applications.* Blackie, Glasgow.

Marsh, J.G., Lerch, F.J., Koblinsky, C.J.,Klosko, S.M., Robbins, J.W., Williamson, R.G., Patel, G.B., *NASA Draft Manuscript,* Goddard Space Flight Centre (1988b).

Marsh, J.G., Lerch, F.J., Putney, B.H., Christodoulidis, D.C., Felsentreger, T.L., Sanchez, B.V., Smith, D.E., Klosko, S.M., Martin, T.V., Paulis, E.C., Robbins, J.W., Williamson, R.G., Colombo, O.L., Chandler, N.L., Rachlin, K.E., Patel, G.B., Bhati, S. and Chinn, D.S. (1988) *An improved model of the Earth's gravitational field GEM–T1,* J. Geophys. Res., 93, 6169.

Marsh, J.G., Lerch, F.J., Putney, B.H., Felsentreger, T.L., Sanchez, B.V., Klosko, S.M., Patel, G.B., Robbins, J.W., Williamson, R.G., Engelis, T.E., Eddy, W.F., Chandler, N.L., Chinn, D.S., Kapoor, S., Rachlin, K.E., Braatz, L.E. and Paulis, E.C. (1989) *The GEM–T2 Gravitational Model.* NASA Technical Memorandum 100746.

Moore, P. (1983) *A resonance problem of two degrees of Freedom.* Celest. Mech., 30, 31.

Moore, P. (1984) *A problem of libration with two degrees of freedom.* Celest. Mech., 33, 49.

Plummer, H.C. (1918) *An introductory Treatise on Dynamical Astronomy.* C.U.P. pp 44–46. Republished by Dover, New York (1960).

Sochilina, A.S. (1982) *On the motion of a satellite in resonance with its rotating planet.* Celest. Mech., 26, 337.

Tisserand, F. (1889) *Traité de Mécanique Celeste, Vol. 1 : Perturbations des Planetes d'aprés la Methode de la Variation des Constantes Arbitraires.* Paris, Gauthier–Villans et Fils, republished 1960.

Walker, D.M.C. (1979) *Cosmos 462 (1971–106A) : orbit determination and analysis.* Phil. Trans. R. Soc., A 292, 473.

Wilson, H.K. (1971) *Ordinary Differential Equations – Introductory and intermediate course using matrix methods.* Addison–Wesley, Reading, Massachusetts.